



Fisheries and Oceans
Canada

Pêches et Océans
Canada

Ecosystems and
Oceans Science

Sciences des écosystèmes
et des océans

Canadian Science Advisory Secretariat (CSAS)

Research Document 2022/062

Newfoundland and Labrador Region

A New Spatial Ecosystem-Based Surplus Production Model for Northern Shrimp in Shrimp Fishing Areas 4 to 6

E.J. Pedersen, K. Skanes, N. Le Corre, M. Koen Alonso, K.D. Baker

Northwest Atlantic Fisheries Centre
Fisheries and Oceans Canada
80 East Whitehills Road
St. John's, NL A1C 5X1

Foreword

This series documents the scientific basis for the evaluation of aquatic resources and ecosystems in Canada. As such, it addresses the issues of the day in the time frames required and the documents it contains are not intended as definitive statements on the subjects addressed but rather as progress reports on ongoing investigations.

Published by:

Fisheries and Oceans Canada
Canadian Science Advisory Secretariat
200 Kent Street
Ottawa ON K1A 0E6

[http://www.dfo-mpo.gc.ca/csas-sccs/
csas-sccs@dfo-mpo.gc.ca](http://www.dfo-mpo.gc.ca/csas-sccs/csas-sccs@dfo-mpo.gc.ca)



© His Majesty the King in Right of Canada, as represented by the Minister of the
Department of Fisheries and Oceans, 2022

ISSN 1919-5044

ISBN 978-0-660-45401-6 Cat. No. Fs70-5/2022-062E-PDF

Correct citation for this publication:

Pedersen, E.J., Skanes, K., le Corre, N., Koen Alonso, M., and Baker, K.D. 2022. A New Spatial Ecosystem-Based Surplus Production Model for Northern Shrimp in Shrimp Fishing Areas 4 to 6. DFO Can. Sci. Advis. Sec. Res. Doc. 2022/062. v + 64 p.

Aussi disponible en français :

Pedersen, E.J., Skanes, K., le Corre, N., Koen Alonso, M., et Baker, K.D. 2022. Un nouveau modèle écosystémique spatial de production excédentaire pour la crevette nordique dans les zones de pêche à la crevette 4 à 6. Secr. can. des avis sci. du MPO. Doc. de rech. 2022/062. v + 69 p.

TABLE OF CONTENTS

ABSTRACT	v
INTRODUCTION	1
BIOLOGY OF NORTHERN SHRIMP IN THE NL OFFSHORE REGIONS	2
NL SHELF NORTHERN SHRIMP FISHERIES.....	3
METHODS AND RESULTS.....	3
REVIEW OF DATA SOURCES.....	3
Historic Northern Shrimp Surveys.....	3
Fisheries and Oceans Canada Multi-Species and Northern Shrimp Research Foundation Surveys	4
Commercial Northern Shrimp Data	5
HISTORIC TRENDS IN NORTHERN SHRIMP PRODUCTIVITY	5
POPULATION AND ECOSYSTEM METRICS FOR CURRENT SURVEY DATA.....	7
Spatial Divisions For The Analysis	7
General Spatial Modelling Strategy.....	8
Current Northern Shrimp Biomass Dynamics	9
Predator Density	11
Bottom Temperature	11
North Atlantic Oscillation Index	11
Plankton	11
Fishing Pressure	12
Spatial Patterns of Recruitment	12
SPATIAL SURPLUS PRODUCTION MODELS	13
Surplus Production Model Background.....	13
Model Specifications	14
Model Comparisons	15
Model Robustness Checks	16
Forecasting Model Parameters	17
Model Sensitivity Tests	18
DISCUSSION.....	19
SCIENTIFIC UNCERTAINTIES	19
Stock Structure Dynamics.....	19
Catchability.....	20
Predation Rates on Northern Shrimp	20
Movement of Larval and Adult Shrimp Between Regions.....	21
Ecosystem Drivers in SFA 4 and 5	21
FUTURE MODEL DEVELOPMENT DIRECTIONS	22
REFERENCES CITED.....	22
TABLES	26

FIGURES	27
SUPPLEMENTAL FIGURES	51
APPENDIX I: AMENDMENT.....	63

ABSTRACT

Although one of the most economically important stocks in Canadian waters, Northern Shrimp (*Pandalus borealis*) in shrimp fishing areas (SFAs) 4-6 currently lack a population model to predict how fishing pressure and changing environmental conditions may affect future shrimp abundance. We tested various surplus production models that included potential predictors, such as predator density, bottom temperature, large-scale climatic conditions, plankton, patterns in recruitment, and fishing pressure to assess their ability to predict annual changes in Northern Shrimp biomass density. A spatially-explicit, lag-1 autoregressive surplus production model that included Atlantic Cod (*Gadus morhua*) density, alternate predator (Greenland Halibut-*Reinhardtius hippoglossoides* and Redfish-*Sebastes* spp.) density, North Atlantic oscillation (NAO) index, and Northern Shrimp biomass as predictors was found to be the best model. This model represents a step forward for assessing Northern Shrimp in SFAs 4-6, but as with any modelling, caution is warranted when applying it outside the range of ecosystem conditions already observed and ongoing evaluations of its efficacy will be required.

INTRODUCTION

Northern (or Pink) Shrimp (*Pandalus borealis*) stocks on the Newfoundland and Labrador (NL) Shelves (Shrimp Fishing Areas [SFAs] 4-7; Figure 1) are some of the most economically important stocks in NL (Carruthers et al. 2019), and are main components of the benthic shelf ecosystem, comprising a substantial portion of the benthic biomass and providing food for a wide range of benthic predators (Lilly et al. 2000). These stocks currently lack a population model to predict how fishing pressure and changing environmental conditions may affect shrimp densities in the short or long term. They are managed under a Precautionary Approach/Decision-making (PA/DM) Framework established following recommendations of a prior working group (DFO 2009), based on an index of average female spawning stock biomass (SSB) during what was considered a productive time period.

Following rapid declines of Northern Shrimp biomass in SFA 6 and 7 (leading to the closure of SFA 7), along with increasing biomass of groundfish predators of Northern Shrimp (with Atlantic Cod, showing the largest increases, but with many predator species increasing from 2010 onward (Rose and Rowe 2015; Pedersen et al. 2017; DFO 2018a), concerns were raised about the appropriateness of the average biomass approach used to manage these stocks, and if it should be updated given changing ecosystem conditions. The biomass-based reference points were re-evaluated in 2017 through a Regional Science Response peer-review process (DFO 2017), where it was concluded that there was some evidence that environmental factors affecting shrimp productivity may have changed since 2009. These findings were consistent with assessments of these stocks, which highlighted increasingly unfavourable environmental conditions, including increasing levels of groundfish predation. The 2017 Science Response concluded that a predictive population model was needed to understand the factors affecting productivity. The need for a population model for these stocks was also identified in the stock-rebuilding plan for SFA 6 following its entry into the Critical Zone of the PA/DM Framework (DFO 2018b).

In this document, we propose a new quantitative population model for these Northern Shrimp stocks. This model was designed to meet five criteria:

1. Predictive: The model should be able to predict changes in biomass at least one year in advance based on information that is measurable in the current year, so that it is useful for providing management advice.
2. Mechanistic: The model should be based on known or hypothesized mechanistic connections between variables and productivity.
3. Ecosystem-based: The model should use information on the current state of the ecosystem when making predictions, rather than simply using the current biomass of shrimp stocks and fishing pressure.
4. Explicitly include uncertainty: The model predictions should include the uncertainty associated with a given prediction and allow for a range of model forecasts.
5. Spatially structured: The NL shelves are strongly spatially structured, so both the Northern Shrimp stock and the drivers affecting it are also spatially structured. As such, shrimp productivity also likely varies in space. By developing an explicitly spatial model of these stocks, it is possible to estimate where productivity is changing most rapidly. Spatially explicit estimates of productivity can easily be scaled to the SFA level, whereas it is not generally possible to use aggregated models to predict smaller-scale changes.

In general, fisheries modelling has focused on developing population models at the level of whole stocks, rather than spatially explicit population models. We consider a spatial approach more fruitful for developing ecosystem-based models, as it allows us to explicitly incorporate the local or multi-scale effects of changing ecosystem conditions on changing productivity. Further, it is often possible to use simpler functional responses to model relationships between productivity and ecosystem variables in spatially explicit models than in stock-level models, as nonlinear averaging effects can lead to functional relationships appearing more nonlinear at large scales than at small scales (Barraquand and Murrell 2013).

BIOLOGY OF NORTHERN SHRIMP IN THE NL OFFSHORE REGIONS

Northern Shrimp are found in the Northwest Atlantic from Baffin Bay south to the Gulf of Maine. Northern Shrimp prefer an ocean floor that is somewhat soft and muddy and where temperatures range from approximately 1-6°C; however, the majority of Northern Shrimp are caught in waters from 2-4°C. These conditions typically occur at depths of 150-600 m and exist throughout the NL offshore area (Parsons 1982; Shumway et al. 1985). Northern Shrimp represents the primary shrimp resource in the North Atlantic, but overlaps in range with the Striped Shrimp (*Pandalus montagui*), which is also commercially exploited, generally as a bycatch fishery (DFO 2019).

SFAs 4-7 are not separated by any substantive barriers to adult or larval shrimp dispersal. The Labrador Current connects all four SFAs, running southward from SFA 4 through SFAs 5, 6, and 7. Research on larval dispersal modeling within SFAs 4-7 indicated strong downstream larval connectivity; the majority of recruits in a particular SFA may come from SFAs farther north. Northern Shrimp larvae may travel several hundreds of kilometers before settlement (Le Corre et al. 2019). Ongoing research has demonstrated that larvae originating in the Arctic also show high settlement in SFAs 4-6 (Le Corre et al. 2020). This research also indicates low larval shrimp retention in SFA 4 and 5, and higher larval retention in SFA 6. Release location, ocean circulation, and larval behaviour were identified as important variables affecting larval dispersal in the study area. Simulations on larval dispersal indicated that larvae released from inshore populations showed higher potential settlement success than larvae released from offshore (shelf edge) sites (Le Corre et al. 2019).

Studies of genetics between Northern Shrimp populations in SFAs 4-7 have demonstrated that Northern Shrimp in these areas are largely homogeneous genetically (Jorde et al. 2015). This is most likely a result of larval and pelagic transport by the Labrador Current. Despite the relationships between SFAs 4-7, the Northern Shrimp resources in these areas are managed (and hence assessed) on an individual SFA basis rather than as a whole.

Northern Shrimp are born and first mature as males, mate as males for one or more years, and then change sex to spend the rest of their lives as females. They are thought to live for more than eight years. Some northern populations exhibit slower rates of growth and maturation, but live longer and reach larger maximum size. Females produce eggs in the late summer-fall and carry the eggs on their pleopods until they hatch in the spring. Shrimp are thought to begin to recruit to the fishery around age three (Parsons 1982; Shumway et al. 1985). Most of the fishable biomass is female; however, the proportion of females in the fishable survey catch varies by SFA and year (DFO 2019).

During the daytime, shrimp rest and feed on or near the ocean floor. At night, substantial numbers migrate vertically into the water column, feeding on zooplankton (Shumway et al. 1985). Currently, there is little information on their diet composition, their food preferences, or the fraction of shrimp diets obtained from benthic/detrital versus pelagic food sources.

They are important prey for many species such as Atlantic Cod, Greenland Halibut, Redfish, American Plaice (*Hippoglossoides platessoides*), Skates (*Raja radiata*, *Raja spinicauda*), Wolffish (*Anarhichas* spp.), and Harp Seal (*Pagophilus groenlandica*), especially during the period of low groundfish abundances on the Newfoundland Shelf (DFO 2019). Varying predation rates have been shown to play an important role in regulating Northern Shrimp abundances across a wide range of systems, including Greenland (Hvingel and Kingsley 2006), Iceland (Björnsson et al. 2017), the Gulf of Maine (Cao et al. 2016b; Hunter et al. 2018), and the Gulf of St. Lawrence (Tamdrari et al. 2018), although recent studies in the Gulf of St. Lawrence also highlight the important role of plankton dynamics on Northern Shrimp growth (Brosset et al. 2018).

NL SHELF NORTHERN SHRIMP FISHERIES

The fishery for Northern Shrimp off the coast of Labrador began in SFA 5 in the mid-1970s, primarily in the Hopedale and Cartwright Channels. Soon after, concentrations of Northern Shrimp were located within SFA 4 and 6 leading to an expansion of the fishery into those areas. As the fishery expanded to Hawke Channel, St. Anthony Basin and Funk Island Deep, and to the slope of the continental shelf in SFAs 4-6 during the early-1990s, total allowable catches (TACs) were increased periodically and taken in most years. The northern Grand Banks (SFA 7) were opened to fishing in 2000 (DFO 2018c). There have been changes in seasonality of fishing effort through time and dependent on various factors, one of those being ice coverage in the various SFAs. Subject to license conditions, the large-vessel fleet fishes throughout the year in different SFAs.

Despite linkages between shrimp populations in SFAs 4-7, they are managed independently (i.e., TACs are allocated only with consideration for that particular SFA). TACs in SFAs 4-6 combined have been decreasing since the 2008/09 management year (Figure 2), mainly due to TAC reductions in SFA 6 which were implemented as a result of declines in survey biomass indices. SFA 7 was closed to fishing in 2015 following declining biomass levels below the established B_{lim} reference point (DFO 2018c), and has not increased above that level. The combined TAC for SFA 4-6 was 50,085 t in 2018/19. Commercial catch trends generally follow TAC trends (Figure 2); however, there have been years during which market conditions and operating costs led to uncaught Northern Shrimp quota.

All Northern Shrimp fisheries in eastern Canada are subject to the *Atlantic Fisheries Regulations*, established under the *Fisheries Act*, regarding territorial waters, by-catch, discards, vessel logs, etc. These include a minimum mesh size of 40 mm and mandatory use of sorting grates to minimize by-catch of non-target species. Grate size is dependent upon area fished. In SFA 6, the minimum bar spacing is 22 mm and in SFAs 4-5 the minimum bar spacing is 28 mm.

METHODS AND RESULTS

REVIEW OF DATA SOURCES

Historic Northern Shrimp Surveys

From the late-1970s to the early-1990s, targeted shrimp surveys were executed in various small areas (corresponding to commercial fishing grounds) of SFA 5 and 6. These surveys were executed from the vessels *A.T. Cameron*, *Zagreb*, and *Gadus Atlantica* and sets were randomly selected. Some of these surveys were experimental (i.e., diurnal) in nature. The fishing gear, seasonality, and spatial coverage were much different than the survey protocols in place today. A Sputnik 1600 trawl was utilized for 30-minute tows at a vessel speed of 3.0 knots. This trawl

had a wing spread of about 72.2 feet and an opening of about 21 feet. The same information (i.e., shrimp maturities, weights and numbers) were captured then, although there have been some refinements to maturity identification and disease/condition characterization.

Fisheries and Oceans Canada Multi-Species and Northern Shrimp Research Foundation Surveys

Fisheries and Oceans Canada (DFO) multi-species surveys employing a shrimp trawl began in 1995 and are executed from Canadian Coast Guard vessels including *CCG Wilfred Templeman* (1995-2008), *CCG Teleost* (1995-present), and *CCG Alfred Needler* (1996, 2001, 2005-06, 2008-present). Northern Shrimp assessments are performed using the autumn (late-September to mid-December) survey data, which covers North Atlantic Fisheries Organization (NAFO) Divisions 2HJ3KLNO; however, complete survey coverage of NAFO Division 2H (i.e., northern SFA 5) has only consistently been completed since 2010. The trends in SFA 5 survey biomass indices during the missing years is unknown. The goal of these surveys is to maintain set allocations, survey coverage, and seasonality across years, however there have been times that the survey has extended into January and planned sets have been dropped due to factors including weather and vessel issues.

Basic DFO fall survey performance statistics and coverage are presented annually at NAFO meetings and are published on the NAFO website (Power et al. 2016; Rideout and Ings 2018).

Northern Shrimp Research Foundation (NSRF) surveys began in 2005 and cover SFA 4 during the summer months (July-August). These surveys are executed from commercial fishing vessels including *Cape Ballard* (2005-11), *Kinguk* (2014), *Katsheshuk II* (2015), and *Aqviq* (2012-13, 2016-18). *Cape Ballard*, *Aqviq*, and *Kinguk* had similar specifications but *Katsheshuk II* was a larger, more powerful vessel. There was no change in the survey gear or design, and it was assumed that any effect of this change in the survey vessel would not be important. However, no among-vessel calibration was conducted.

A Campelen 1800 trawl is utilized on the research vessel (RV) surveys and is towed for a targeted 15 minutes of bottom contact at a vessel speed of 3.0 knots. This trawl has a wing spread of about 55.25 feet and an opening of about 13 feet; details of the survey design and fishing protocols are outlined in Brodie (1996) and McCallum and Walsh (1996).

A trawl-mounted CTD also provides information on bottom temperatures and depths at survey locations. When the CTD does not function properly, an expendable bathythermograph (XBT) is deployed to provide bottom temperature readings and depth readings are taken from the vessel sounder or Scanmar sensors.

The data from these surveys are subject to two data review processes: once on-board the ship by the person in charge of each particular trip, and again when the data are returned to DFO-Science upon the completion of the entire seasonal survey. Trained technicians on these surveys count and weigh every species that is caught. This includes known predators of shrimp (e.g., Greenland Halibut, Redfish, and Atlantic Cod) in addition to shrimp species identification, maturities, parasite presence, and carapace lengths. Shrimp maturity classes include males, transitional, primiparous females, ovigerous females, and multiparous females. A sample weight by maturity and disease condition (e.g., black gill) is captured before capturing the numbers at size (i.e., carapace length) for the survey shrimp sample. Carapace lengths are measured to the nearest tenth of a millimeter, however survey results are normally grouped in 0.5 mm length bins for analyses.

Over a number of early years, experiments were conducted during which individual shrimp were measured and weighed such that formulas could be derived for conversion from numbers to

weights. These formulas are applied to numbers at size in order to convert abundance to weight of fishable-sized (i.e., carapace length >17 mm) shrimp from each survey tow. These formulas are as follows:

$$\text{Individual Weight (g)} = \begin{cases} \text{males: } 0.00088 \times (\text{Carapace Length (mm)})^{2.857} \\ \text{females: } 0.00193 \times (\text{Carapace Length (mm)})^{2.663} \end{cases} \quad (1)$$

Commercial Northern Shrimp Data

Canadian Observer Data

The current Northern Shrimp fishery in SFA 4-6 is executed by about 13 large vessels and 250 small vessels. Coverage of these areas is available to all large vessels, but the small-vessel fishery is largely concentrated in SFA 6. Observer coverage is mandatory on all large vessels. The goal for observer coverage on the small-vessel fleet is 10%; however, coverage is usually much less than that, with about 5-8% coverage in recent years.

Observers onboard vessels are responsible for recording positions, catch size, discards, etc. They measure one random detailed sample of Northern Shrimp per day, which consists of 250-300 individual Northern Shrimp and includes information on maturity, lengths, and pathogens. This provides a reasonable snapshot of size frequencies throughout the fishing season in various areas.

Given the complete observer coverage of the large-vessel Northern Shrimp fishery, observer data are utilized to calculate commercial catch per unit effort (CPUE) for assessment purposes and are used to determine the spatial distribution of commercial catch in this model. The assessment takes place while the fishery is ongoing and there is a delay receiving the data such that the most recent commercial data are not available for analysis in the assessment (i.e., 2018/19 data is not available for the 2019 assessment) and the last point presented is preliminary. There are some differences in how data are collected and depends on the province in which the fishing vessel is registered together with the company responsible for the observers. Some trips capture detailed sampling that includes males, primiparous females, multiparous females, and ovigerous females, while others only record whether a shrimp is ovigerous or non-ovigerous.

Canadian Logbook Data

Logbooks are completed for every Canadian vessel targeting Northern Shrimp. They are returned to the province in which the vessel is registered and stored in databases that differ by province. These data include information such as catch size, position, and discards.

Given the low observer coverage rates of the small-vessel Northern Shrimp Fishery, logbooks are utilized to generate small-vessel CPUE indices for the assessments, and to determine the spatial distribution of small-vessel fishing effort.

HISTORIC TRENDS IN NORTHERN SHRIMP PRODUCTIVITY

While the fishery for Northern Shrimp on the NL Shelves started in the early-1970s, the current RV biomass time series starts in 1995 (for SFA 5-7) or 2005 (for SFA 4). Northern Shrimp abundance may have increased somewhat during the 1980s and increased rapidly from 1990 in SFA 6 (Lilly et al. 2000). This followed a reverse trend from the bulk of the groundfish stocks on the Newfoundland Shelf, with average groundfish biomasses declining from the mid-1980s, with the most rapid declines occurring from 1990-95 (Pedersen et al. 2017). However, the extent of this growth has been previously unknown, as there were no validated metrics of pre-1995 Northern Shrimp abundances to compare with current abundance metrics based on multi-

species RV surveys. Measures of changes in Northern Shrimp historical biomass to current biomass can provide a useful baseline to determine the approximate magnitude of changes in shrimp productivity from the period of high to low groundfish abundances, and provides a useful test case to compare model predictions out of the sample of the current trawl survey. In this section, we survey the existing historical data on Northern Shrimp abundances prior to 1995, to determine the extent of the change in biomass from the 1980s to 1995.

As noted, prior to 1995, limited historical shrimp surveys had been conducted in three channels: Hopedale Channel, Cartwright Channel (both in SFA 5), and Hawke Channel (at the northern end of SFA 6). The spatial distribution of these trawls is shown in Figure 3A in red, compared to the spatial extent of current (1995 onwards) trawls in black. A comparative index of shrimp biomass in these channels was developed by matching trawls in the RV survey with historic trawl surveys by finding the 10 nearest RV trawls across all RV survey years to each historic trawl. The RV trawls for comparison were then further filtered by excluding all trawls not falling within a non-convex bounding polygon (Blangiardo and Cameletti 2015) around each channel. The spatial distribution of matched RV and historic trawls are shown in Figure 3B.

Total Northern Shrimp biomass from each trawl was transformed into a density by dividing by the area swept by the trawl. Means and confidence intervals of biomass in each channel from before and after 1995 was calculated by fitting a spatiotemporal smoothed GAM model to the observed densities across both sets of trawls.

The second index of historical shrimp productivity was based on inferred abundance of Northern Shrimp based on the presence of shrimp in the diets of Atlantic Cod in SFA 6¹. The fall RV survey has consistently collected data on the presence or absence of prey as primary components in predator stomachs across SFA 6 since the 1980s (from historic Groundfish Engels surveys and current DFO RV surveys), referred to as ‘called stomach’ data. The fraction of Atlantic Cod stomachs in SFA 6 that contained shrimp as one of the main components correlated closely with Ogmap estimates of biomass of shrimp in the RV data for the years where Northern Shrimp were consistently measured (Figure 4). These data were used to infer past Northern Shrimp biomasses by regressing RV biomass on diet fraction using a generalized linear model (GLM) assuming Tweedie-distributed RV biomass, and then past biomass levels in SFA 6 were inferred by using the fitted GLM to give the estimated biomass for those years where only diet fraction data were available.

Both shrimp biomass proxies suffer from data issues that result in them not being optimal for assessing biomass trends; the RV and historical shrimp surveys differed in survey gear and survey timing, the difference in catchability between historical and RV surveys is unknown, and the presence of shrimp in cod diets may have been influenced by factors other than changes in shrimp biomass, such as the availability of alternative prey or changes in the spatial distributions of cod or shrimp. However, both comparative trawl biomass time series (Figure 5A) and diet-inferred biomass time series (Figure 6A) are consistent with a general increase in shrimp biomass between 1990 and 1995, to a level between four to ten times the biomass of the pre-1990 level (Figure 5B and Figure 6B). These metrics also indicate that in recent years shrimp biomass has declined to a level consistent with their 1979-90 levels in SFA 6. As the two time series use very different information to estimate changes in abundance, this indicates that this rapid increase very likely occurred in SFA 6 (and to a lesser extent across SFA 5; see Figure 5B

¹ Greenland Halibut diets were also available for this period, but showed very similar relationships between diet fraction and Northern Shrimp biomass, and using both species did not improve model predictions relative to using Atlantic Cod diets alone.

Cartwright and Hopedale channels), and the increase in biomass in the 1990s was similar to the decline in biomass after 2008.

POPULATION AND ECOSYSTEM METRICS FOR CURRENT SURVEY DATA

Spatial Divisions For The Analysis

One of the goals for the surplus production model was to explicitly account for the spatial structure of the stock, including the possibility of spatially varying demographic factors (e.g., growth and mortality) and incorporate modelled patterns of larval recruitment. As such, the models had to explicitly account for stock spatial structure. This requires discretizing space in some way, as any modelling approach requires some form of discretization.

While the region is already divided into SFAs, these were considered too coarse-scale for the purposes of this model. The sampling scheme used for the summer and fall surveys was already based around depth strata, which could have been used as a discretization scheme. However, this approach was also not optimal, because there were a large number of strata (increasing computational time for any model), and many strata were long and thin, so that determining the probability of dispersing from one stratum to another became complicated in any future modelling of shrimp dispersal. As such, it was determined that it was necessary to develop a new discretization scheme for the region.

When developing the discretization, four factors were prioritized:

1. Spatial patches should be compact (ideally, convex), avoiding patches that were spatially complex or divided into sub-patches.
2. The range of depths within each patch should be relatively homogeneous, as depth was recognized as one of the major factors that would affect shrimp demographics and dispersal.
3. Patches should be structured such that each patch covered an area that typically included multiple trawl survey tows per year, to stabilize population estimates (although given the variability in sampling coverage, no discretization scheme could achieve this for all patches in all years).
4. Patches should respect the existing SFA boundaries, so it would be possible to assign growth and biomass occurring within each patch to a specific SFA for management purposes.

This required developing a novel method to meet these criteria. All spatial analyses for this procedure were done using the **sf** package for **R 3.5.1** (Pebesma 2018; R Core Team 2018). For each SFA in the model (SFAs 4-7), a random sample of locations of previous trawls were drawn from the fall survey. These draws included 10 trawls from SFA 4, 30 from SFA 5, 30 from SFA 6, and 5 from SFA 7. The overall number of draws was chosen arbitrarily and within each SFA the numbers were chosen because SFA 4 is a smaller area than SFA 5 and 6 and less depth-structured. As well, shrimp occur less frequently in SFA 7 and it was decided that less computational effort should be dedicated to estimates for that region.

A Voronoi tessellation was calculated based around the selected points. This procedure creates a set of polygons, where the interiors of each polygon around a specific point contain all of the locations that are closer to that point than to any other point in the set (Fortin and Dale 2005). All polygons that overlapped a SFA boundary were cut into two pieces, and any resulting polygons that fell outside of any SFA were discarded. As there were a number of very small polygons after clipping to SFA boundaries, any polygon with an area of less than 1,500 km² was

merged with its nearest neighbour within the SFA. One polygon in SFA 4 was also cut into four separate ones as it previously covered too large an area, and was not homogeneous for depth, covering both the shelf and shelf edge. As the SFA boundaries included several inshore areas near Labrador that are not sampled as part of the multi-species of NSRF surveys, these areas were excluded by clipping polygons to the area bounded by the current trawl strata. This procedure resulted in 71 total patches (Figure 7). The distribution of depths within each polygon is shown in Figure 8.

General Spatial Modelling Strategy

A model-based, penalized regression approach was used to estimate spatiotemporal trends for shrimp biomass density and for environmental predictor variables. Spatial statistical models were fit using generalized additive models (GAMs) (Wood 2017; Pedersen et al. 2019) for all predictors that were derived from RV trawl data, commercial logbooks, or commercial observer data. This includes Northern Shrimp biomass, bottom temperature, and biomass of potential shrimp predators (here using three of the most abundant species as proxies for the groundfish predation field: Atlantic Cod, Greenland Halibut, and Deepwater Redfish). These models assume that any given outcome y is a random observation from a statistical distribution, so that the probability of observing a given value $y_{t,i}$ at a specific year (t) and in a given patch (i) is given by $y_{t,i} \sim f(\mu_{t,i}, \phi)$ where f is some statistical distribution with a mean $\mu_{t,i}$ and a scale factor that does not depend on time or location, and determines the variability around the mean value. Mean value fields $\mu_{t,i}$ are assumed to come from the sum of one or more *smooth terms*, by transforming the predictor variables into a group of simple functions (*basis functions*, $b_{1\dots n}(t, i)$) that can be multiplied by coefficients and linearly summed across all functions, then taking the resulting sum and transforming it by a distribution-specific *link function* ($g(x)$) to give the predicted mean.

To estimate the appropriate coefficients to best predict observed patterns in the data, the GAM model maximizes the sum of the log-likelihood of observing all of the observed data $\sum \log(p_f(y_{i,t}|\mu_{i,t}, \phi))$, minus a penalty term that penalizes how far each estimated coefficient in a given smooth term is away from the other coefficients, using a smoother-specific penalty term λ and penalty matrix P that determines which coefficients should be “close” to each other, by penalizing the quadratic products of all pairs of coefficients. The penalties in turn are selected using restricted maximum likelihood (REML) (Wood 2011). See Pedersen et al. (2019) section II for a more detailed introduction to these methods.

GAM models of predictors were fit using the **mgcv** package (Wood 2017). For all spatially-resolved model inputs, spatiotemporal trends were estimated using three smooth terms:

1. A year-effect, where each year was treated as a single basis function; this term estimated the mean value of each variable over time.
2. A spatial term, where each patch was treated as a single basis function, and each trawl was assigned to one patch (using the patch structure identified above); this term estimated the average distribution of each predictor across space.
3. A year-spatial interaction, calculated as a tensor-product interaction (Wood 2006a) of the year and spatial terms; this term estimated how much each model term varied around the year- and location-specific averages.

The year terms were penalized using a random-effect penalty (Wood 2017), that penalized all coefficients towards the global mean (with the penalty for each coefficient being proportionate to the squared value of that coefficient; Figure 9). This penalty acts to smooth estimates, but does not specifically penalize years that were close to each other more strongly towards one another

than to other years, so that rapid year-to-year changes were not penalized away. The spatial terms were fit using a Markov Random Field (MRF) smoother (Wood 2017), that penalizes the squared differences between coefficients of the polygons directly adjacent to one another. This acts to spatially smooth adjacent polygons towards each other (sharing information between nearby areas on the average value of a given predictor variable), with a penalty that drops off with distance, so that polygons far away from one another are able to be freely estimated. The spatiotemporal interaction term was penalized with a tensor product of a MRF and random effect penalty, using the `ti` function in **mgcv** (Wood 2006a), so that neighbouring polygons in the same year were penalized towards one another and toward the global mean.

This model-based approach to estimating Northern Shrimp density and spatial predictors enables estimation not only of the mean value of each predictor at a given location and time, but also ranges of uncertainty associated with each estimate, both for location-specific estimates and for functions of those estimates, such as average biomass across the year. To calculate uncertainty for any given point, the GAM model was treated as a Bayesian regression (Wood 2006b; Marra and Wood 2012), with the penalty terms and matrices corresponding to multivariate normal priors on the various smooth terms (when treated as a Bayesian model estimate, REML smoothing estimation corresponds to an approximation of Empirical Bayesian model fitting with flat priors on the log of the smoothing parameters; Wood 2006b). To estimate posterior uncertainty intervals for desired values, new random coefficient values were generated from a multivariate normal distribution with a mean of the estimated coefficient values and the variance-covariance matrix equal to the model posterior variance-covariance matrix. These posterior sample coefficient vectors were multiplied by the basis functions that corresponded to the predictor values that an uncertainty interval was desired for. This yielded a vector of predicted values for each combination of predictors of interest, and the quantiles of this distribution were used to calculate the desired intervals. In all cases, 1,000 simulated coefficient vectors were generated to calculate uncertainty intervals. These simulated values were also used to calculate uncertainty intervals for derived statistics (such as total biomass in a given SFA). The procedure for this is the same as above, except the desired summary statistics are calculated from the simulated values prior to aggregating values into uncertainty intervals.

Current Northern Shrimp Biomass Dynamics

The above procedure was used to model the spatiotemporal dynamics of shrimp biomass density across the three survey regions that are the focus of this document, as well as the dynamics of SFA 7. While SFA 7 is managed under a separate NAFO management framework, it is spatially connected to SFA 6 and the population changes in this area can provide additional information about factors that may be driving the stock. Currently more northern stocks (the Eastern Assessment Zone and Western Assessment Zone) are not included in these models, but it would be possible to extend this approach to incorporate these regions in future models.

All trawl survey catches were first converted into densities by dividing the total weight of Northern Shrimp caught in a given trawl by the area swept by that trawl in km^2 , where area swept equaled the distance traveled by the trawl multiplied by the wingspread of the Campelen trawl (16.8 m). The spatiotemporal pattern of biomass across the four SFAs was then calculated using the GAM model described in the “General spatial modelling strategy” section. Shrimp density was assumed to be distributed following a Tweedie distribution (Wood 2017). The Tweedie distribution assumes that observed weight caught in a trawl follows a compound Poisson-Gamma distribution, where shrimp are assumed to live in aggregations each of which has a specific biomass following a Gamma distribution, and the probability of capturing n aggregations follows a Poisson distribution. This distribution allows for the possibility of both trawls with zero catch (when no aggregations are captured) and trawls with very high catches

(when one or more aggregations are captured) and has been shown to be effective for modelling complex spatial patterns of population abundance in other fisheries (Lecomte et al. 2013).

The spatial pattern of Northern Shrimp densities estimated by the model are shown in Figure 10. There are consistent patterns of spatial aggregation in shrimp biomass occurring across the shelf, but the declines in biomass across the range in the last several years are apparent.

The current assessment for Northern Shrimp in SFAs 4-6 relies on biomass estimates derived using the ogive mapping method (Ogmap) (Evans et al. 2000), instead of GAM-based estimates as used in this model. The Ogmap method relies on using observed shrimp biomasses in trawls to create a weighted empirical cumulative distribution function (WECDF) for each point in the domain of interest, with the weights based on distances and differences in depth between that location and other survey points. These WECDFs are then used to estimate mean or median biomass (or other quantiles of the local distribution), at each point in a grid, which are then summed across to estimate quantities such as total biomass in a region. This approach can also be used to estimate uncertainty intervals for aggregate biomass, by bootstrap resampling (Efron 1982) from the set of WECDFs to generate a new sample trawl survey and generate a new estimate of population biomass.

We chose to use GAM-based estimates of the spatial distribution of biomass and other indicators rather than Ogmap because there is currently no method in place in the Ogmap approach to propagate uncertainty of estimates for multiple spatial locations simultaneously (which the Empirical Bayesian approach described above does). Further, Ogmap currently tends to generate unrealistically tight confidence intervals, due to unresolved issues with how trawls at a given location are included when fitting parameters for the weighting function versus when using Ogmap for estimating derived quantities (Evans, personal communication). However, to ensure that the approach for estimating biomass used for this model was comparable to the Ogmap approach, we compared Ogmap and GAM outputs for each SFA and for each patch within the SFAs.

The smooth GAM model of biomass density was integrated into an estimate of biomass within each SFA for each year by multiplying the estimated density of each patch by its area then summing across all patches within each SFA. Uncertainty intervals for these yearly biomass estimates were calculated as described in the “General spatial modelling strategy” section. These biomass estimates and 95% confidence intervals are shown in Figure 11, with biomass estimates and 95% confidence intervals for the estimates used in the current Northern Shrimp SFAs 4-6 assessment (DFO 2019). The GAM procedure resulted in very similar biomass estimates in all SFAs compared to the Ogmap procedure (Evans et al. 2000), and broader confidence intervals for SFA 6 and 7. This discrepancy may be a result of the current version of Ogmap returning overly narrow uncertainty intervals, due to the issue with the inclusion of individual trawl points noted above. Furthermore, both methods gave very similar estimates of the dynamics of mean biomasses within each patch (Figure 12), with the only notable differences between average patch densities between the two patches occurring in small patches on the boundary of the range, such as V3, V4, and V60 (Figure 7). As such, the GAM biomass estimates were considered to be consistent with Ogmap biomass estimates, as were used in the remainder of this model as the primary estimate of biomass.

These biomass indicators can be converted into estimates of fishable biomass, by multiplying total biomass values by the fraction of the total weight estimated to occur as shrimp larger than 17 mm carapace length in each year for each SFA. This conversion factor was calculated by transforming counts of shrimp in each size bin observed in the RV survey into weights using equation (1) then dividing the average weight per tow of all shrimp found in the RV survey trawl

in given SFA and year by the summed weights. The ratio of fishable to total biomass has stayed relatively constant within each SFA, but varied between SFAs, with the average fishable fraction increasing from south to north, from 84% in SFA 7 to 98% in SFA 4 (Figure 13).

Predator Density

Density of shrimp predators was estimated from biomass estimates taken from summer (NSRF) and fall (DFO RV) trawl surveys². Three potential predators (previously identified as significant consumers of shrimp) were identified: Atlantic Cod, Deepwater Redfish, and Greenland Halibut. For each species, the total biomass in each trawl was transformed into density per km² by scaling biomass by trawl area. Spatiotemporal regression models were fit for each species using a Tweedie family and the procedure described in “General spatial modelling strategy” section. The estimated maps of density for these species are shown in Figures 14, 15, and 16. Average densities of each of the three species in SFAs 4-7 are shown in Figure 17.

Bottom Temperature

The bottom temperature field was estimated from measurements of temperature taken at each station as part of the summer and fall RV surveys. The spatiotemporal pattern of bottom temperature was estimated by using the smooth modelling approach, assuming residual temperatures were normally distributed around their mean field estimates. Estimated spatial patterns of temperature are shown in Figure 18. Average bottom temperatures are shown in Figure 19.

North Atlantic Oscillation Index

The NAO is a large-scale climate state indicator, defined as the difference in winter sea level atmospheric pressures between the Azores and Iceland. It correlates quite strongly with general climate conditions on the NL Shelves, with positive NAO conditions being associated with generally colder and fresher waters on the shelf (Colbourne et al. 2017). This predictor was calculated for the whole shelf on an annual scale by averaging all the monthly NAO values in a given year (Figure 20A), obtained from the National Oceanic and Atmospheric Administration (NOAA) climate prediction center. As winter NAO (the average NAO index from December to March) has been identified as an important predictor of shrimp dynamics in Greenland (Hamilton et al. 2003), this index was also calculated for all years.

Plankton

Estimates of zooplankton abundance were derived from summer data from the Atlantic Zonal Monitoring Program (AZMP), from the Station 27, Bonavista, Seal Island, Makkovik Bank, and Flemish Cap lines. Following the standardization procedure in Pepin et al. (2017), scaled biomass estimates for each line were derived from total zooplankton biomass measurements by subtracting the average biomass recorded in the summer in that survey line during the AZMP zooplankton reference period of 1998 to 2010, and dividing by the standard deviation of biomass measurements in the same reference period. Biomass deviations for all measurements within given year were then averaged to give a single zooplankton biomass deviation for that

² These estimates do not represent estimates of fish biomass for stock assessment purposes, and are only designed as metrics of relative abundance of these species at the spatial scales used to model shrimp dynamics.

year, indicating how many standard deviations, on average, zooplankton biomass exceeded or fell below the average biomass for the reference period (Figure 20B).

Estimates of phytoplankton abundance were based on satellite images of the spring phytoplankton bloom, using estimates of the magnitude (chlorophyll concentration integrated across the whole bloom, Figure 20C) and timing (Figure 20D) of the bloom from Pepin et al. (2017). Phytoplankton abundance indicators were scaled using the same method as that used for zooplankton abundances.

Fishing Pressure

Total Northern Shrimp catch was determined for each patch in each year by summing catches from all trawls that occurred in each patch based on observer records from large-vessel catch and logbook records from small-vessel catch. These measures were scaled by the total reported landings in that year, as total catches based on logbook or observer data did not always exactly sum to total landings. Catches for the most recent year (2018) were scaled based on total assigned quota for the SFA, as final observer, logbook, and landings data were not available at the time of writing. Catches were transformed into catch densities by dividing the catch assigned to each patch in each year by the patch area.

Spatial Patterns of Recruitment

Given the strong and consistent southerly Labrador Current and the extended larval duration of Northern Shrimp, new recruits entering the population at any given location likely originated substantially north of that location, and a high degree of recruitment connectivity between SFAs is expected (Le Corre et al. 2019). As such, spatially structured patterns of recruitment were considered as one potential driver of shrimp population dynamics. To estimate dispersal rates of larvae originating from each patch to the others, the oceanographic dispersal model developed in Le Corre et al. (2019) was used to simulate larval drift paths from a grid of 267 points spread across all four SFAs (Figure 21). For each starting point, 100 simulated larvae per day were released and tracked for 105 days, in three separate simulation years (1999, 2009, and 2010, chosen to span a range of NAO conditions). Any larvae that was found in a given patch between the 86th to 105th day since the beginning of its dispersal (the assumed larval competency period; Le Corre et al. 2019) was assumed to be able to disperse there from its starting point. For each pair of patches, a and b , the fraction of individuals dispersing from a to b was calculated as the number of days that a settlement-competent larvae from a was in patch b , divided by the total number of settlement competent larvae-days for all larvae from a . This was repeated for all pairs of patches.

These observed fractions were used to estimate a connectivity matrix by regressing fraction settled between patch a and b on a MRF interaction between all sites (so that sites near each other were penalized to have similar numbers of larvae dispersing from them to other sites, and from other sites to them). This connectivity matrix was then scaled by the total patch size of the sending and receiving patch, to account for the fact that different patches would differ in density, as a fixed number of larvae moving into a smaller patch would have a greater effect on the patch's density than the same number moving into a larger patch.

Finally, this modified connectivity matrix was converted into an estimated index of recruitment for each patch in each year, by multiplying the connectivity matrix by a vector of estimated densities for all starting locations (calculated from the model in "Current Northern Shrimp biomass dynamics" section). This implied that the recruitment index for any given site was a weighted average of the estimated shrimp densities for all other sites, where the weighting depended on the modelled connectivity rate and the relative areas of the two patches.

Spatial Surplus Production Models

Surplus Production Model Background

Patch-specific rates of change for biomass across the region were modelled using a series of ecosystem-based spatially structured surplus production models (SPM). These SPMs assumed that population density in a given patch i and year t ($D_{i,t}$) is equal to the density in the location observed in the previous year ($D_{i,t-1}$) times a year and patch-specific annual production rate $e^{r_{t,i}}$, minus the total catch density in that location, $C_{i,t}$ (where $C_{i,t}$ equals the total mass of all Northern Shrimp caught in the patch divided by patch area). The growth term captures all non-fishing effects that lead to biomass change, including recruitment, growth, and mortality:

$$D_{i,t} = D_{i,t-1} e^{r_{t,i}} - C_{i,t} \quad (2)$$

These models assumed that fisheries removals happen after recruitment, growth, and mortality has occurred, so that in the absence of fishing pressure, all of the caught shrimp would still be present in the population at the time of the survey.

The instantaneous productivity is assumed to in turn depend on the density in the patch in the previous year ($D_{i,t-1}$) and other potentially year- and patch-specific factors ($\mathbf{V}_{i,t}$):

$$r_{t,i} = f(D_{i,t-1}, \mathbf{V}_{i,t}) \quad (3)$$

Rearranging equation (2) then log-transforming both sides and substituting in equation (3) gives the following equation for production:

$$\log\left(\frac{D_{i,t} + C_{i,t}}{D_{i,t-1}}\right) = f(D_{i,t-1}, \mathbf{V}_{i,t}) \quad (4)$$

The models developed focused on linear additive versions of equation (4), where ecosystem predictors were assumed to be linearly related to instantaneous productivity. This would correspond to a simple Ricker model if $f(D_{i,t-1}, \mathbf{V}_{i,t}) = \hat{r} - \beta \cdot D_{i,t-1}$, where \hat{r} is the density-independent rate of growth and β accounts for density-dependence on growth rates. In the linear additive case, equation (5) can be estimated by regressing the log of the ratio of current density plus catch to the density in the past year on past density and other potential predictors:

$$\log\left(\frac{D_{i,t} + C_{i,t}}{D_{i,t-1}}\right) = \hat{r}_i + \beta_i \cdot D_{i,t-1} + \sum_j \gamma_j \cdot V_{j,i,t-1} + \epsilon_{i,t} \quad (5)$$

Spatial variability in maximum productivity is captured by the term \hat{r}_i , which corresponds to the expected rate of growth in patch i at low densities in the absence of other drivers. Spatial variability in density dependence is captured by the term β_i , which determines how rapidly growth rates decline with increasing density; lower values of β_i would correspond to higher local carrying capacity in a site, all else equal. Effects of other measured ecosystem predictors are measured by the terms γ_j , with positive terms meaning that productivity is expected to be high on average when that predictor is high, and negative terms implying reduced productivity when that predictor is at high levels. If ecosystem predictors are changing over time, this will have the net effect of shifting both the maximum possible productivity and the maximum carrying capacity in a patch at any given time. All unmeasured factors affecting productivity were assumed to enter through the error term $\epsilon_{i,t}$ (which also incorporates effects of measurement errors in the prior and current year's biomasses). For all models, the error $\epsilon_{i,t}$ was assumed to follow a Student's t-distribution, which is similar to the standard Gaussian distribution but has longer tails, allowing for the possibility of occasional large positive or negative changes.

Model Specifications

Four SPM models were fit, to determine which ecosystem predictors were able to accurately predict annual changes in biomass density, and to determine if more complex model structures were able to better predict population dynamics. All models were estimated by regressing mean estimated values of $\log\left(\frac{D_{i,t} + C_{i,t}}{D_{i,t}}\right)$ from spatial Northern Shrimp density models on different combinations of environmental predictors, using the gam function from the **mgcv** R package. All models included a MRF smoother across patches to model spatially varying patterns in growth rates. Biomass for Redfish and Greenland Halibut densities in each patch were summed to produce a single composite alternate predator (besides Northern Cod), as estimated Greenland Halibut density stayed relatively constant throughout the time series in all SFAs. Patch-specific density, recruitment, and predator densities were used as patch-level predictors of biomass change. While bottom temperature estimates were available at the trawl and patch level, temperature was aggregated to the SFA-scale by taking the mean temperature in each SFA across patches. We aggregated temperature to the SFA-scale as the spatial pattern of temperature did not show substantial variation across years, and was strongly co-linear with spatial location and thus effectively already accounted for by including patch-specific predictors of average growth rates. Only yearly estimates were available for all other predictors included in the models (zooplankton indices, phytoplankton indices, NAO).

The four tested models were:

1. Lag-1 autoregressive: this model included all of the potential predictors (zooplankton, phytoplankton, NAO, temperature, recruitment index, cod density, and alternative predator density) as linear terms with 1-year lag from the current year. The density of Northern Shrimp in the previous year was included as 1-year lagged term with a spatially varying slope, using a MRF smoother on the slope to prevent over-fitting observed trends:

$$\log\left(\frac{D_{i,t} + C_{i,t}}{D_{i,t}}\right) = \hat{r}_i + \beta_i \cdot \text{shrimp density}_{i,t-1} + \\ \gamma_1 \cdot \text{recruitment index}_{i,t-3} + \\ \gamma_2 \cdot \text{cod density}_{i,t-1} + \gamma_3 \cdot \text{other predator density}_{i,t-1} + \\ \gamma_4 \cdot \text{NAO index}_{t-1} + \gamma_5 \cdot \text{bottom temperature}_{sfa,t-1} + \\ \gamma_6 \cdot \text{phytoplankton magnitude}_{t-1} + \gamma_7 \cdot \text{phytoplankton timing}_{t-1} + \\ \gamma_8 \cdot \text{zooplankton biomass}_{t-1} + \\ \epsilon_{i,t}$$

2. Simplified lag-1 autoregressive: this model included only the significant terms from the prior model: cod density, alternative predator density, NAO index, and Northern Shrimp biomass:

$$\log\left(\frac{D_{i,t} + C_{i,t}}{D_{i,t}}\right) = \hat{r}_i + \beta_i \cdot \text{shrimp density}_{i,t-1} + \\ \gamma_1 \cdot \text{cod density}_{i,t-1} + \gamma_2 \cdot \text{other predator density}_{i,t-1} + \\ \gamma_3 \cdot \text{NAO index}_{t-1} + \\ \epsilon_{i,t}$$

3. Multi-lag autoregressive: this model included lags of up to five years for all predictors, so that the effect of a given predictor on rate of growth was given by $\sum_l \gamma_l \cdot V_{t-l}$. The γ_l for each smoother were penalized toward one another using a thin-plate spline. The goal of this model was to determine if there was evidence for lagged effects beyond a single year.

$$\log\left(\frac{D_{i,t} + C_{i,t}}{D_{i,t}}\right) = \hat{r}_i + \sum_{k=1}^5 \beta_k \cdot \text{shrimp density}_{i,t-k} + \\ \gamma_{1,k} \cdot \text{recruitment index}_{i,t-k} + \\ \gamma_{2,k} \cdot \text{cod density}_{i,t-k} + \gamma_{3,k} \cdot \text{other predator density}_{i,t-k} + \\ \gamma_{4,k} \cdot \text{bottom temperature}_{sfa,t-k} + \gamma_{5,k} \cdot \text{NAO index}_{t-k} + \\ \gamma_{6,k} \cdot \text{zooplankton biomass}_{t-k} + \\ \epsilon_{i,t}$$

4. Spatially varying lag-1 autoregressive: this model had the same structure as model 1, except the effect of each predictor on growth rates was allowed to vary across patches, so the effect of a given predictor on growth rates in a given patch would be given by $\gamma_i \cdot V_{t-1}$ with the spatially varying regression terms γ_i fit using a MRF smoother to penalize estimates of nearby patches towards one another.

$$\log\left(\frac{D_{i,t} + C_{i,t}}{D_{i,t}}\right) = \hat{r}_i + \beta_i \cdot \text{shrimp density}_{i,t-1} + \gamma_{1,i} \cdot \text{recruitment index}_{i,t-3} + \\ \gamma_{2,i} \cdot \text{cod density}_{i,t-1} + \gamma_{3,i} \cdot \text{other predator density}_{i,t-1} + \\ \gamma_{4,i} \cdot \text{bottom temperature}_{sfa,t-1} + \gamma_{5,i} \cdot \text{NAO index}_{t-1} + \\ \gamma_{6,i} \cdot \text{zooplankton biomass}_{t-1} + \\ \epsilon_{i,t}$$

To assess the goodness of fit of each model, several years of data were held as a test set, not used to fit the model. The years used for model testing were 2006-08 (occurring during the period of peak Northern Shrimp biomass) and 2016-18 (during the period of rapid population declines), effectively acting as a retrospective test. Goodness of fit was evaluated by comparing how well each model predicted within-patch rates of change for all test years. Holding out the last three years of data acts as a retrospective analysis, to determine whether the model tends to over- or under-estimate changes in biomass in the years following when it was fit. Goodness of fit was based on visual comparisons between predicted and observed within-patch rates of change, and by comparing the root mean squared error (RMSE) of model predictions of productivity versus observed patch-specific productivities, using both held-out data sets.

Model Comparisons

All models accurately estimated within-patch productivity for test years during the period prior to shrimp declines (2006-08; Figure 22 red points), except in SFA 7, where all models consistently predicted a slower rate of decline than was observed. The lag-1 and simplified lag-1 autoregressive models gave the most accurate predictions of out-of-sample productivity for the years following population declines (Figure 22). The simplified lag-1 model gave as accurate or better predictions as the full lag-1 model for all SFAs for both the 2006-08 and 2016-18 period (Table 1) with fewer predictors, so it was adopted as the primary model for subsequent model comparisons and sensitivity tests.

The simplified lag-1 model was able to accurately estimate SFA-level instantaneous productivity rates for all SFAs, and for all three sets of data (training, testing prior to decline, and testing data after the decline; Figure 23). This model was also able to effectively capture the dynamics within most patches on the landscape (see Supplemental Figures). The most substantive misfits between model predictions and observed patch-level productivities occurred in shallow-water patches, such as patch V6 (Figure S1), V4 (Figure S2), V33 (Figure S10), or V70 (Figure S12), or small patches in deep water at the shelf edge, such as V17 (Figure S3), V44 (Figure S6) or

V55 (Figure S7). In all cases, these patches only account for a small fraction of total biomass in their respective SFAs, so this level of misfit is likely not an issue. However, it does indicate that model predictions in very shallow or deep regions should be given less weight than predictions in the core depth ranges for Northern Shrimp (200-500 m).

Model Robustness Checks

Several alternative model specifications were also tested to determine the robustness of the assumptions used to develop the simplified lag-1 model were. Three alternative models were compared with the simplified lag-1 model:

1. Single-species: This model only included a spatially-varying intercept and Northern Shrimp density effect, assuming time-independent (i.e., constant) maximum productivity. This was used as a null model to determine if the inclusion of ecosystem-based predictors substantially improved the model fit, both within and out-of-sample.
2. Winter NAO: Winter NAO (the average NAO index from December to March) has been identified as an important predictor of shrimp dynamics in Greenland (Hamilton et al. 2003), and multidecadal variability in the winter NAO correlates with North Atlantic sea surface temperature variability (Chelliah and Bell 2004). This index was also calculated for all years. To test if winter NAO was a better predictor than full-year NAO, we refit the simplified lag-1 model using winter NAO as a covariate.
3. Non-spatial: This model was used to determine if including spatial variability in recruitment improved model forecasts compared to a more typical single-stock approach. Northern Shrimp, Atlantic Cod, and other predator abundances were calculated for each SFA for each year by summing estimated densities multiplied by patch areas across patches. Productivity for each year was calculated by adding the SFA-level catch for that year to the biomass in the year. Then SFA-level productivity was regressed on SFA-level shrimp abundance, alternate predator abundance, and NAO, all lagged by 1 year, with SFA-specific slopes for shrimp and predator abundances, to account for the fact that both carrying capacities and the expected spatial overlap in shrimp with predator ranges should vary with SFA.

To compare the three sensitivity tests with the simplified lag-1 model on similar measurement scales, all models were used to estimate yearly productivities for each SFA for training and test data sets. Models were compared using RMSE (Table 2) and via visual comparison (Figure 25). Both groups of test data sets were pooled together for RMSE comparisons between sensitivity tests, as there were only six total test points to compare, and RMSE will tend to be a very noisy measure of fit in small data sets.

The simplified lag-1 model fit observed yearly productivities better than the single species model in all SFAs except 5 in the training data set, but was outperformed by the single species model in SFAs 4 and 5 in the test data set (Table 2). The winter NAO model fit approximately as well as the forecasting model in all SFAs in the training data, and slightly out-performed the forecasting model when predicting trends in the test data set (Table 2). However, the winter NAO term was not actually statistically significant in this model, indicating that the sign of the effect of the winter NAO term was uncertain. The non-spatial model had worse predictive performance than the simplified lag-1 model for all SFAs in the training data set, and worse predictive performance in SFA 4 and 5 compared to the simplified lag-1 model in the test data set. However, the non-spatial model did outperform the simplified lag-1 model in SFAs 6 and 7 in the test data set (Table 2).

Overall, the single-species model did a poorer job of predicting periods of rapid increase or decrease in SFA 6 and 7 (Figure 25, column 2), which is consistent with the evidence presented

previously that these stocks have undergone at least two large-scale changes productivity in this time series. The winter NAO model fit as well or better than the simplified lag-1 model (Figure 25, column 3). The non-spatial model tended to under-predict periods of both increase and declines in SFAs 4-6, and over-predict changes in productivity in SFA 7 (Figure 25, column 4). Although the simplified lag-1 model was outperformed by alternate models test in some incidences (e.g., multi-year lags, SFA 7 post-decline test data), the simplified lag-1 model was chosen for its relatively simplicity and overall fit and was adopted as the primary model for forecasting changes in this stock. This model was refit using data from all years to ensure that model parameters were estimated using all available data. This refit model was used to generate the remainder of the results in this report, and is hereafter referred to as the forecasting model.

The final forecasting model included terms for Atlantic Cod density, alternative predator density, NAO, a spatially varying intercept, and a spatially varying density-dependence term. The full equation describing the forecasting model is:

$$\log\left(\frac{D_{i,t} + C_{i,t}}{D_{i,t}}\right) = \hat{r}_i + \beta_i \cdot \text{shrimp density}_{i,t-1} + \\ \gamma_1 \cdot \text{cod density}_{i,t-1} + \gamma_2 \cdot \text{other predator density}_{i,t-1} + \\ \gamma_3 \cdot \text{NAO index}_{t-1} + \\ \epsilon_{i,t} \\ \epsilon_{i,t} \sim \sigma \cdot t(df)$$

Forecasting Model Parameters

The forecasting model showed substantial spatial variation in demographic parameters. Estimated growth-rate intercepts (Figure 24A) varied from 0.37 year^{-1} in SFA 7 to $>1.5 \text{ year}^{-1}$ in the northern edge of SFA 4 and in the center of SFA 5 (this being the assumed growth rate in the absence of all predation and harvest in a neutral NAO year). Estimated density-dependent effects (Figure 24B) varied from $-5 \times 10^{-4} \text{ kg}^{-1} \cdot \text{km}^2 \cdot \text{year}^{-1}$ in the center of SFA 5 to $-5 \times 10^{-5} \text{ kg}^{-1} \cdot \text{km}^2 \cdot \text{year}^{-1}$ in the south of SFA 4 and in regions in SFA 6 (where values closer to zero indicate weaker density dependence).

The estimated parameter for Atlantic Cod was $-3.7 \times 10^{-4} \text{ kg}^{-1} \cdot \text{km}^2 \cdot \text{year}^{-1}$ ($\pm 0.5 \cdot 10^{-4}$ 2 s.e.) (Figure 24C), meaning that an increase in cod density of $1 \text{ tonne} \cdot \text{km}^{-2}$ in a given patch would correspond to a decrease of 0.37 year^{-1} in instantaneous productivity in that patch. The estimated parameter for other predators was $-1.8 \times 10^{-5} \text{ kg}^{-1} \cdot \text{km}^2 \cdot \text{year}^{-1}$ ($\pm 1.8 \cdot 10^{-4}$ 2 s.e.) (Figure 24D), meaning that an increase in Redfish and Greenland Halibut density of $1 \text{ tonne} \cdot \text{km}^{-2}$ in a given patch would correspond to a decrease of 0.018 year^{-1} in instantaneous productivity. The estimated parameter for NAO was 0.12 year^{-1} (± 0.07 2 s.e.) (Figure 24E), which would result in shrimp instantaneous productivities being 0.24 year^{-1} higher in positive NAO years (indicating cold and fresh conditions) compared to negative NAO years.

The estimated degrees-of-freedom parameter (df) for the error term was 4.3, and the scale parameter (σ) was 0.4, implying the estimated variance of the per-patch residuals was 0.3 year^{-1} (as the variance of a t-distribution is equal to $\frac{df}{df-2} \cdot \sigma^2$). The low estimated df indicates that patch-specific surplus productivity levels showed significantly longer-than-Gaussian tails, indicating the possibility of unmodelled heterogeneity.

Model Sensitivity Tests

Several analyses were conducted to test how sensitive the forecasting model was to changes in the driving parameters (predator density and NAO).

The first test was a retrospective analysis to see what the model would have predicted for Northern Shrimp dynamics in the period before the start of the multispecies trawl survey. As there are no comparable biomass estimates for this time period, making it impossible to generate predicted rates of change prior to 1995, the forecasting model was instead used to predict the carrying capacity in different years, as a proxy for the maximum abundance of shrimp possible in that time period.

As there was a gear change between 1994 and 1995, which would impact the catchability of predator species (and thus the predicted effect on shrimp productivity rates), pre-1995 predator densities were scaled by an estimated catchability factor. These catchability factors were calculated by looking at a subset of the trawl data in the two years immediately before and after 1995 (i.e., 1993-96), using only trawls from SFA 6 and 7 (the only two SFAs that were consistently sampled during this period). This approach was adapted from the method used in Pedersen et al. (2017). Predator species weights from these data were modelled using a GAM with a Tweedie distribution for the error term, a MRF smoother term for patch (to model spatially varying patterns in predator density), and a random year effect (to model inter-year differences in biomass), plus a fixed survey effect, to model mean differences between 1993/94 and 1995/96. This estimated fixed effect was then used as a gear conversion factor, by multiplying predator densities prior to the gear change by the inverse of the conversion factor. The gear effect was estimated for Atlantic Cod to be 2.1 (i.e., catchability of cod in the Engel gear was half that of the Campelen gear), 3.4 for Redfish, and 2.5 for Greenland Halibut.

The forecasting model was used to estimate the time-varying carrying capacity K_t for each SFA by finding the shrimp density for each patch in each year that would result in the mean value of equation (5) equaling zero given the predictors for the patches in those years (i.e., Atlantic Cod density, alternative predator density, and NAO), and then multiplying all of the patch-level $K_{i,t}$ values by patch area and summing within each SFA. This was done for all years from 1995-2018 for all SFAs that had data, and for 1990-95 for SFA 6 and 7, to determine the model-predicted carrying capacity prior to the collapse of Atlantic Cod.

The model predicted that carrying capacities in SFA 6 and 7 were very low in 1990, and rose rapidly to reach a peak in 1995 (Figure 26). This carrying capacity was above estimated Northern Shrimp biomass until 2000 in SFA 6 and 2001 in SFA 7, but this is consistent with the fact that these stocks started at a very low density, and would take time to reach their carrying capacity. The modelled carrying capacities imply that SFA 7 should have started increasing in density prior to its first major increases in 2000, and indicated that it had declined substantially below its carrying capacity following 2010. This may be evidence of dependence of SFA 7 on SFA 6 for recruitment, as predicted by Le Corre et al. (2019), and may indicate the need for inclusion of inter-regional connectivity for predicting SFA 7 in future.

The forecasting model predicted that shrimp carrying capacity should have been zero in 1990 (Figure 26), when Atlantic Cod were last at a high level (the model uses cod biomass from 1989 as the predictor). This indicates that the model is likely overestimating either the effect of Atlantic Cod at very high cod densities, or is missing a low-density refuge effect for shrimp, as a carrying capacity of zero is inconsistent with the previously observed shrimp densities in these regions, which we estimated to be around 250,000 tonnes in these two SFAs in the same period based on diet information (Figure 4).

To test the sensitivity of the forecasting model to large changes in the predictor values, the forecasting model was used to predict the carrying capacity for each SFA using the covariates for 2019 (i.e., covariates from data collected in 2018), and for the same data but with predator abundances and NAO scaled by fixed levels. Predator abundances were varied from -75% of 2018 levels to +300% (four times) their densities in 2018, and NAO index values for the current year, +1, 0, and -1 were tested.

The model predicted that doubling the current density of predators would substantially negatively affect the carrying capacity for Northern Shrimp in SFA 6 and 7, with the largest effects in SFA 6 (Figure 27). It would have a smaller impact in SFA 5, and an almost unnoticeable effect on abundances in SFA 4, indicating that at current predator densities, SFA 4 Northern Shrimp is not under strong top-down control. Large swings in the NAO index (from its 2018 level of 1.08 to a low index of -1, close to the minimum observed level of -1.15) were predicted to have substantial effects on carrying capacity in all four regions. This sensitivity test also indicated that predator densities 300% higher than current (i.e., four times the present density) would lead to zero carrying capacities in SFA 6, regardless of NAO.

This sensitivity analysis is consistent with the first sensitivity analysis, indicating that the forecasting model is likely overestimating the effects of very high predator densities, and it may be overestimating the effect very large NAO swings. As such, it is recommended that this model be re-evaluated if predator densities increase above more than 50% their current abundances, or if the NL shelves undergo another extensive period of warming or cooling.

DISCUSSION

SCIENTIFIC UNCERTAINTIES

This proposed model incorporates the most current ecological knowledge of the state of these stocks. However, there are several outstanding scientific questions that could affect model predictions.

Stock Structure Dynamics

The proposed assessment model focuses on total productivity, and does not partition growth rates into size classes or life-stages. Further, it does not attempt to measure whether changes in ecosystem variables result in changes in patterns of recruitment dynamics, individual growth over time, or mortality rates. Size-structured models have been developed for the Northern Shrimp stock in the Gulf of Maine (Cao et al. 2016a, 2016b) that incorporate dynamics of growth, mortality, and recruitment, including the effect of ecosystem drivers such as predation on mortality; this approach forms the core of the Gulf of Maine Northern Shrimp assessment (Hunter et al. 2018). However, this model is not directly transferable to NL stocks, as it is parameterized for very different environmental conditions and does not include mechanisms for larval or adult transport between regions.

Fitting this kind of model is challenging for NL stocks, as they do not typically show discrete cohorts of recruits moving through the population over time, and the exact patterns of movement of adult shrimp within and among regions over time is currently poorly understood. Currently, DFO is partnering with academia in an attempt to develop a Bayesian length-structured model of these stocks, with the goal of partitioning effects of fishing pressure, predation, and bottom-up environmental drivers on recruitment, individual growth, and mortality in these stocks. However, this model is currently not reliable enough for assessment purposes. If a reliable version of this model is developed, it may be used to generate stock predictions in future assessments.

Catchability

One of the most substantial uncertainties is the catchability of Northern Shrimp in the RV trawl survey. Currently, both Ogmap and GAM population estimates assume that all shrimp that occurred in the volume swept by the trawl were caught. As shrimp spend at least a portion of time in the water column away from the benthos feeding, the RV survey is likely missing at least a fraction of the total available population. Further, the RV trawl survey does not seem to effectively capture Northern Shrimp below 15 mm in size, meaning that new recruits are not well sampled.

As long as catchability does not depend on density, this will not affect estimated per-unit-biomass rates of change, as these metrics depend on the ratio between biomass estimates in any two years, rather than the absolute value. However, low catchability would imply that current biomass estimates would be underestimating the true population size, and thus overestimating the impacts of fishing on productivity.

There is currently no externally validated metric of gear catchability, so it has to be assumed to be equal to one. We recommend further research on this issue be undertaken, and estimates of catchability could readily be worked in to the model developed here.

Predation Rates on Northern Shrimp

The SPM proposed in this document relies on the abundance of Atlantic Cod, Deepwater Redfish, and Greenland Halibut in trawl RV surveys as a proxy for the effects of the entire predator field on Northern Shrimp. Atlantic Cod, Greenland Halibut, and Redfish were chosen as the primary metrics as these species have been consistently sampled throughout the assessment period, shown large-scale population changes, and are readily identifiable, so catches from the NSRF survey are the most likely to be comparable with fall RV catches. It is noteworthy, that the partial effect of Atlantic Cod is much stronger (~10x) than the partial effect of other predators, indicating that Atlantic Cod have a strong and disproportionate effect on shrimp abundance. The significant effect of Atlantic Cod on shrimp abundance has also been noted in Iceland (Björnsson et al. 2017). However, a wide range of groundfish species are known to feed on shrimp, and many of these species have been fluctuating over different time scales than these three species (Pedersen et al. 2017). Further, the SPM assumes that instantaneous mortality of shrimp depends linearly on both predator abundance and shrimp abundance, which ignores the potential for predator satiation when shrimp densities are locally high, or reduced predation rates at very low shrimp densities due to refuge effects or other mechanisms (Walters and Martell 2004).

This is one potential explanation for why the model predicts much lower abundance of Northern Shrimp than historical surveys indicate in 1990, as Atlantic Cod levels may still have been very high in that time period. If predator levels increase substantially, it is recommended that new functional responses be tested to prevent the model from forecasting consistent negative population growth rates. A current research project at DFO has been focusing on estimating spatial variation in predation rates of multiple groundfish species on Northern Shrimp across all Canadian Atlantic waters. This research is still in progress, but results from it may be incorporated into future assessment models for these stocks, and developing new predation functional responses.

This modelling also does not include the effects of other Northern Shrimp predators, such as marine mammals. Prior research has noted that Harp Seals prey on Northern Shrimp (although generally Striped Shrimp are a more common prey item; Parsons 2005). It is unlikely that predation by Harp Seals was the primary cause of declining shrimp abundances, as seal abundances were increasing at the same time as shrimp populations in the 1980s and 1990s,

and had largely stabilized before the beginning of the decline in Northern Shrimp in SFA 6 and 7 (DFO 2014). However, fluctuations in Harp Seals and other marine mammal predators may result in changes Northern Shrimp stocks in future, as environmental conditions continue to change, and the higher abundance of seals currently compared to the 1980s may mean that equilibrium biomass of shrimp could be lower than it was in the 1980s if groundfish predators increase to their prior abundances.

Movement of Larval and Adult Shrimp Between Regions

Dispersal simulations for the four regions indicate that there should be substantial transport of larvae from SFAs 4 and 5 to SFA 6, and from SFA 6 to SFA 7. However, the recruitment index used in the SPMs had poor predictive performance relative to other ecosystem indicators. This could be caused by several factors:

1. The current growth models only track total growth in population, rather than explicitly following cohorts of recruits; as such, recruitment effects may be obscured by other changes in shrimp stock structure. Ongoing work on developing length-structured ecosystem models for these stocks may improve the fit of this index.
2. The poor fit of this index may be a result of the lack of biomass estimates from populations upstream of SFA 4. The current recruitment model ignores populations north of SFA 4, and as such likely underestimates the number of recruits available for SFA 4 and 5.
3. There may be a mismatch between where Northern Shrimp stocks are located at the time of the survey versus where the populations are when females release eggs. Northern Shrimp are known to undergo seasonal movements, but the scale and timing of those movements in SFA 4-7 are poorly understood.
4. It may represent a model misfit, where simulated patterns of larval dispersal do not match up with true dispersal trajectories.

Beyond larval dispersal, very little is known about the small-scale (patch-to-patch) movement of post-larval shrimp, either via seasonal migrations or via dispersive movement. The potential for post-larval movement is currently implicitly included in the spatial smoother models for population density, as the MRF penalty in the smoother implies that changes in population density in one patch should predict changes in nearby patches. However, substantially more work is needed to understand post-larval movement in these stocks.

The forecasting model developed in this report does not explicitly include inter-regional connectivity. Connectivity could be included in the model if it could be demonstrated that over-exploitation in SFA 4-5 leads to downstream effects on growth rates in SFA 6-7. However, there is currently only limited evidence to suggest that recruitment from upstream is limiting population growth rates.

Ecosystem Drivers in SFA 4 and 5

The proposed SPM is most accurate at predicting biomass dynamics in SFA 6 and 7, where observed groundfish abundances are highest. Both SFA 4 and 5 have shown multiple years of declines in biomass that are not predicted by the model, including significant declines in the most recent years (2016-18). The drivers of these declines are not well understood. More research into environmental conditions affecting these stocks is needed.

FUTURE MODEL DEVELOPMENT DIRECTIONS

The forecasting model developed in this report should not be viewed as a final tool, but instead the first version of a set of predictive models to be developed over time. As noted above, there are still substantial questions about how to include known important ecosystem effects, such as larval or adult movement, and nonlinear predation effects. Further, the current model does not include any bottom-up effects (i.e., food, shelter, or disease) on Northern Shrimp production except the implied effect of climate via the NAO index. While the NAO index is strongly predictive of North Atlantic ocean climate (Chelliah and Bell 2004), it is still not a direct measurement of current climate conditions that may be affecting shrimp production.

This model could be improved using several techniques. The first would be to include the size structure of Northern Shrimp, as has been done in the Gulf of Maine (Cao et al. 2016b; Hunter et al. 2018). This would allow explicitly modelling spatial recruitment dynamics and size-specific effects of fishing pressure on stock productivity. As the size structure of Northern Shrimp in SFAs 4–7 has remained stable over the last two decades, it may be difficult to parameterize the size-specific mortality and growth terms required for this type of model in the absence of very strong prior assumptions about growth dynamics.

The second way to extend this model would be to include explicit estimates of predator consumption based on predator diet data currently collected as part of the trawl survey. This would require an estimate of the amount of biomass predators consume per unit time, and a functional response model that can predict how this amount would vary with predator and prey density.

REFERENCES CITED

- Barraquand, F., and D.J. Murrell. 2013. Scaling up predator–prey dynamics using spatial moment equations. *Meth. Ecol. Evol.* 4(3):276–289.
- Björnsson, B., Burgos, J.M., Sólmundsson, J., Ragnarsson, S.Á., Jónsdóttir, I.G., and U. Skúladóttir. 2017. Effects of cod and haddock abundance on the distribution and abundance of northern shrimp. *Mari. Ecol. Prog. Ser.* 572:209–221.
- Blangiardo, M., and M. Cameletti. 2015. Spatial and spatio-temporal Bayesian models with R - INLA. John Wiley & Sons, West Sussex, UK.
- Brodie, W. 1996. A Description of the 1995 Fall Groundfish Survey in Division 2J3KLMNO. NAFO SCR Doc 27: N2700.
- Brosset, P., Bourdages, H., Blais, M., Scarratt, M., Plourde, S., and Handling Editor: Emory Anderson. 2018. Local environment affecting northern shrimp recruitment: A comparative study of Gulf of St. Lawrence stocks. *ICES J. Mar. Sci. fsy185-fsy185*.
- Cao, J., Chen, Y., and R.A. Richards. 2016a. Improving assessment of *Pandalus* stocks using a seasonal, size-structured assessment model with environmental variables. Part II: Model evaluation and simulation. *Can. J. Fish. Aqua. Sci.* 74(3):363–376.
- Cao, J., Chen, Y., and R.A. Richards. 2016b. Improving assessment of *Pandalus* stocks using a seasonal, size-structured assessment model with environmental variables. Part I: Model description and application. *Can. J. Fish. Aqua. Sci.* 74(3):349–362.
- Carruthers, E.H., Parlee, C.E., Keenan, R., and P. Foley. P. 2019. Onshore benefits from fishing: Tracking value from the northern shrimp fishery to communities in Newfoundland and Labrador. *Marine Policy* 103:130–137.

-
- Chelliah, M., and G.D. Bell. 2004. Tropical multidecadal and interannual climate variability in the NCEP–NCAR reanalysis. *J. Clim.* 17(9):1777–1803.
- Colbourne, E., Holden, J., Snook, S., Han, G., Lewis, S., Senciall, D., Bailey, W., Higdon, J., and N. Chen. 2017. Physical oceanographic conditions on the Newfoundland and Labrador shelf during 2016. NAFO SCR Doc. 2017/079.
- DFO. 2009. [Proceedings of the precautionary approach workshop on Canadian shrimp and prawn stocks and fisheries; November 26-27, 2008](#). DFO Can. Sci. Advis. Sec. Proceed. Ser. 2008/031.
- DFO. 2014. [Status of Northwest Atlantic Harp Seals, *Pagophilus groenlandicus*](#). DFO Can. Sci. Advis. Sec. Sci. Advis. Rep. 2014/011.
- DFO. 2017. [Review of reference points used in the precautionary approach for Northern Shrimp \(*Pandalus borealis*\) in Shrimp Fishing Area 6](#). DFO Can. Sci. Advis. Sec. Sci. Resp. 2017/009.
- DFO. 2018a. [Stock assessment of Northern cod \(NAFO Divisions 2J3KL\) in 2018](#). DFO Can. Sci. Advis. Sec. Sci. Advis. Rep. 2018/038.
- DFO. 2018b. [Annex J - Rebuilding plan for Northern shrimp SFA 6](#).
- DFO. 2018c. [Integrated Fisheries Management Plan-Northern shrimp and striped shrimp- Shrimp fishing areas 0, 1, 4-7, the Eastern and Western Assessment Zones and North Atlantic Fisheries Organization \(NAFO\) Division 3M](#).
- DFO. 2019. [An Assessment of Northern Shrimp \(*Pandalus borealis*\) in Shrimp Fishing Areas 4–6 and of Striped Shrimp *Pandalus montagui*\) in Shrimp Fishing Area 4 in 2018](#). DFO Can. Sci. Advis. Sec. Sci. Advis. Rep. 2019/027.
- Efron, B. 1982. The jackknife, the bootstrap and other resampling plans. Society for Industrial; Applied Mathematics, Philadelphia, PA, USA.
- Evans, G., Parsons, D., Veitch, P., and D. Orr. 2000. A local-influence method of estimating biomass from trawl surveys, with Monte Carlo confidence intervals. *J. North. Atl. Fish. Sci.* 27:133–138.
- Fortin, M.-J., and M.R.T. Dale. 2005. Spatial analysis: A guide for ecologists. Cambridge University Press, Cambridge.
- Hamilton, L.C., Brown, B.C., and R.O. Rasmussen. 2003. West Greenland’s cod-to-shrimp transition: Local dimensions of climatic change. *Arctic* 56(3):271–282.
- Hunter, M., Whitmore, K., Atwood, R., Richards, A., Miller, A., Drew, K., and M. Ware. 2018. Assessment report for Gulf of Maine Northern Shrimp-2018. Northern Shrimp Technical Committee Stock Assessment Report, Atlantic States Marine Fisheries Commission.
- Hvingel, C., and M.C. Kingsley. 2006. A framework to model shrimp (*Pandalus borealis*) stock dynamics and to quantify the risk associated with alternative management options, using Bayesian methods. *ICES J. Mar. Sci.* 63(1):68–82.
- Jorde, P.E., Søvik, G., Westgaard, J.-I., Orr, D., Han, G., Stansbury, D., and K.E. Jørstad. 2015. Genetic population structure of northern shrimp, *Pandalus borealis*, in the Northwest Atlantic: adaptation to different temperatures as an isolation factor. *Mole. Ecol.* 24(8):1742–1757.

-
- Lecomte, J.-B., Benoît, H.P., Ancelet, S., Etienne, M.-P., Bel, L., and E. Parent. 2013. Compound Poisson-gamma vs. Delta-gamma to handle zero-inflated continuous data under a variable sampling volume. *Meth. Ecol. Evol.* 4(12):1159-1166.
- Le Corre, N., Pepin, P., Han, G., Ma, Z., and P.V.R. Snelgrove. 2019. Assessing connectivity patterns among management units of the Newfoundland and Labrador shrimp population. *Fish. Ocean.* 28(2):183-202.
- Le Corre, N., Pepin, P., Burmeister, A., Walkusz, W., Skanes, K., Wang, Z., Brickman, D., and P.V.R. Snelgrove. 2020. Larval connectivity of northern shrimp (*Pandalus borealis*) in the Northwest Atlantic. *Can. J. Fish. Aqua. Sci.* 77(8):1332-1347.
- Lilly, G.R., Parsons, D.G., and D.W. Kulka. 2000. Was the increase in shrimp biomass on the northeast Newfoundland shelf a consequence of a release in predation pressure from cod? *J. North. Atl. Fish. Sci.* 27:45-62.
- Marra, G., and S.N. Wood. 2012. Coverage properties of confidence intervals for generalized additive model components. *Scand. J. Stat.* 39(1):53-74.
- McCallum, B., and S. Walsh. 1996. Groundfish survey trawls used at the Northwest Atlantic Fisheries Centre, 1971-present. NAFO SCR Doc. 96/50.
- Parsons, D.G. 1982. Biological characteristics of northern shrimp (*Pandalus borealis* Kroyer) in areas off Labrador. Master's thesis, Memorial University, St. John's, NL, Canada.
- Parsons, D.G. 2005. Predators of northern shrimp, *Pandalus borealis* (Pandalidae), throughout the North Atlantic. *Mar. Bio. Res.* 1(1):48-58.
- Pebesma, E. 2018. Simple features for R: Standardized support for spatial vector data. *The R Journal.*
- Pedersen, E.J., Thompson, P.L., Ball, R.A., Fortin, M.-J., Gouhier, T.C., Link, H., Moritz, C., Nenzen, H., Stanley, R.R.E., Tararu, Z.E., Gonzalez, A., Guichard, F., and P. Pepin. 2017. Signatures of the collapse and incipient recovery of an overexploited marine ecosystem. *Royal Society Open Science* 4(7).
- Pepin, P., Maillet, G., Fraser, S., Doyle, G., Robar, A., Shears, T., and G. Redmond. 2017. [Optical, chemical, and biological oceanographic conditions on the Newfoundland and Labrador Shelf during 2014-2015.](#) DFO Can. Sci. Advis. Sec. Res. Doc. 2017/009.
- Power, D., Ings, D., Rideout, R., and B.P. Healey. 2016. Performance and description of Canadian multi-species bottom trawl surveys in NAFO Subarea 2 + Divisions 3KLMNO, with emphasis on 2014-2015. NAFO SCR Doc. 16/28.
- R Core Team. 2018. R: A language and environment for statistical computing. R Foundation for Statistical Computing, Vienna, Austria.
- Rideout, R., and D. Ings. 2018. Temporal and spatial coverage of Canadian (Newfoundland and Labrador Region) spring and autumn multi-species RV bottom trawl surveys, with an emphasis on surveys conducted in 2017. NAFO SCR Doc. 18/017.
- Rose, G.A., and S. Rowe. 2015. Northern cod comeback. *Can. J. Fish. Aqua. Sci.* 1789-1798.
- Shumway, S.E., Perkins, H.C., Schick, D.F., and A.P. Stickney. 1985. Synopsis of biological data on the pink shrimp, *Pandalus borealis* Kroyer, 1838. NOAA Technical Report.

-
- Tamdrari, H., Benoît, H.P., Hanson, J.M., Bourdages, H., and J.C. Brêthes. 2018. Environmental associations and assemblage structure of shrimp species in the Gulf of St. Lawrence (Canada) following dramatic increases in abundance. *Mar. Ecol. Prog. Se.* 596:95-112.
- Walters, C.J., and S.J.D. Martell. 2004. *Fisheries ecology and management*. Princeton University Press, Princeton, N.J., U.S.A.
- Wood, S.N. 2006a. Low-rank scale-invariant tensor product smooths for generalized additive mixed models. *Biometrics* 62(4): 1025-1036.
- Wood, S.N. 2006b. On confidence intervals for generalized additive models based on penalized regression splines. *Australian & New Zealand J. Stat.* 48(4):445-464.
- Wood, S.N. 2011. Fast stable restricted maximum likelihood and marginal likelihood estimation of semiparametric generalized linear models. *J. Roy. Stat. Soc. Series B (Statistical Methodology)* 73(1):3-36.
- Wood, S.N. 2017. *Generalized Additive Models: An Introduction with R*, 2nd Edition. *In 2nd editions*. CRC Press, Boco Raton, FL.

TABLES

Table 1: Out-of-sample goodness of fit (RMSE) for four tested model specifications.

	Lag-1 (full)	Lag-1 (simplified)	Multi-year lags	Spatially varying lag-1
Pre-decline test data (2006-08)				
SFA 4	0.70	0.69	0.84	0.77
SFA 6	0.52	0.47	0.56	0.52
SFA 7	0.52	0.51	0.63	0.57
Post-decline test data (2016-18)				
SFA 4	0.93	0.99	1.03	1.18
SFA 5	0.61	0.60	0.68	0.64
SFA 6	0.60	0.56	0.62	0.55
SFA 7	0.80	0.82	0.73	0.79

Table 2: SFA-level out-of-sample goodness of fit (RMSE) for model sensitivity comparisons.

	Forecasting	Single species	Winter NAO	Non-spatial
Training data				
SFA 4	0.29	0.32	0.32	0.43
SFA 5	0.27	0.24	0.28	0.30
SFA 6	0.14	0.20	0.14	0.22
SFA 7	0.38	0.47	0.41	0.52
Test data (2006-08, 2016-18)				
SFA 4	0.28	0.22	0.24	0.39
SFA 5	0.33	0.28	0.31	0.37
SFA 6	0.30	0.36	0.28	0.17
SFA 7	0.55	0.57	0.54	0.36

FIGURES

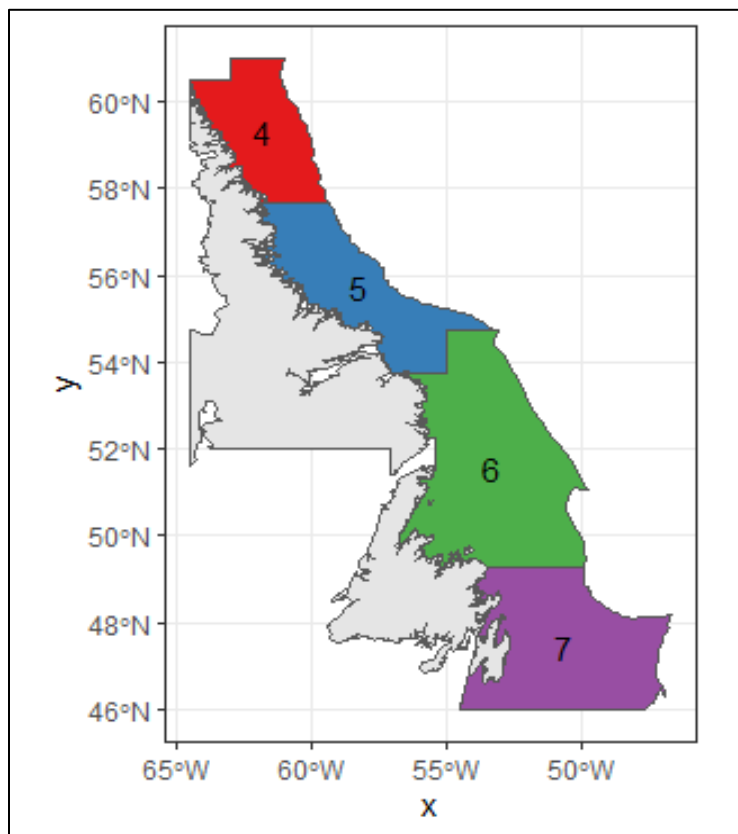


Figure 1: Map of Northern Shrimp management areas on the Newfoundland and Labrador Shelves. SFA 7, on the Grand Banks, is included for clarity, but is managed under a separate NAFO management plan.

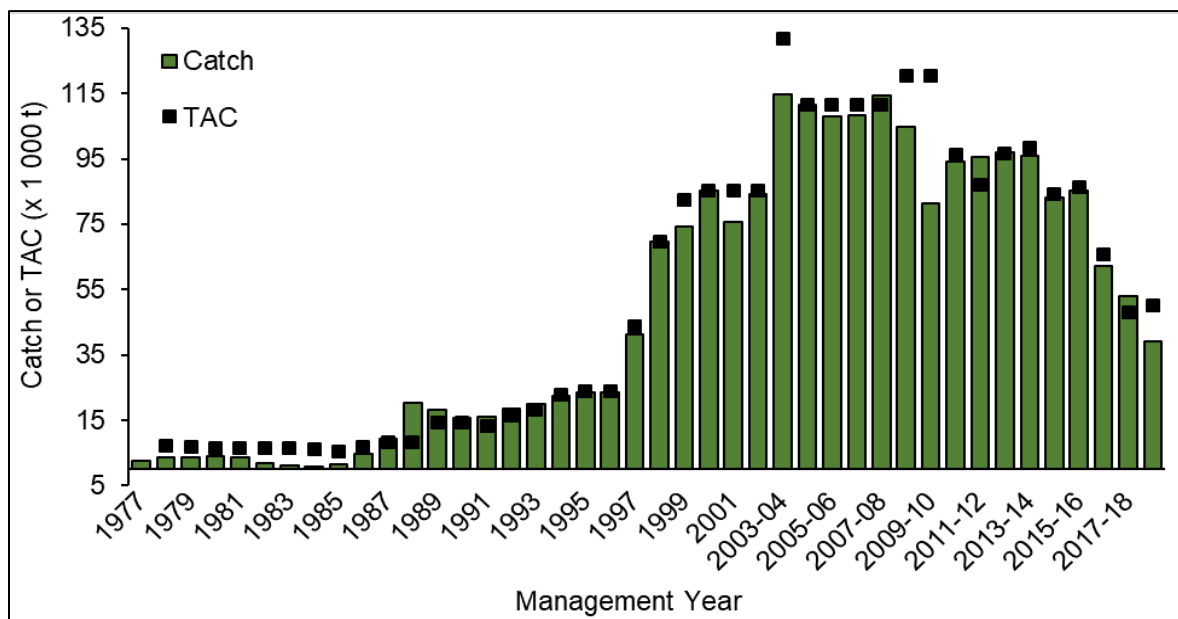


Figure 2: Historical Northern Shrimp catches and TACs (SFAs 4-6 combined) for the period 1977-2018/19. Catches for 2018/19 are preliminary as of February 7, 2019.

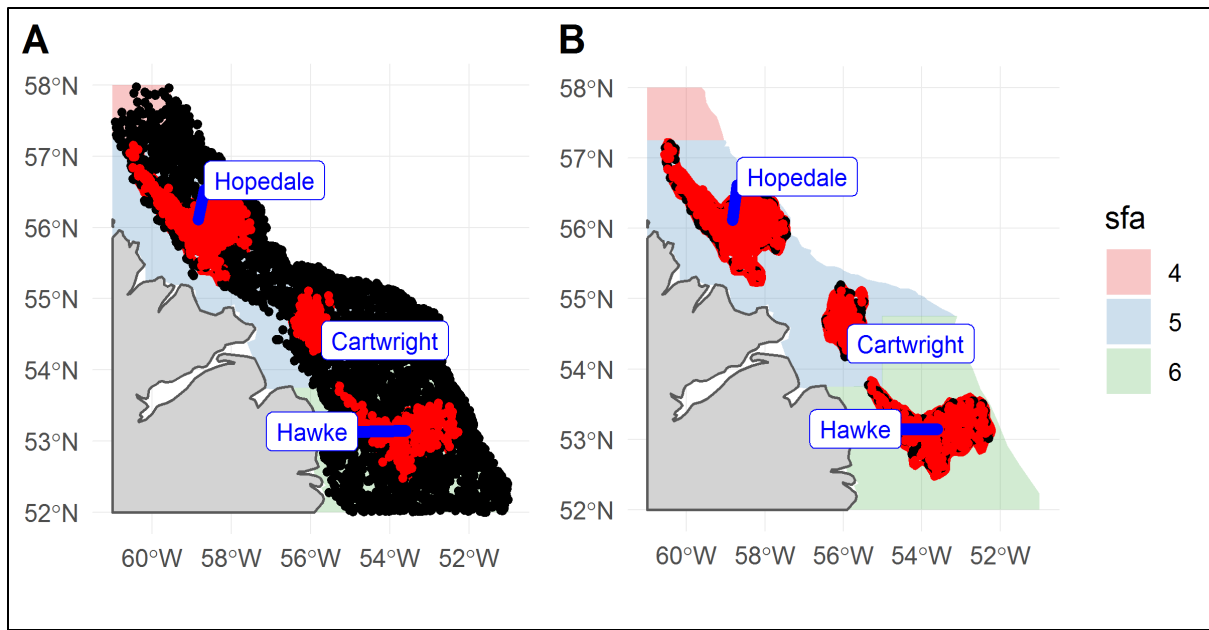


Figure 3: A) Distribution of historic and current RV trawls around the three channels with historical trawl data. B) Distribution of matched historic and current RV surveys for comparative time series analysis. Red points indicate historical trawls, and black points indicate locations of trawls from the current RV survey.

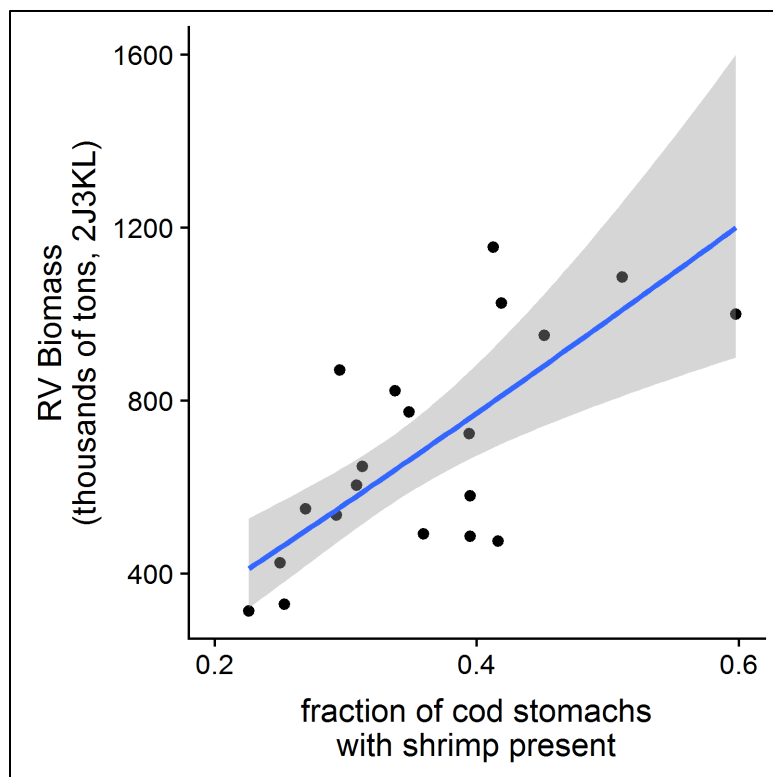


Figure 4: Regression of RV biomass of Northern Shrimp in SFA 6 on fraction of Atlantic Cod diets with shrimp present. Blue line represents estimated relationship (GLM regression of biomass on stomach fraction, assuming Tweedie-distributed biomass). Grey band indicates 95% CI for the regression relationship.

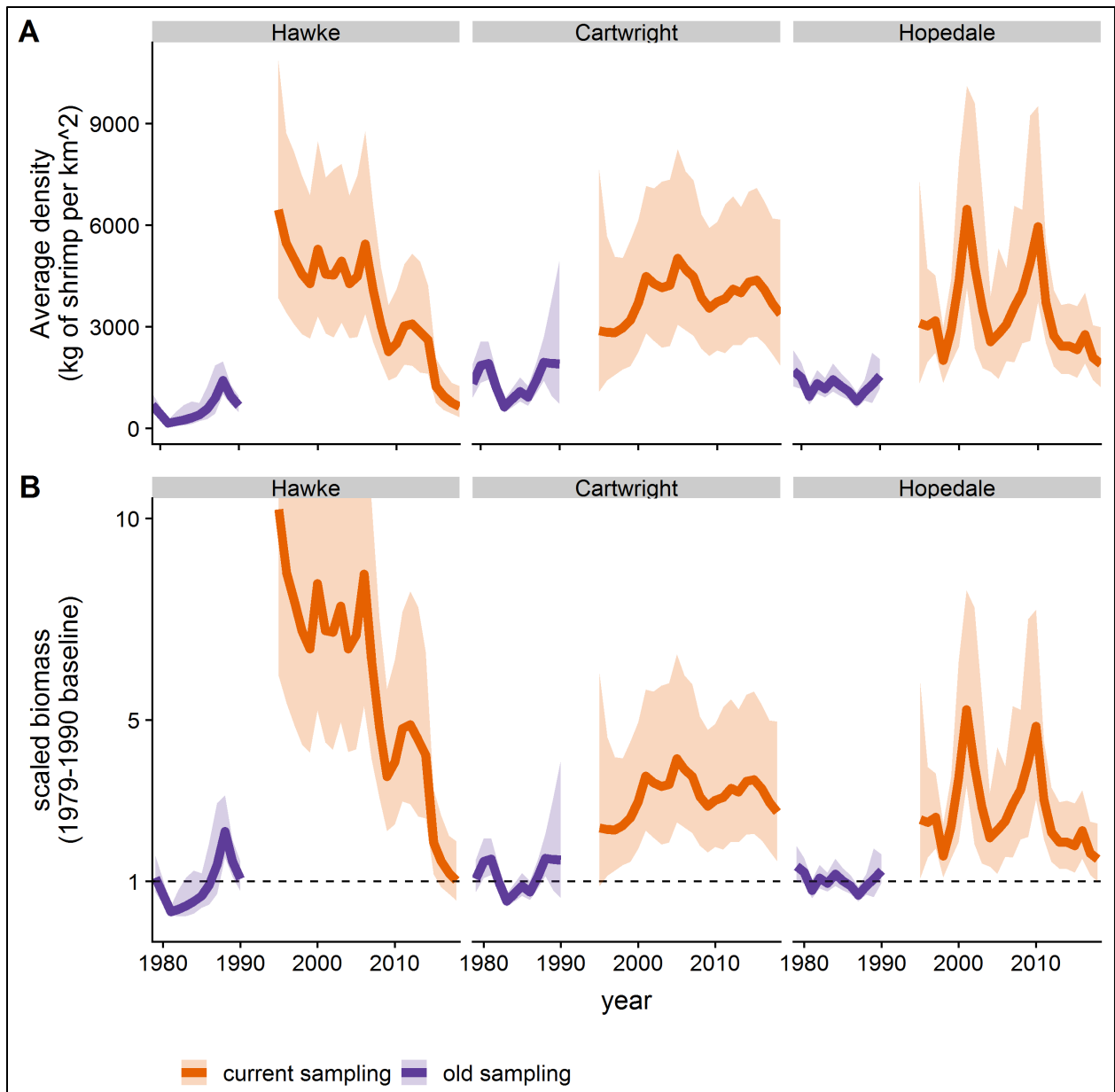


Figure 5: Time series of estimated Northern Shrimp density in three focal channels before and after start of the multispecies RV survey based on matched trawl surveys. A) Estimated density under historical (purple) and current (orange) sampling regimes, with lines indicating estimated mean density and ribbons indicating 95% CIs. B) Scaled density estimates to determine magnitude of change between 1990 and 1995. Time series were scaled by dividing all observations by the average value from 1980-90. Dashed line indicates the reference level.

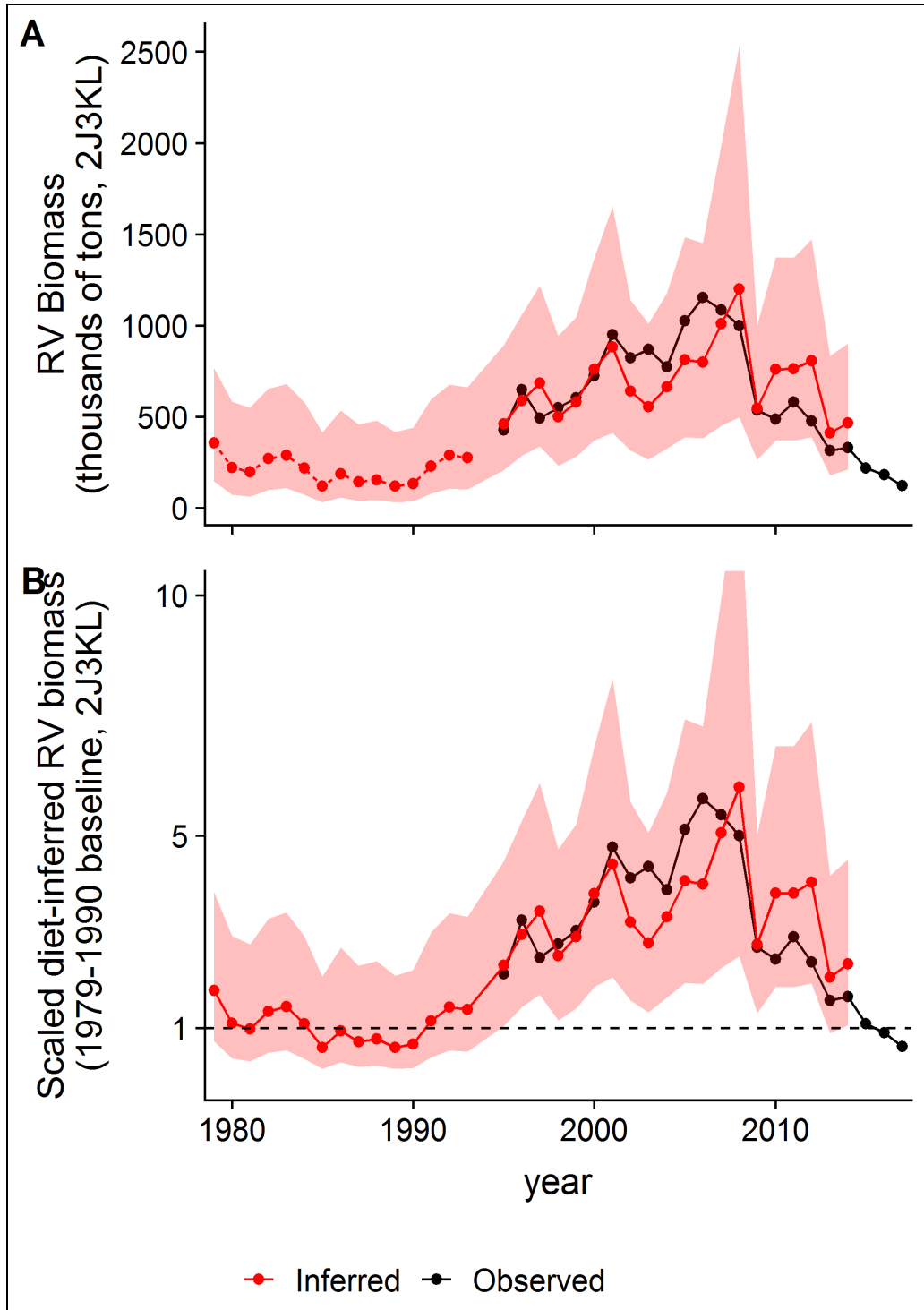


Figure 6: Time series of estimated Northern Shrimp density in SFA 6 before and after start of the RV survey, based on biomass inferred from cod diets. A) Observed RV biomass (black) and biomass inferred from diets (red), with line indicating mean of the inferred relationship and ribbon illustrating the 95% CI. Dotted line indicates points where no multispecies RV biomass estimate was available. B) Scaled diet-based biomass estimates to determine magnitude of change between 1990 and 1995. Time series were scaled by dividing all observations in A) by their average value from 1980-90.

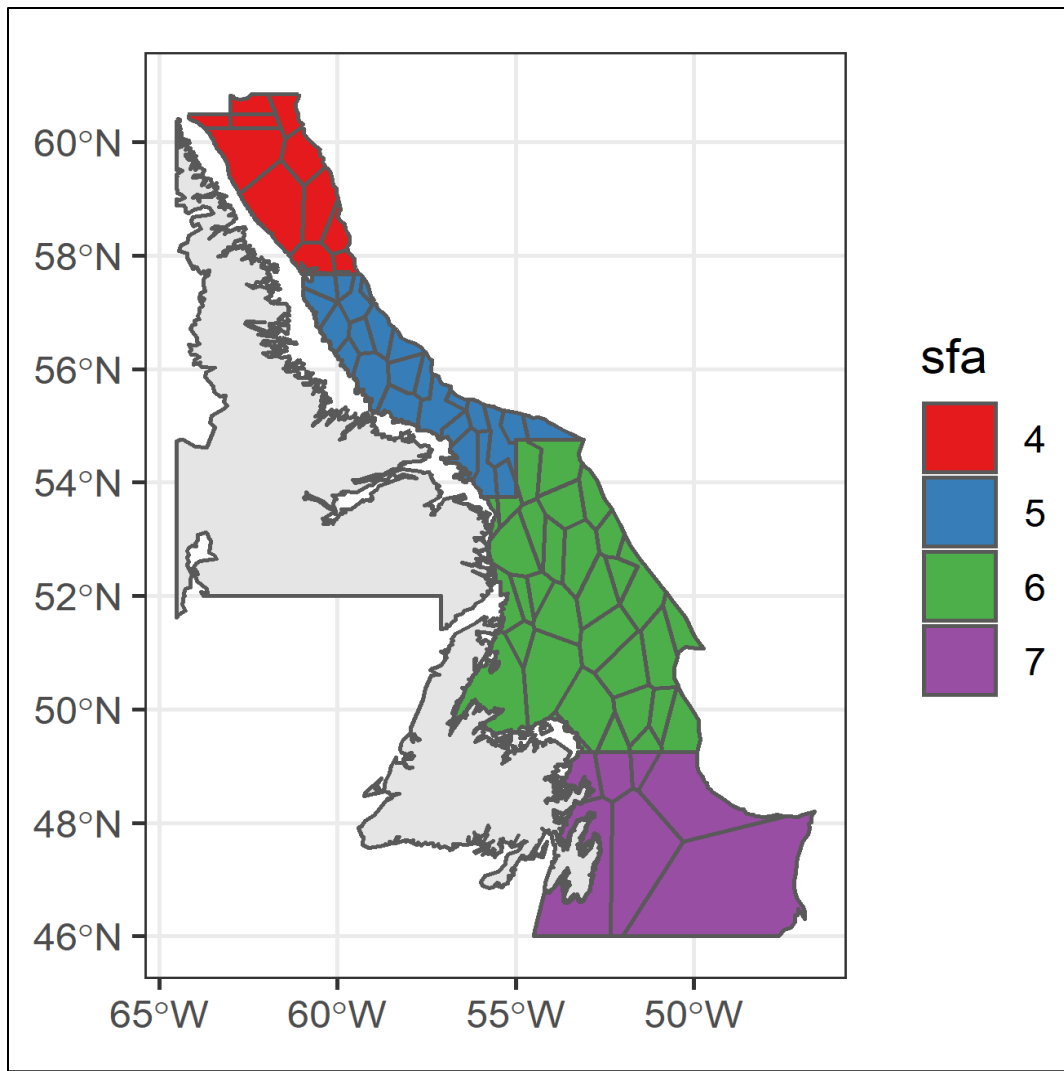


Figure 7: Voronoi-tessellation-based patches used for spatially structured analyses, colored by SFA.

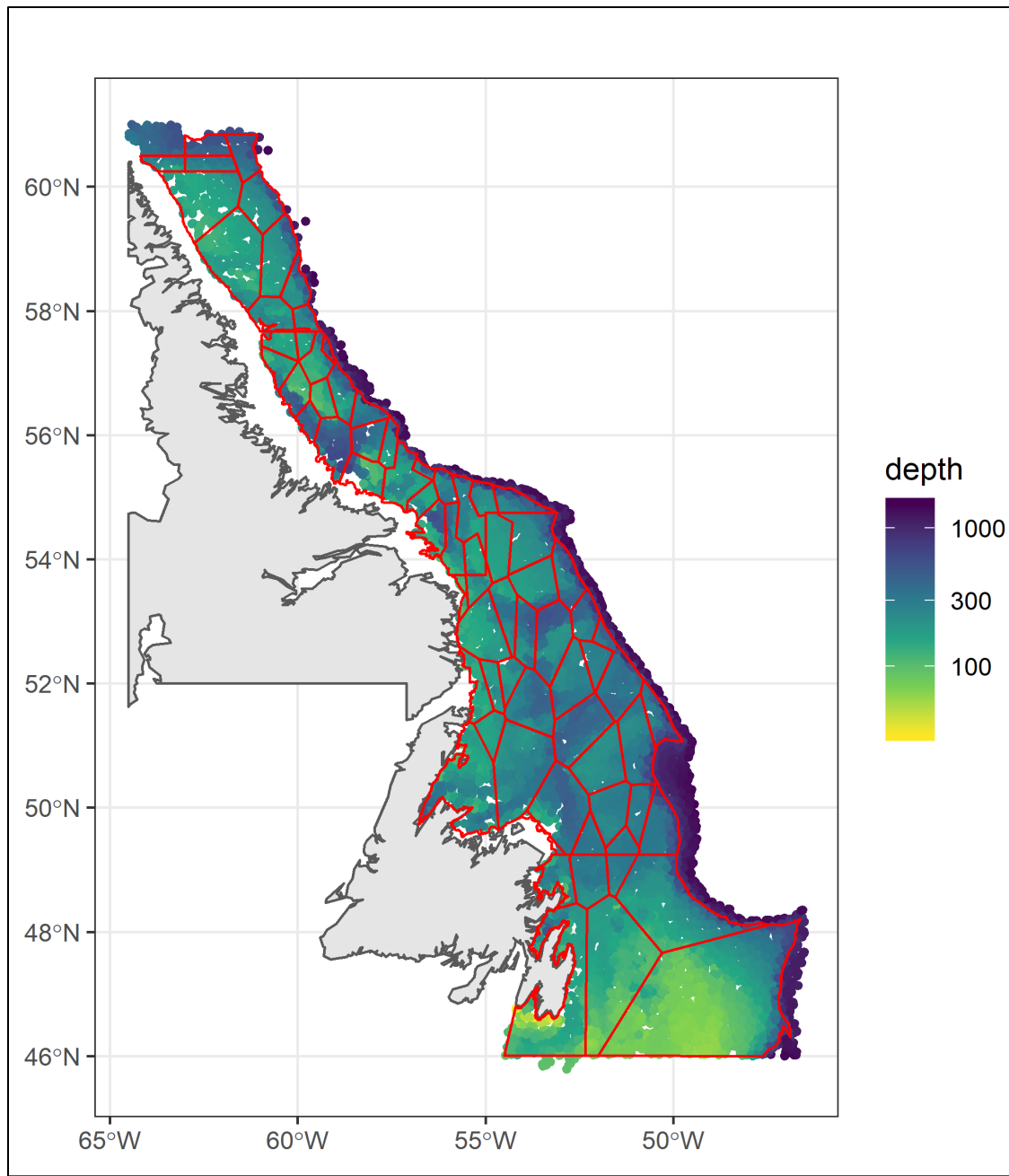


Figure 8: Voronoi patches with trawl depth distribution. Red lines indicate patch boundaries. Colours represent trawl depths, with yellow colours corresponding to shallower depths and blue to deeper ones (note that the depth color scale is log-scaled to better illustrate contrasts). Colours cover all RV survey locations from 1995-2016, including summer survey data.

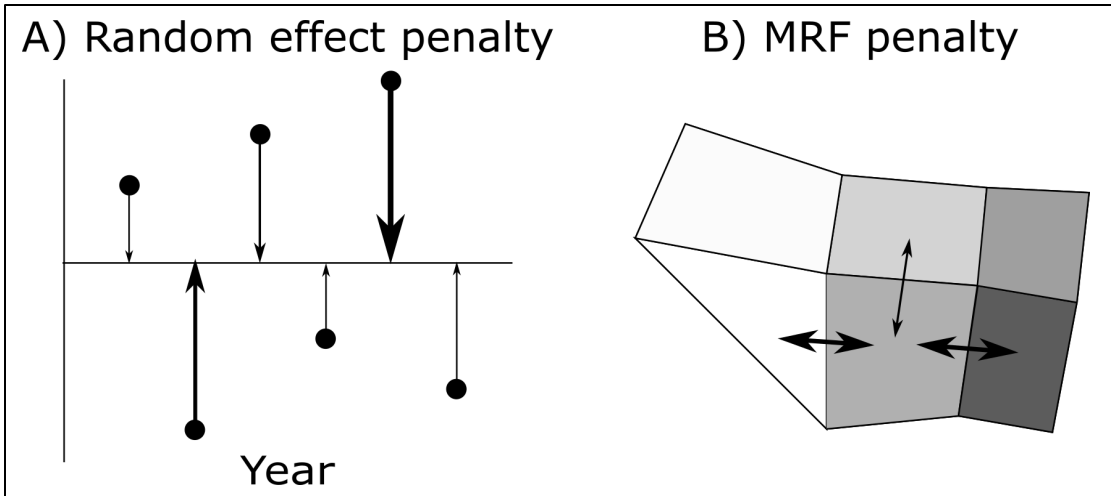


Figure 9: Illustration of how penalty terms work to smooth estimates towards one another. For (A) random effect smoothers, all coefficients are penalized toward the global mean; the size of the arrow denotes the strength of the penalty applied to each coefficient. (B) For MRF penalties, all terms are penalized toward the average of their immediate neighbours; for example, estimates toward the lower middle grey polygon (where the color denotes the fitted parameter value) would be penalized towards its three adjacent polygons, denoted by arrows; the penalty will be stronger for the neighbours to the left and right that differ strongly in value from the middle polygon, compared to polygon above the focal one which has a very similar value. These neighbours would also be penalized symmetrically toward the grey polygon, as well as to their other immediate neighbours.

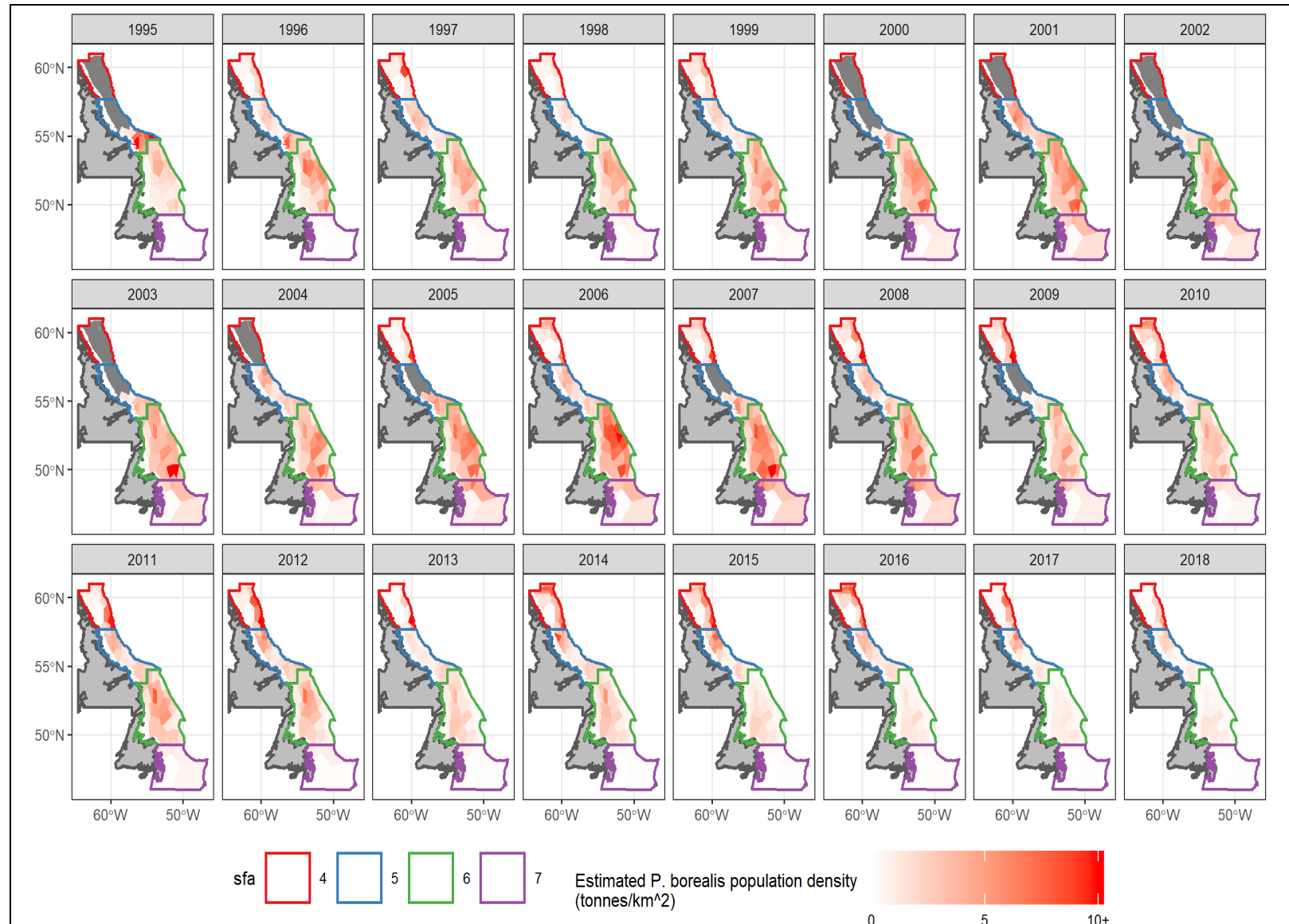


Figure 10: Spatial distributions of Northern Shrimp density in tonnes per square km, with darker colors indicating lower density, and lighter colors indicating higher densities. Dark grey polygons indicate areas where data were missing for a given year.

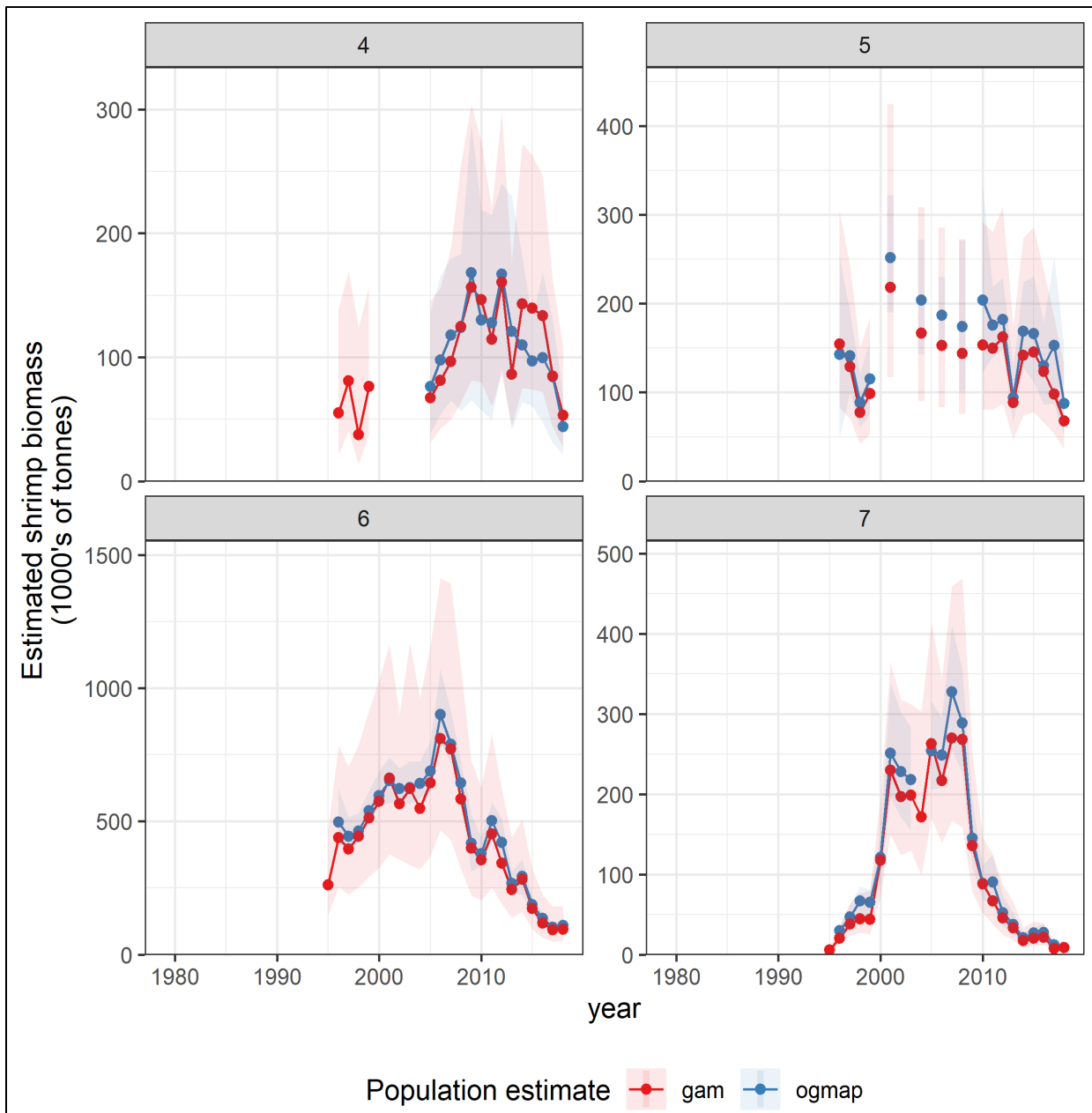


Figure 11: Comparison of GAM smoothed biomass versus prior Ogmap estimates. Red points and lines indicate yearly means estimated by the GAM model, and blue points and lines indicate estimates from the current Ogmap estimation approach. Colored ribbons indicate 95% CIs for both methods.

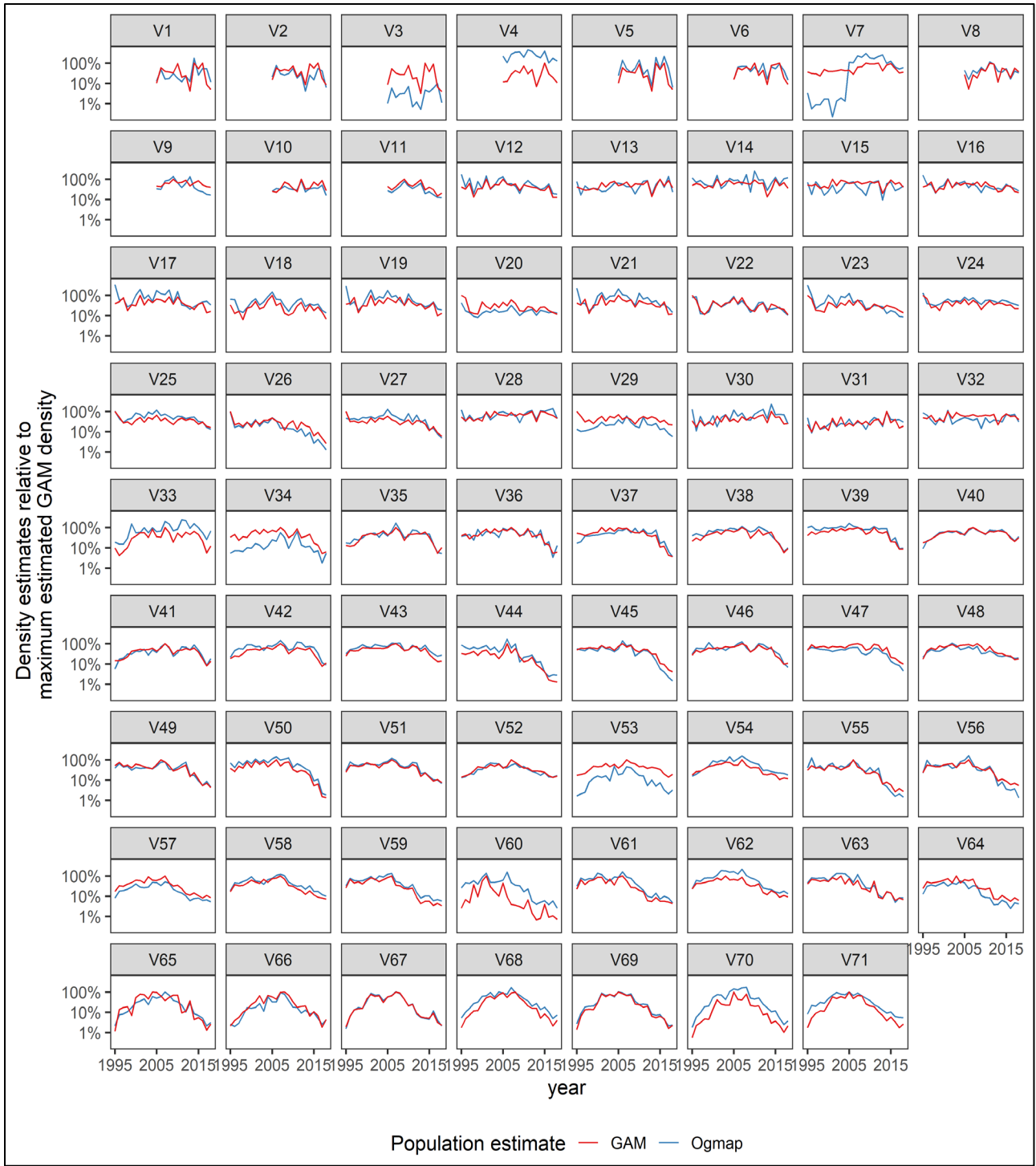


Figure 12: Comparison of GAM smoothed biomass versus prior Ogmap estimates within each patch. Red lines indicate yearly means estimated by the GAM model, and blue lines indicate estimates from the current Ogmap estimation approach. All density estimates have been scaled by the maximum estimate of biomass for that patch from the GAM method, to allow for easier within-patch comparisons.



Figure 13: Fraction of total biomass in each SFA considered to be fishable biomass (carapace length >17 mm).

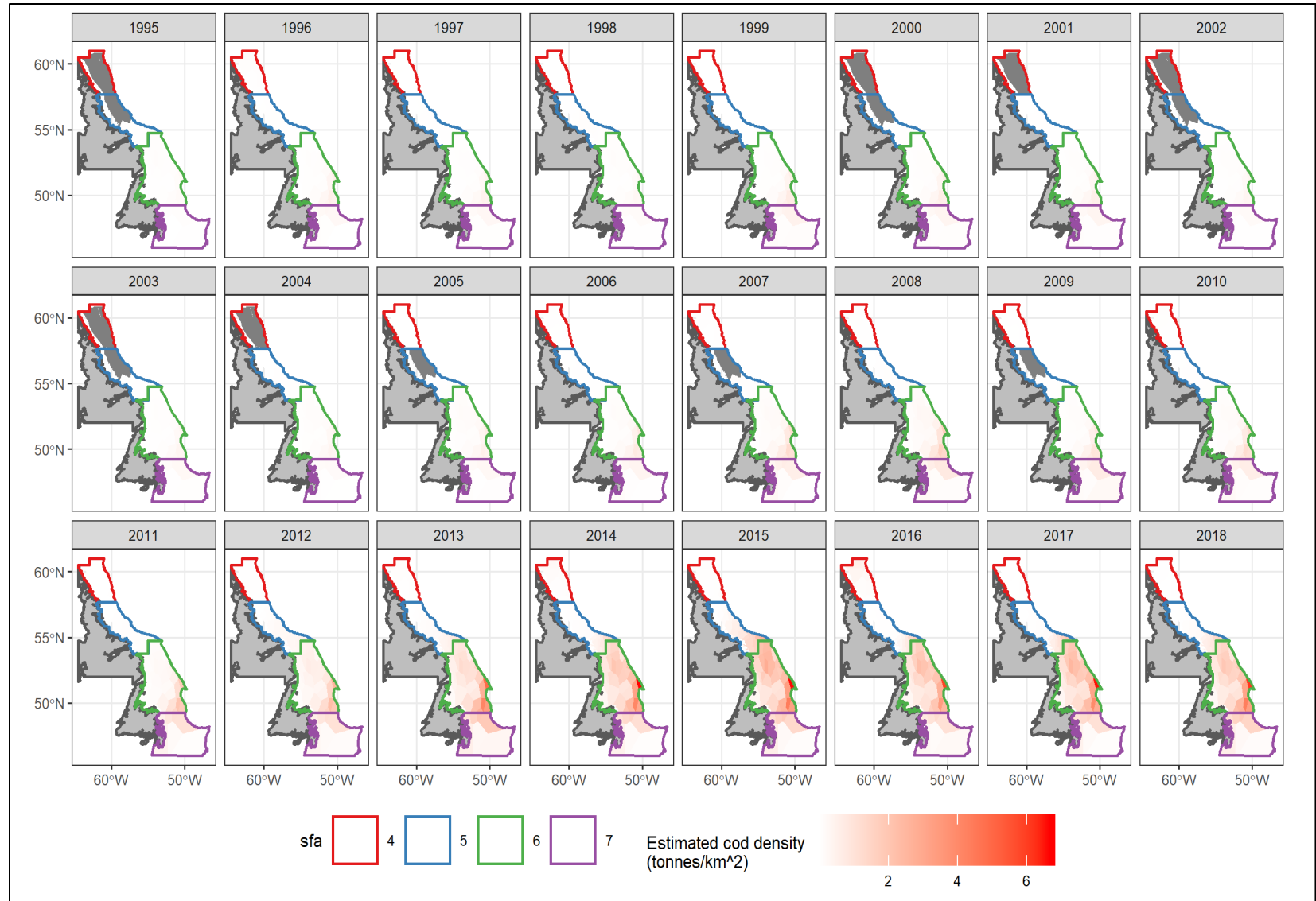


Figure 14: Spatial distributions of Atlantic Cod (*Gadus morhua*) density in tonnes per square km, with darker colors indicating lower density, and lighter colors indicating higher densities. Dark grey polygons indicate areas where data were missing for a given year.

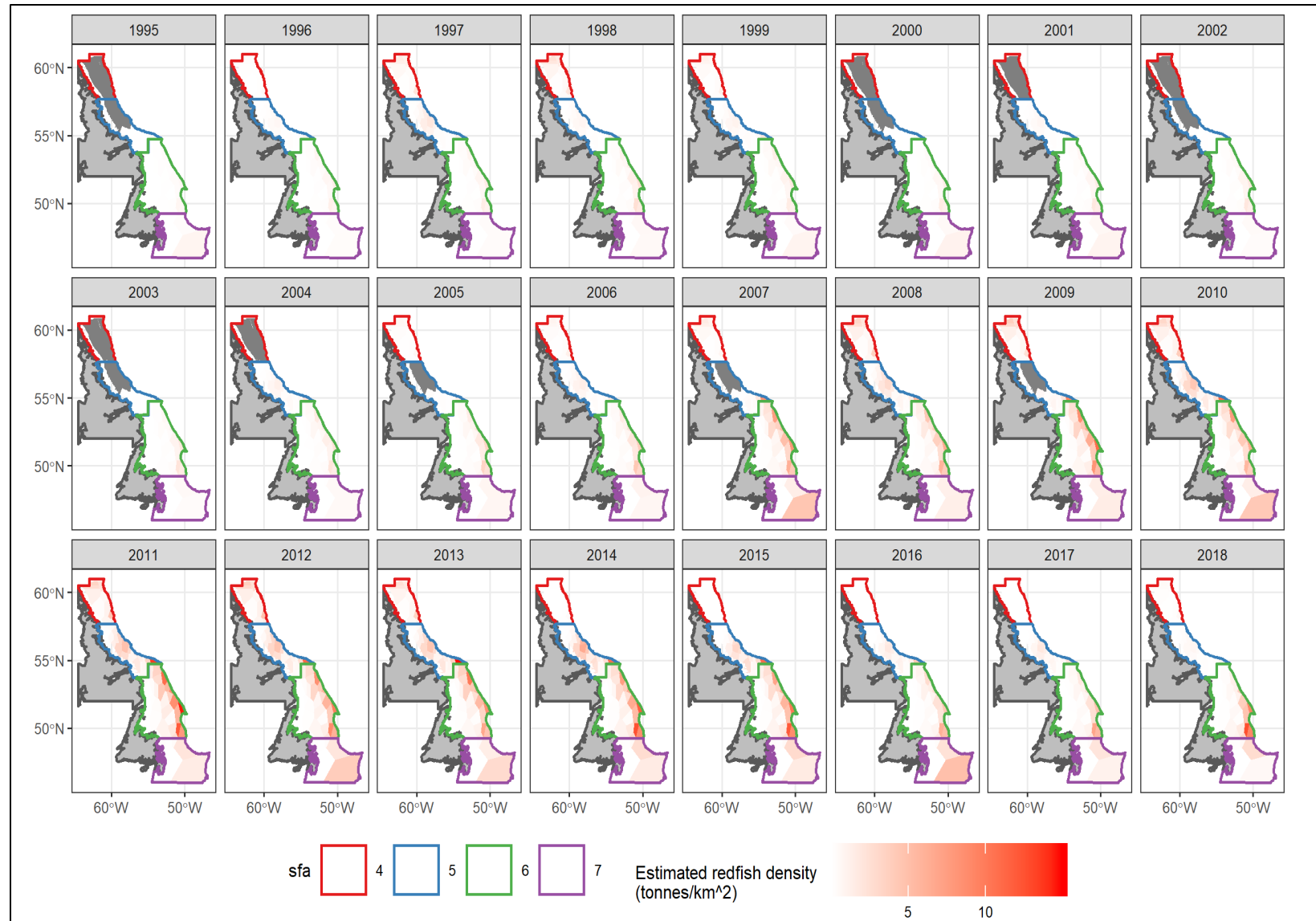


Figure 15: Spatial distributions of Deepwater Redfish (*Sebastodes mentella*) density in tonnes per square km, with darker colors indicating lower density, and lighter colors indicating higher densities. Dark grey polygons indicate areas where data were missing for a given year.

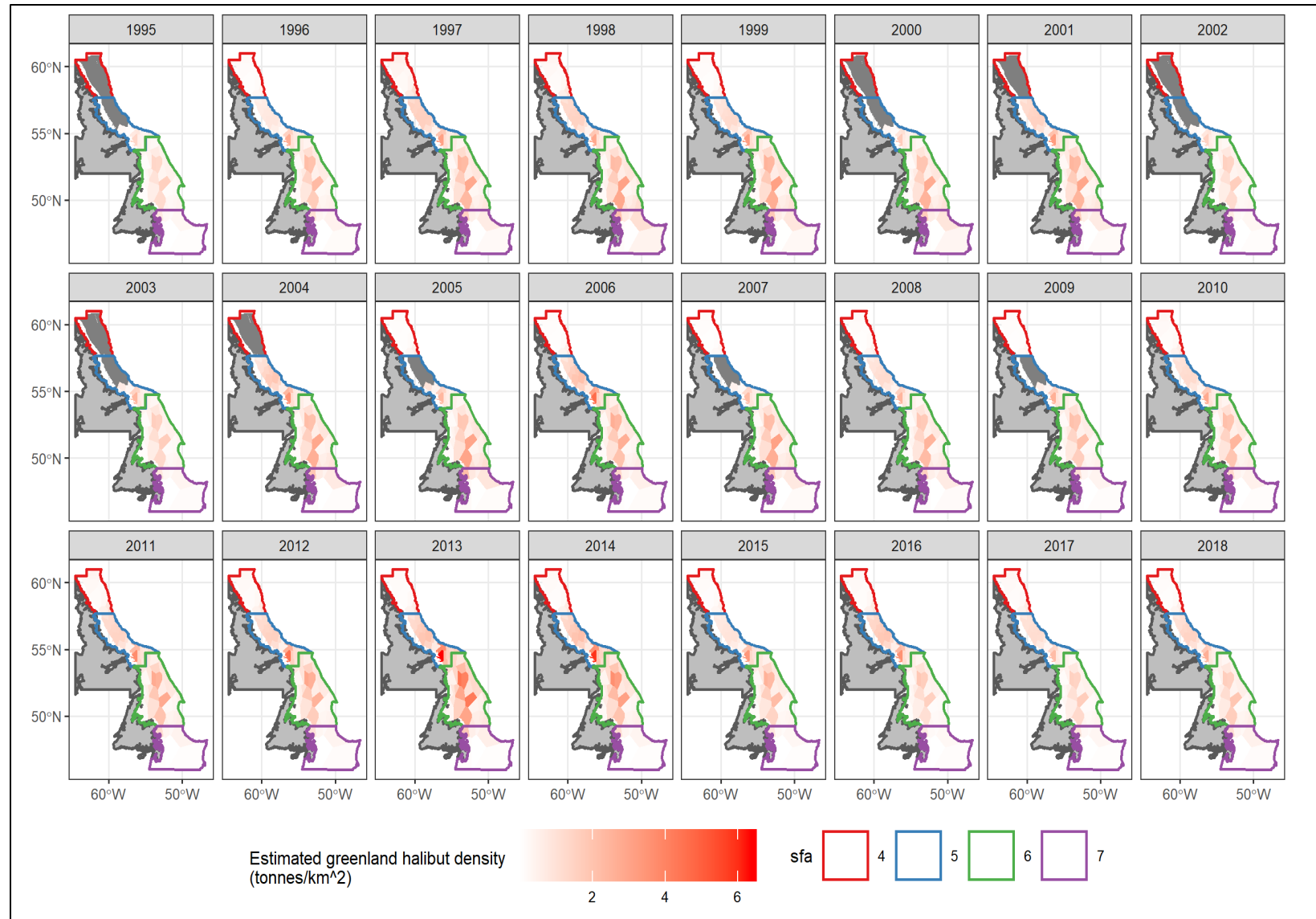


Figure 16: Spatial distributions of Greenland Halibut (*Reinhardtius hippoglossoides*) density in tonnes per square km, with darker colors indicating lower density, and lighter colors indicating higher densities. Dark grey polygons indicate areas where data were missing for a given year.

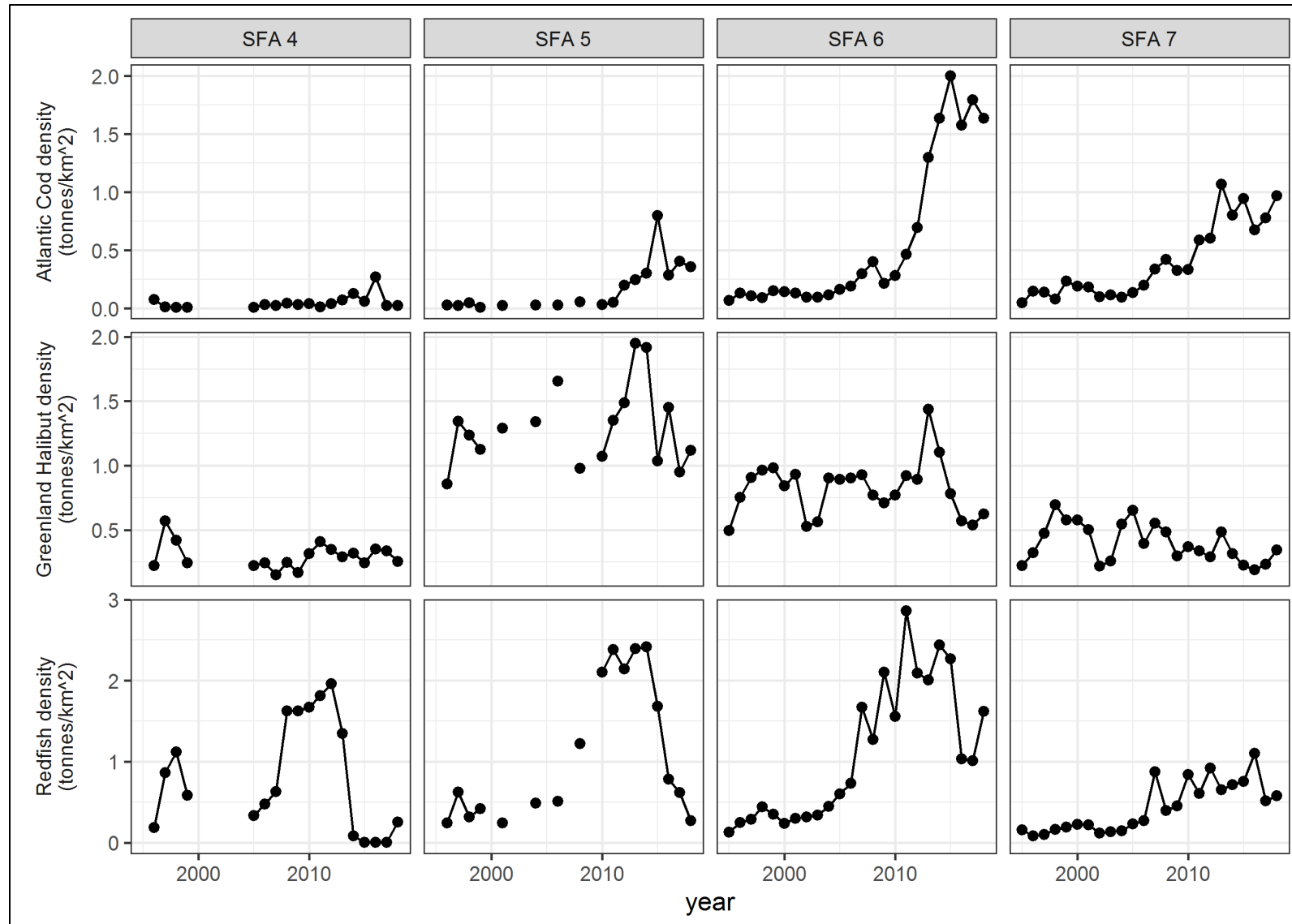


Figure 17: Densities of primary predators (Atlantic Cod, Redfish, and Greenland Halibut) within each SFA across years, averaged across spatiotemporal regression model fits for each species.

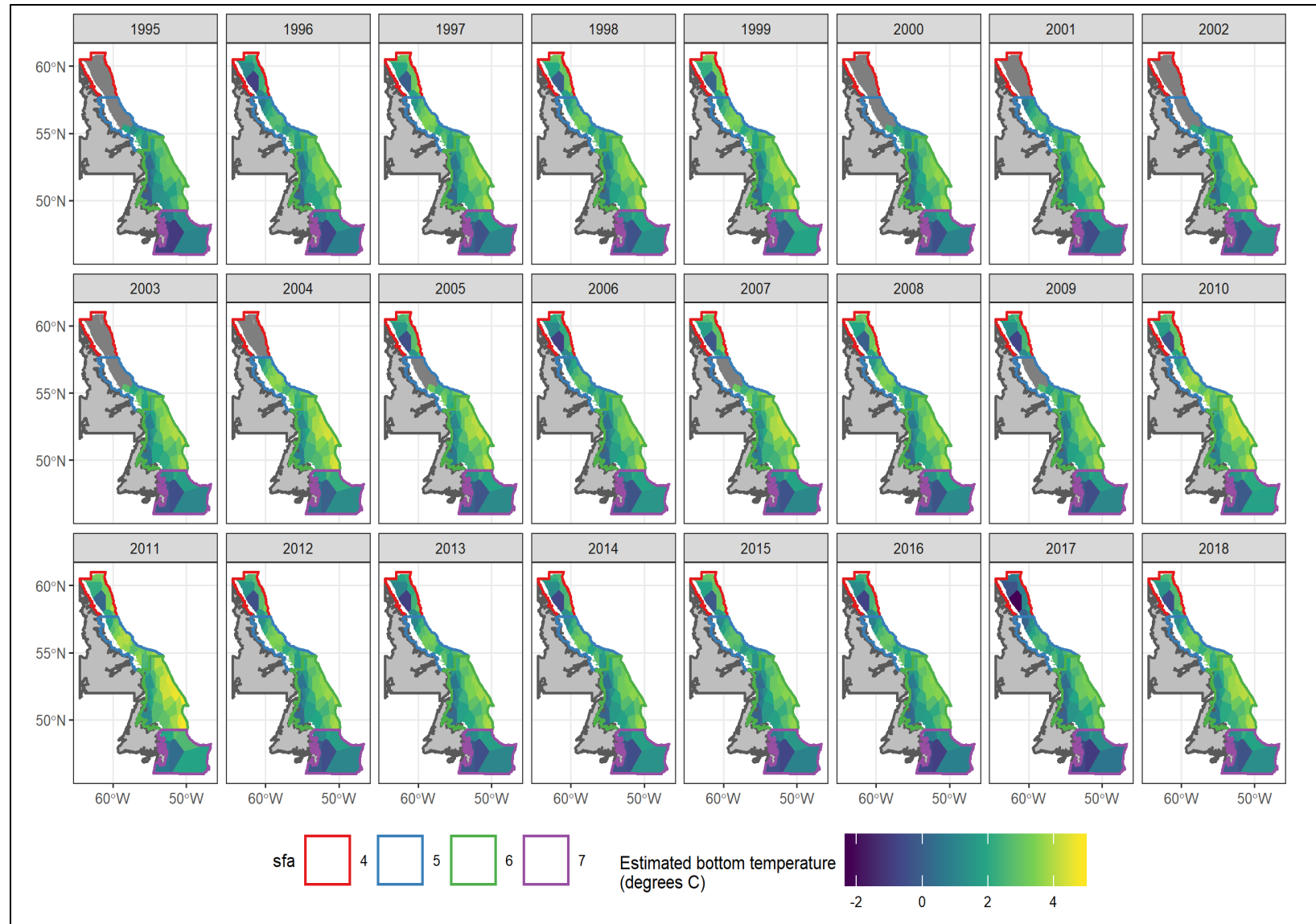


Figure 18: Spatial distributions of bottom temperature in °C, with darker colors indicating lower temperature, and lighter colors indicating higher temperatures. Dark grey polygons indicate areas where trawl data were missing for a given year.

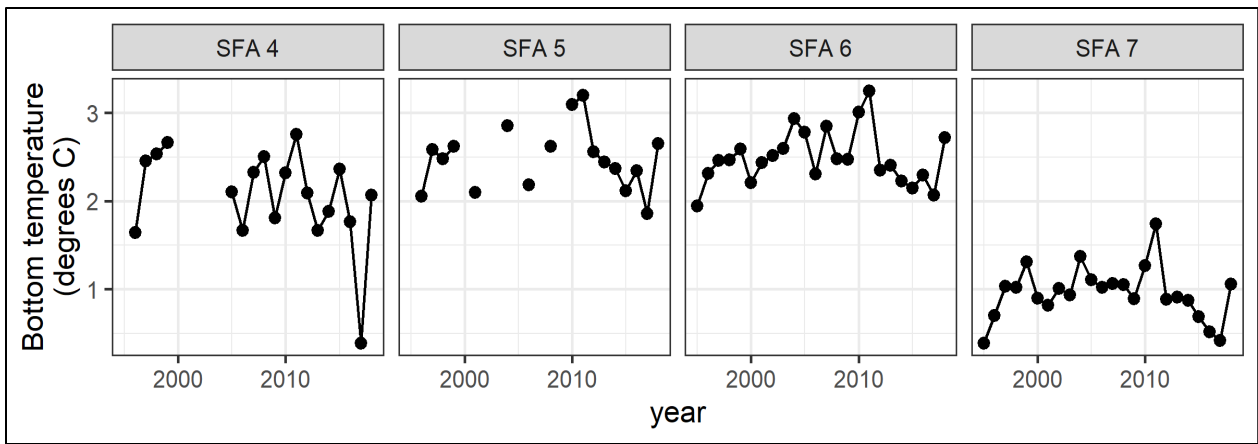


Figure 19: Average yearly bottom temperature in each SFA, aggregated across patches.

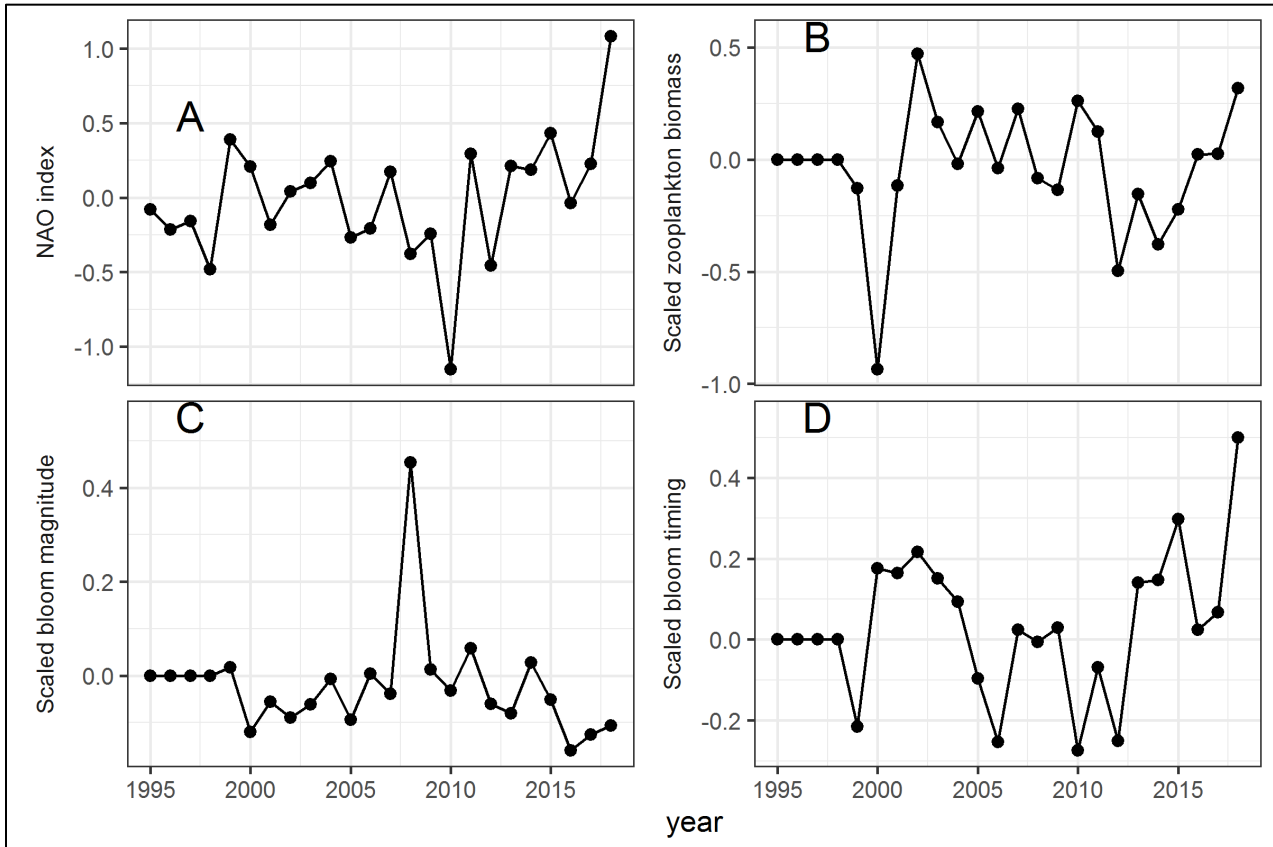


Figure 20: Average yearly mean time series of (A) NAO index, scaled phytoplankton bloom magnitude (B), scaled phytoplankton timing (C), and (D) scaled zooplankton abundance.

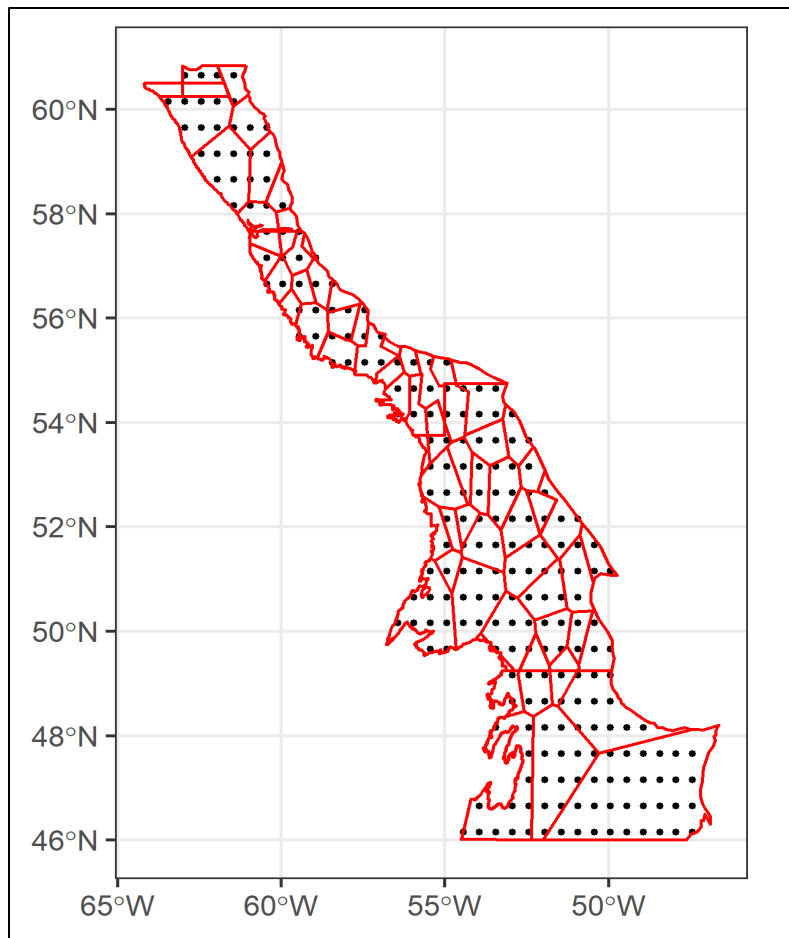


Figure 21: Starting points for larval drift simulations.

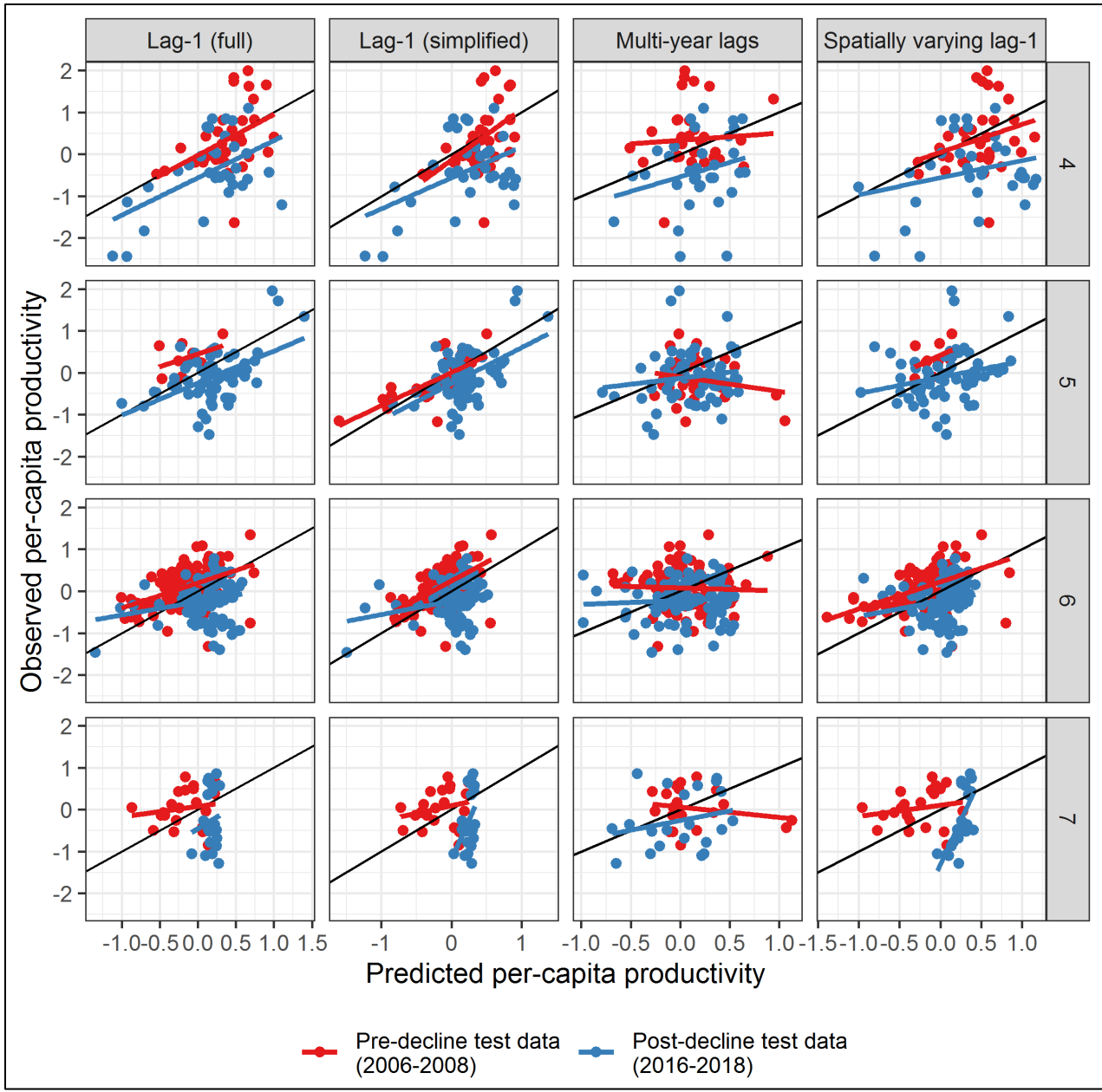


Figure 22: Observed per-patch productivity values in years reserved for model testing, compared to predicted productivity rates. A model that perfectly predicted growth rates would result in all points lying on the 1-1 equality line (in black). Variation around this line indicates unexplained variation in productivity. Colored lines represent simple linear regressions of observed on predicted values, to illustrate the actual relationship between predicted and observed rates of change; flat linear regressions correspond to models with no predictive power, and regression lines occurring consistently above (below) the 1-1 line indicate models that consistently predict lower than (greater than) observed growth rates. Red points and lines indicate data from 2006-08, prior to significant Northern Shrimp declines. Blue points and lines indicate data from 2016-18, following the declines in shrimp biomass.

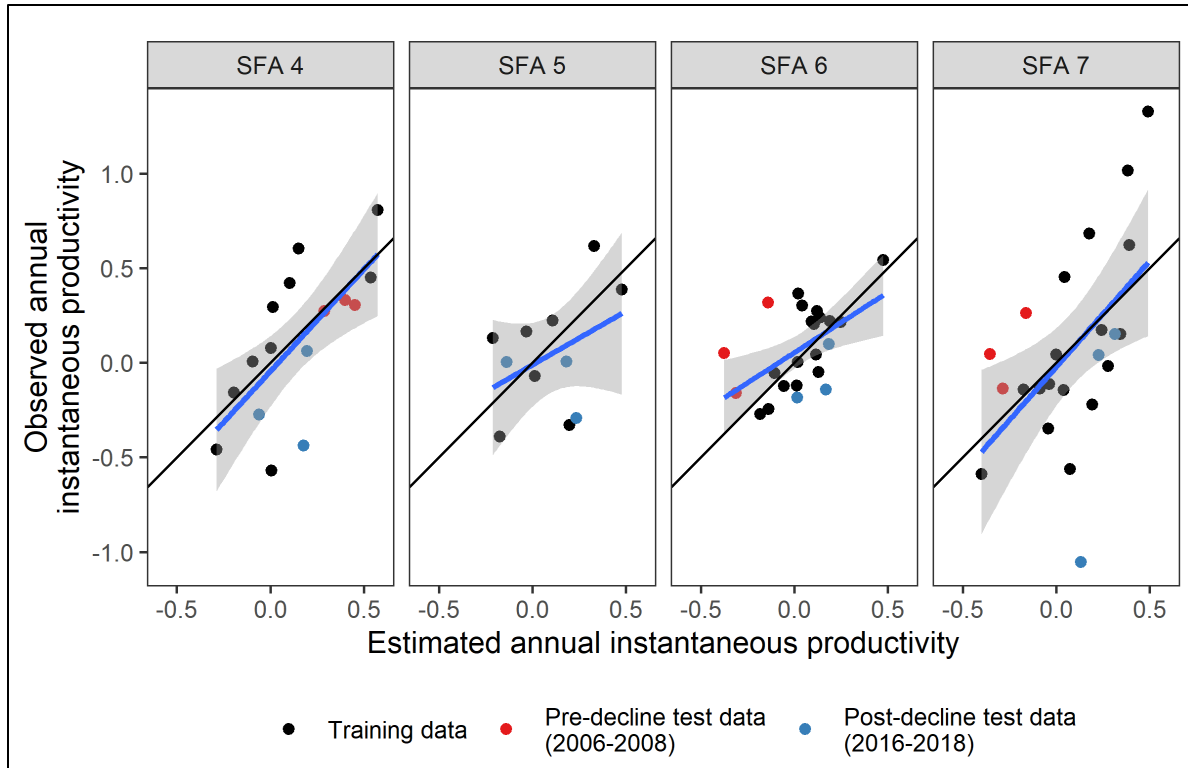


Figure 23: Observed SFA-level productivity values for all SFAs. Black line indicates the 1-1 equality line, and the blue lines represent a simple linear regressions of observed on predicted values. Red points and lines indicate data from 2006-08, prior to significant Northern Shrimp declines. Blue points and lines indicate data from 2016-18, following the decline in shrimp biomass.

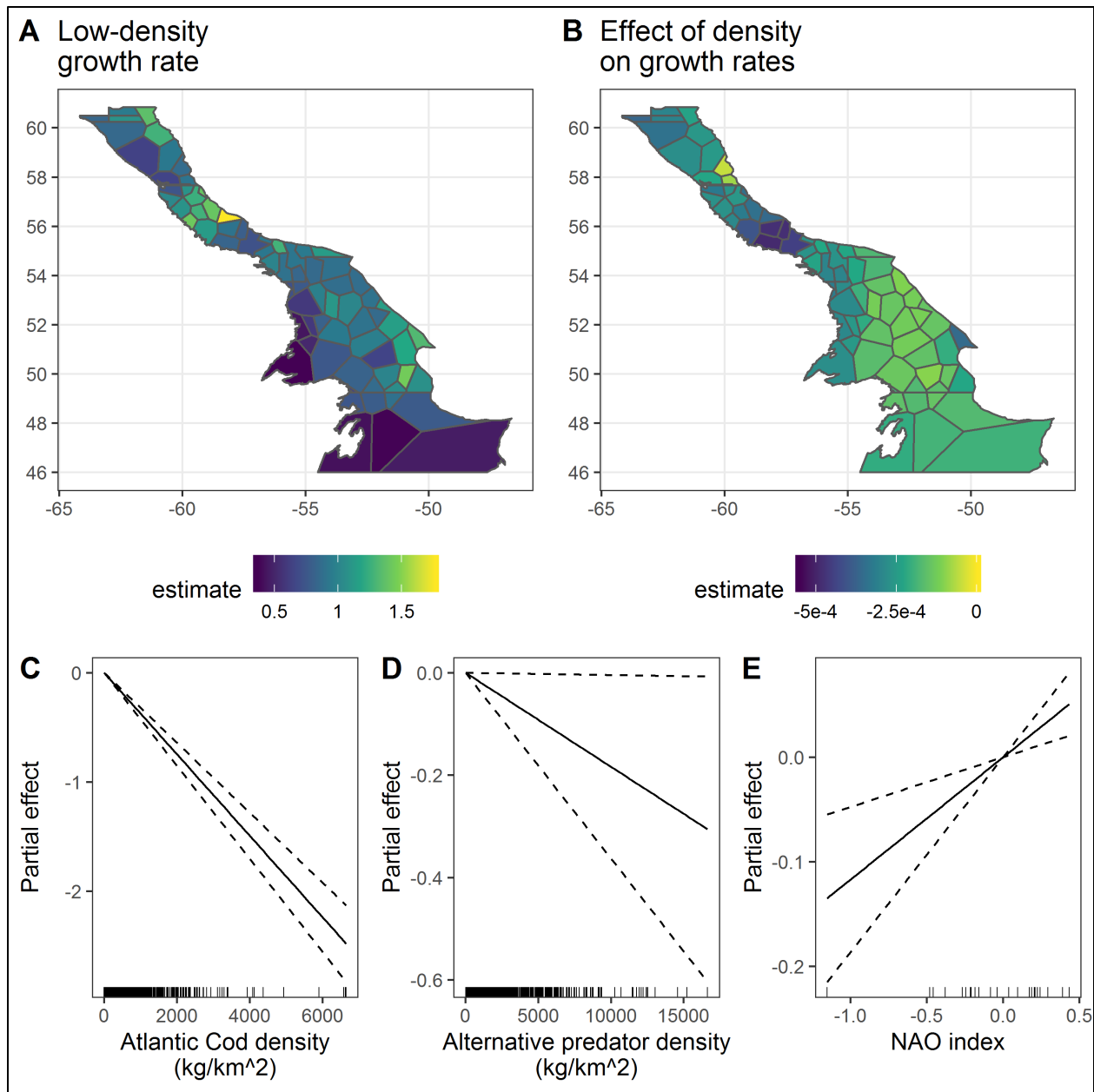


Figure 24: Estimates of coefficients from the forecasting model. A) The estimated instantaneous productivity in each patch in the absence of density-dependence, cod predation, and NAO effects. B) The estimated density-dependence term, indicating how quickly productivity is expected to decline with each additional kg per km^2 of shrimp. C) Effect of Atlantic Cod density, indicating how quickly productivity is expected to decline with each additional kg per km^2 of Atlantic Cod. D) Effect of alternative predator density. E) Effect of NAO on productivity, with high NAO values corresponding to generally colder and fresher conditions.

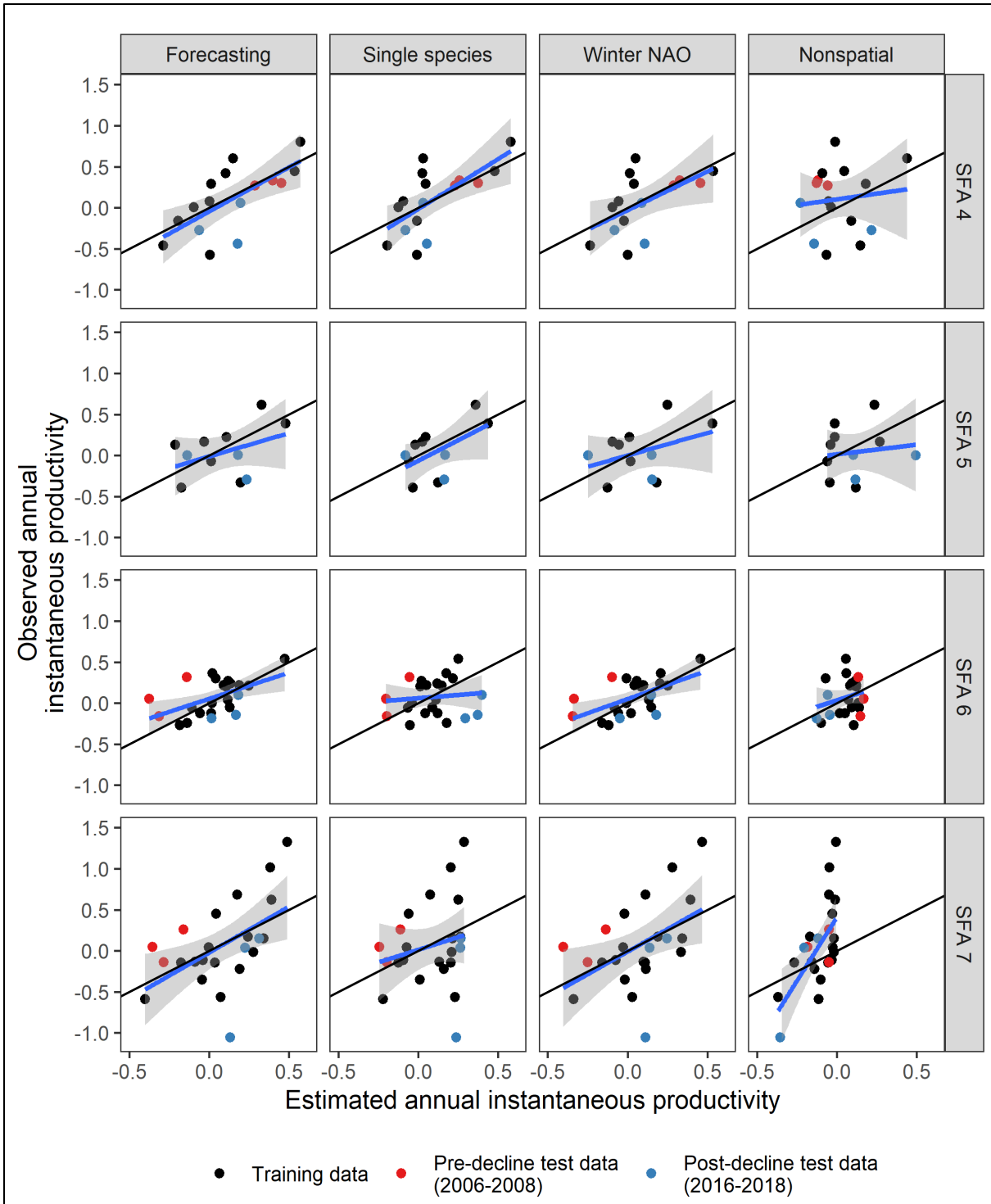


Figure 25: Observed SFA-level productivity values for all SFAs for sensitivity tests. Black line indicates the 1-1 equality line, and the blue lines represent a simple linear regressions of observed on predicted values. Red points and lines indicate data from 2006-08, prior to significant Northern Shrimp declines. Blue points and lines indicate data from 2016-18, following the decline in shrimp biomass.

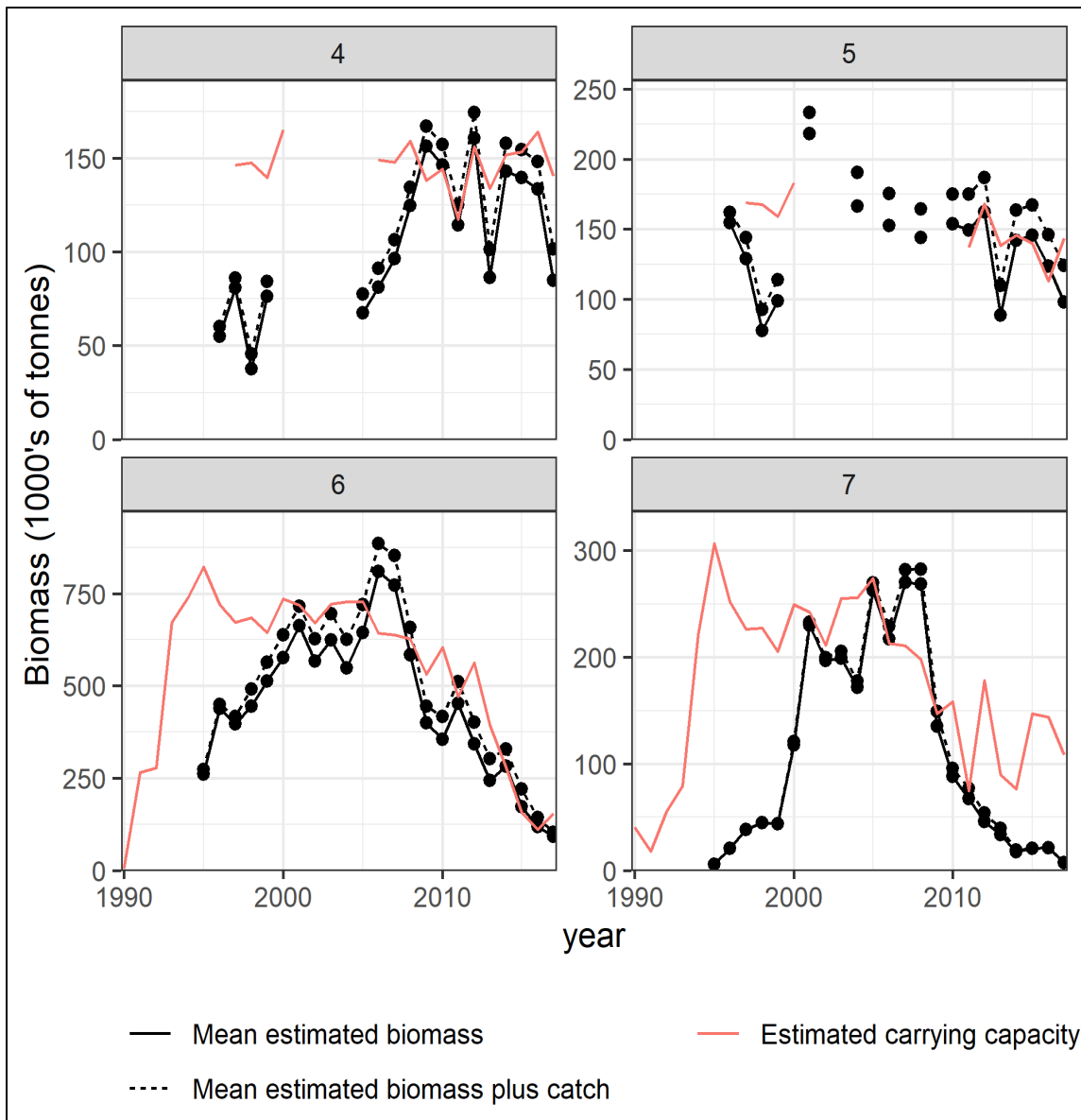


Figure 26: Modelled biomass for each SFA with commercial catch included (dashed black line) and remaining after harvest (solid black line). Estimated time-varying SFA-scale carrying capacities for each year given observed environmental conditions are shown as red lines.

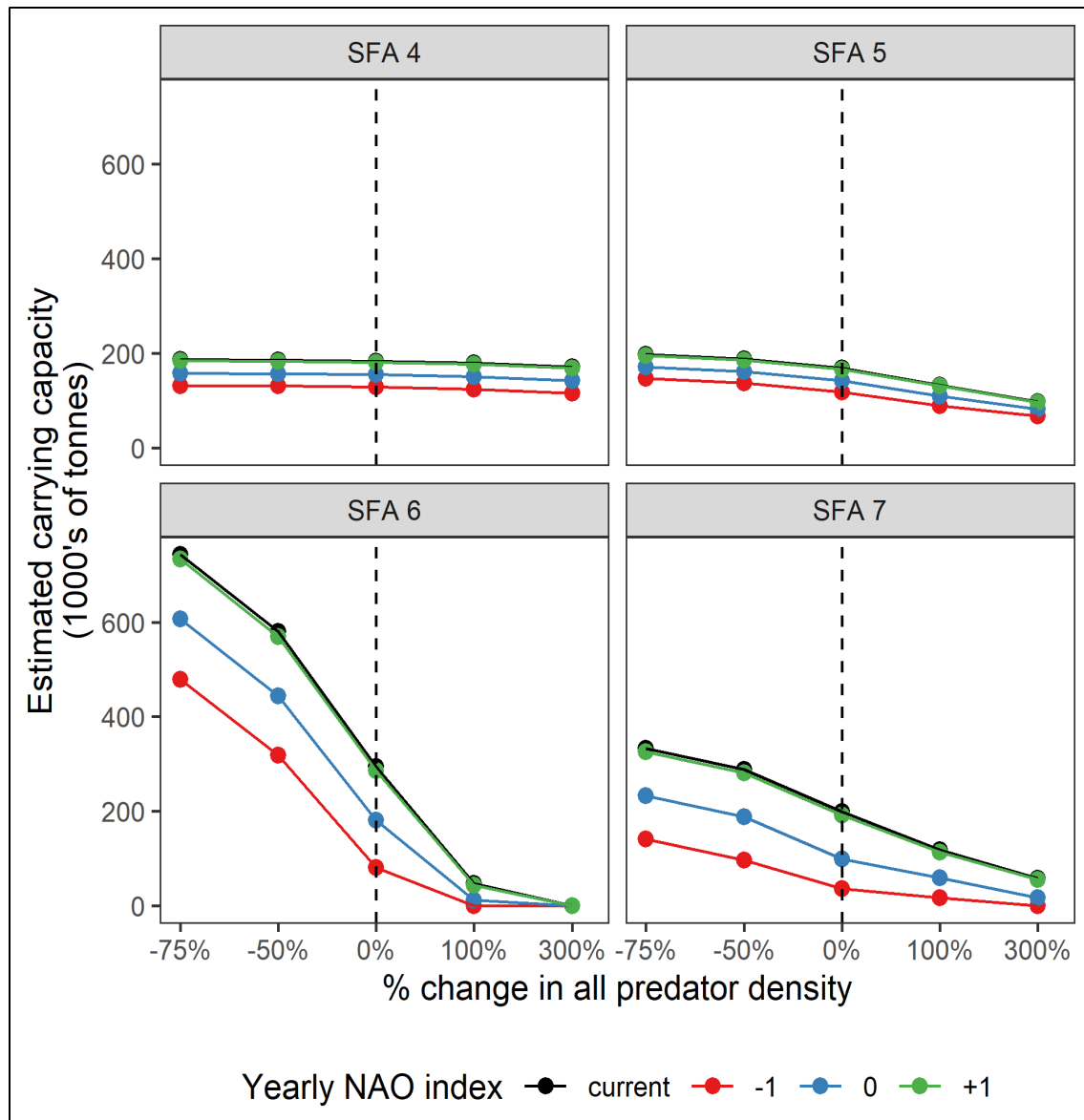


Figure 27: Sensitivity of estimated carrying capacity for each SFA for 2019 to variation in model inputs.

SUPPLEMENTAL FIGURES

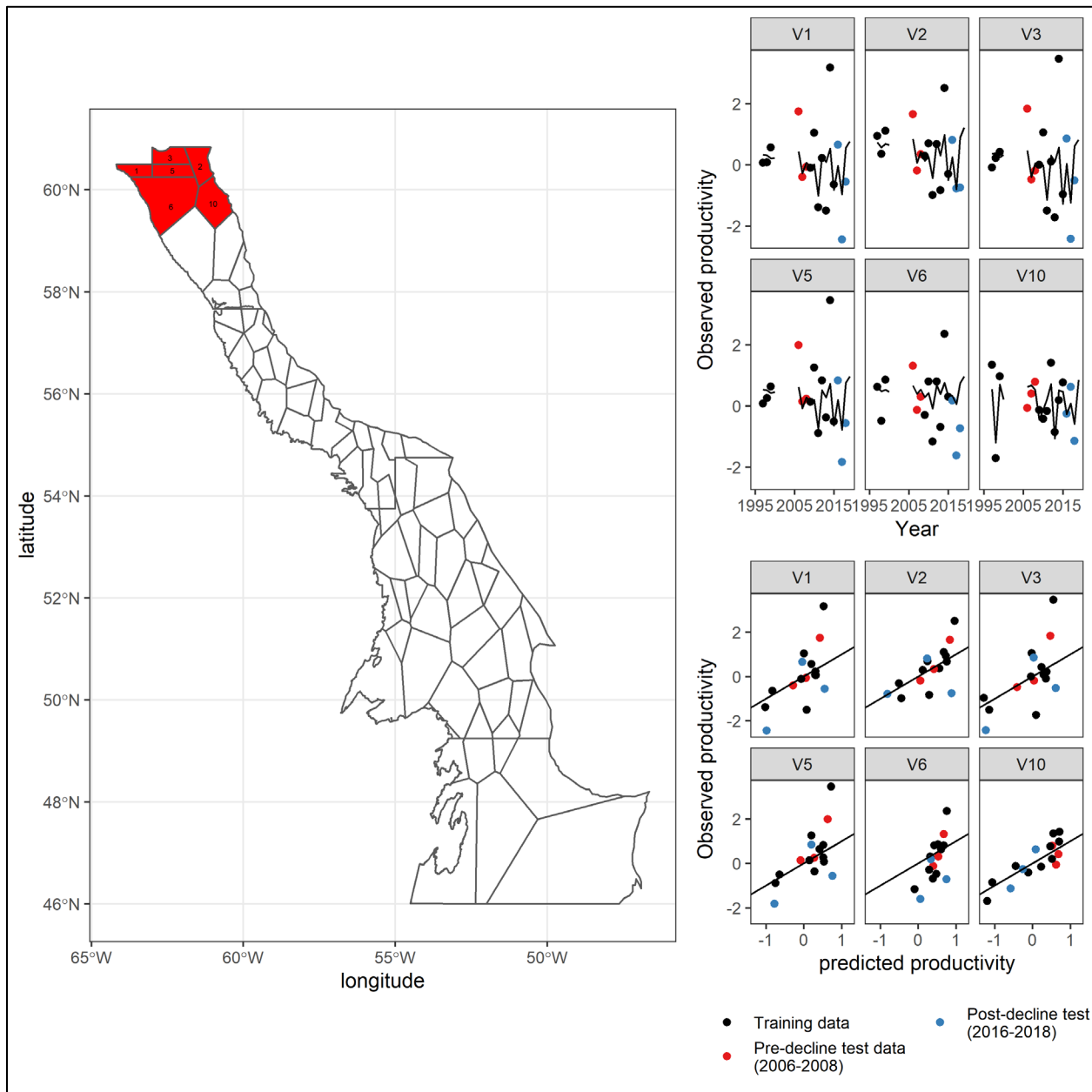


Figure S1: Model fits for patches V1, V2, V3, V5, V6, and V10. Left: map illustrating patch locations. Top right: plot of observed patch-level productivities plotted against time. Black line indicated model-predicted productivity. Bottom right: observed versus expected productivity in each patch in each year. Black line indicates the 1-1 line.

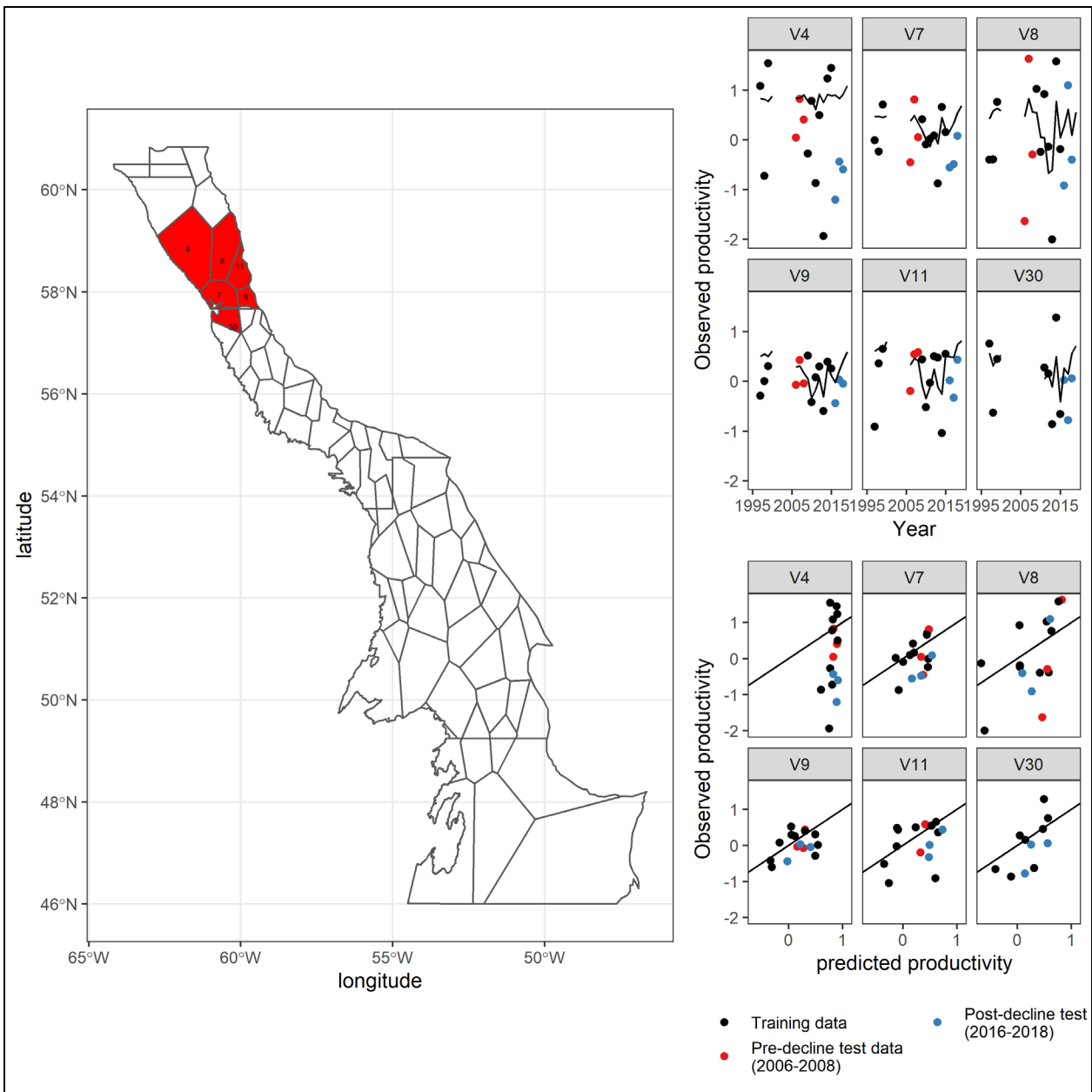


Figure S2: Model fits for patches V4, V7, V8, V9, V11, and V30. Left: map illustrating patch locations. Top right: plot of observed patch-level productivities plotted against time. Black line indicated model-predicted productivity. Bottom right: observed versus expected productivity in each patch in each year. Black line indicates the 1-1 line.

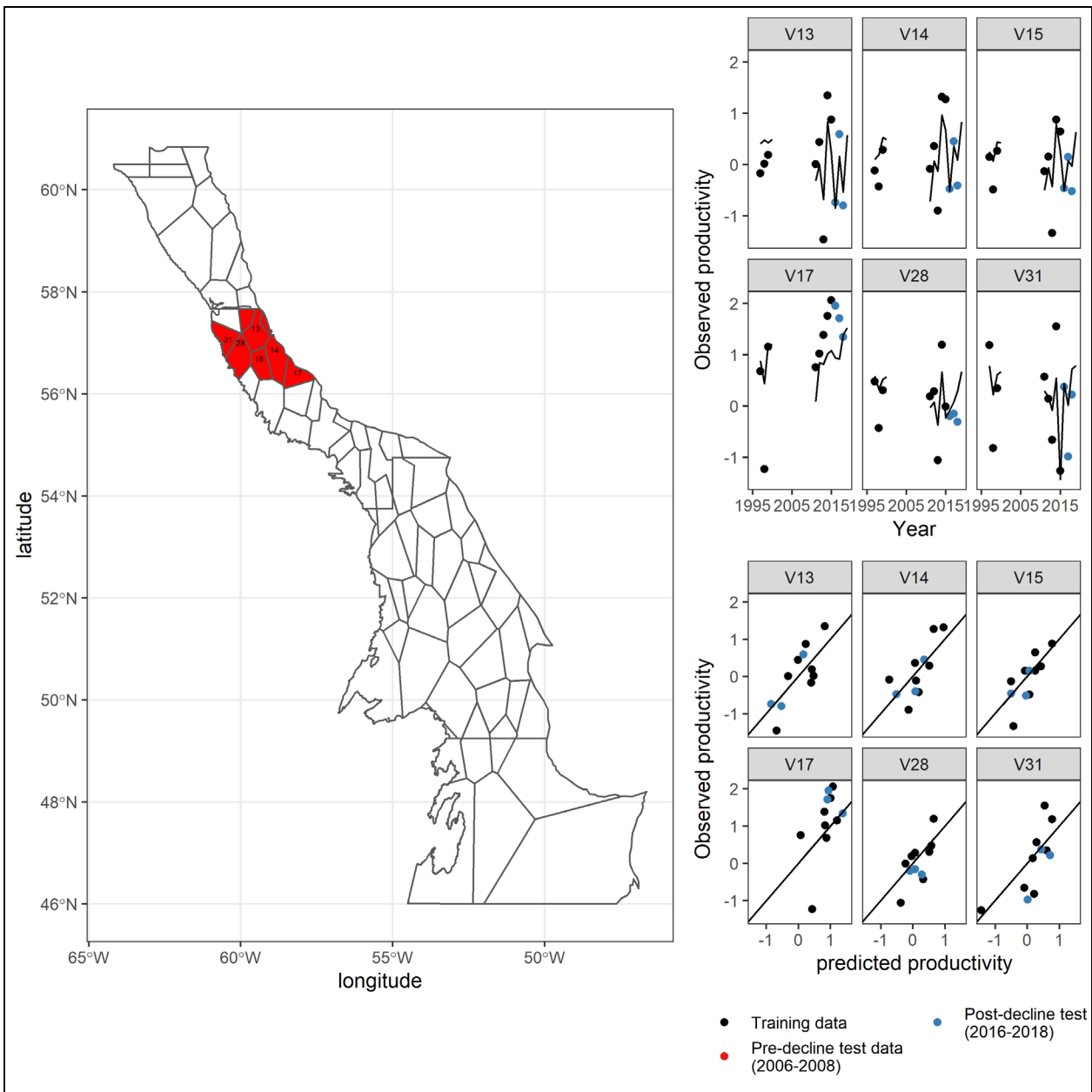


Figure S3: Model fits for patches V13, V14, V15, V17, V28, and V31. Left: map illustrating patch locations. Top right: plot of observed patch-level productivities plotted against time. Black line indicated model-predicted productivity. Bottom right: observed versus expected productivity in each patch in each year. Black line indicates the 1-1 line.

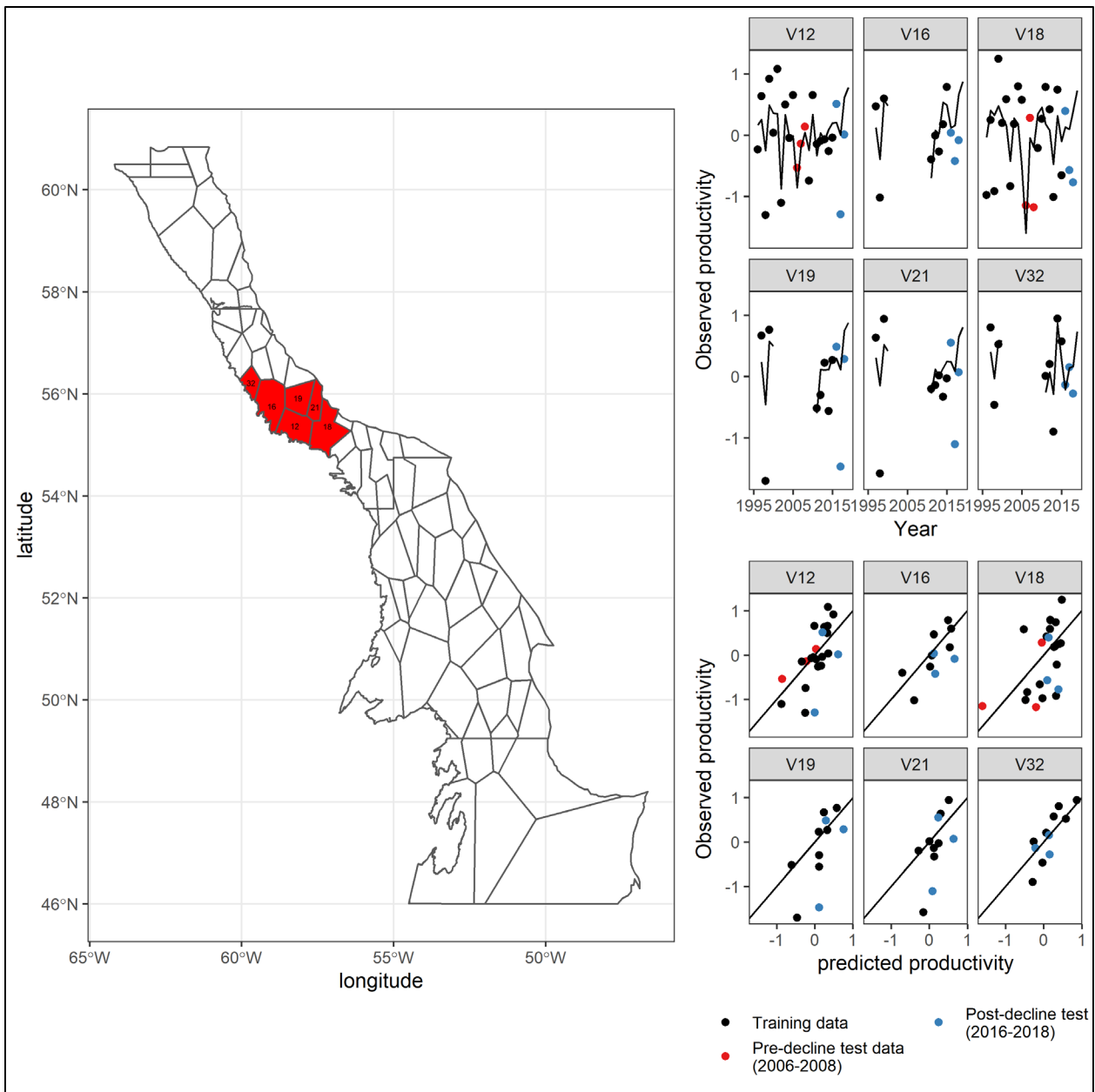


Figure S4: Model fits for patches V12, V16, V18, V19, V21, and V32. Left: map illustrating patch locations. Top right: plot of observed patch-level productivities plotted against time. Black line indicated model-predicted productivity. Bottom right: observed versus expected productivity in each patch in each year. Black line indicates the 1-1 line.

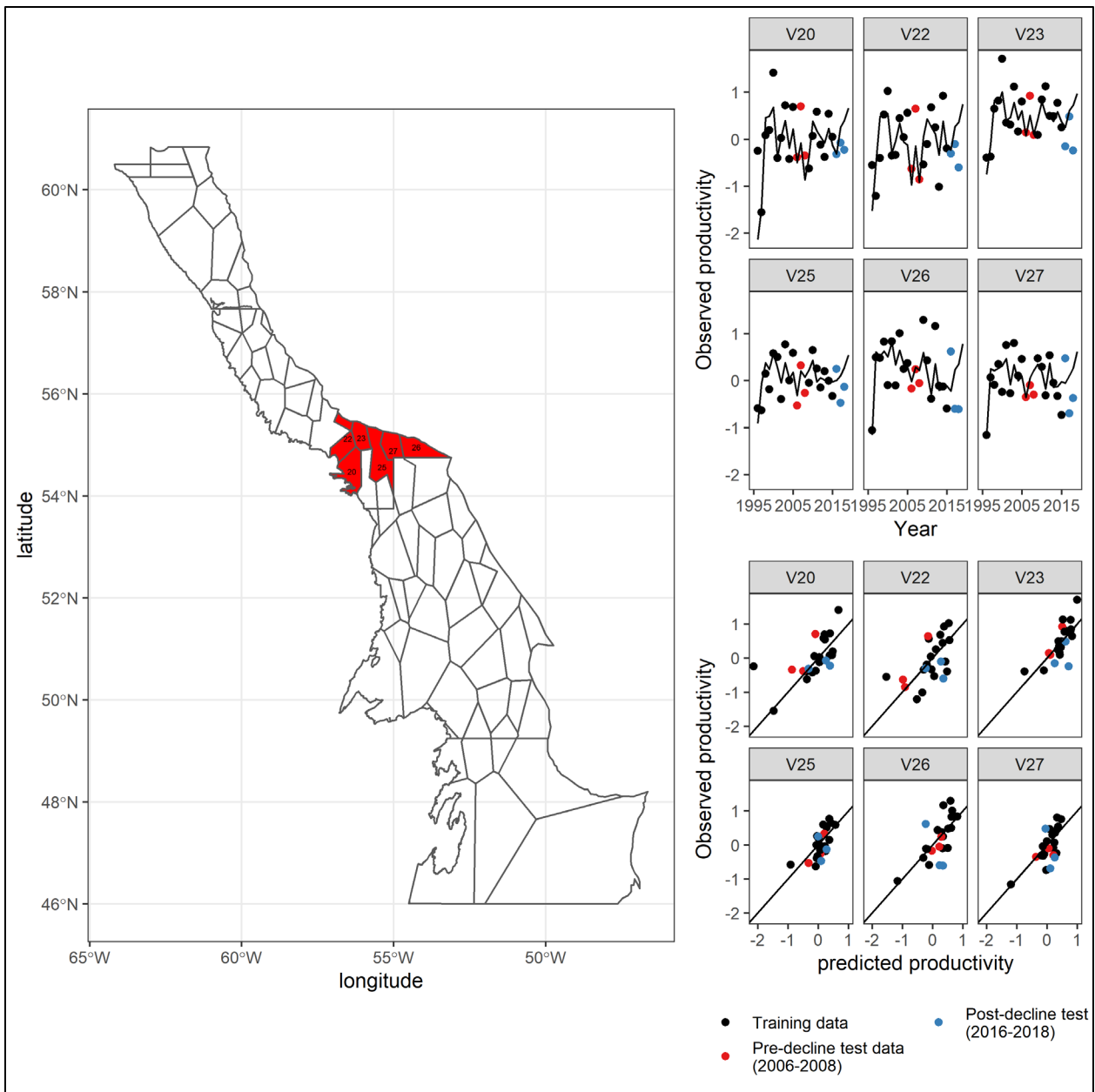


Figure S5: Model fits for patches V20, V22, V23, V25, V26, and V27. Left: map illustrating patch locations. Top right: plot of observed patch-level productivities plotted against time. Black line indicated model-predicted productivity. Bottom right: observed versus expected productivity in each patch in each year. Black line indicates the 1-1 line.

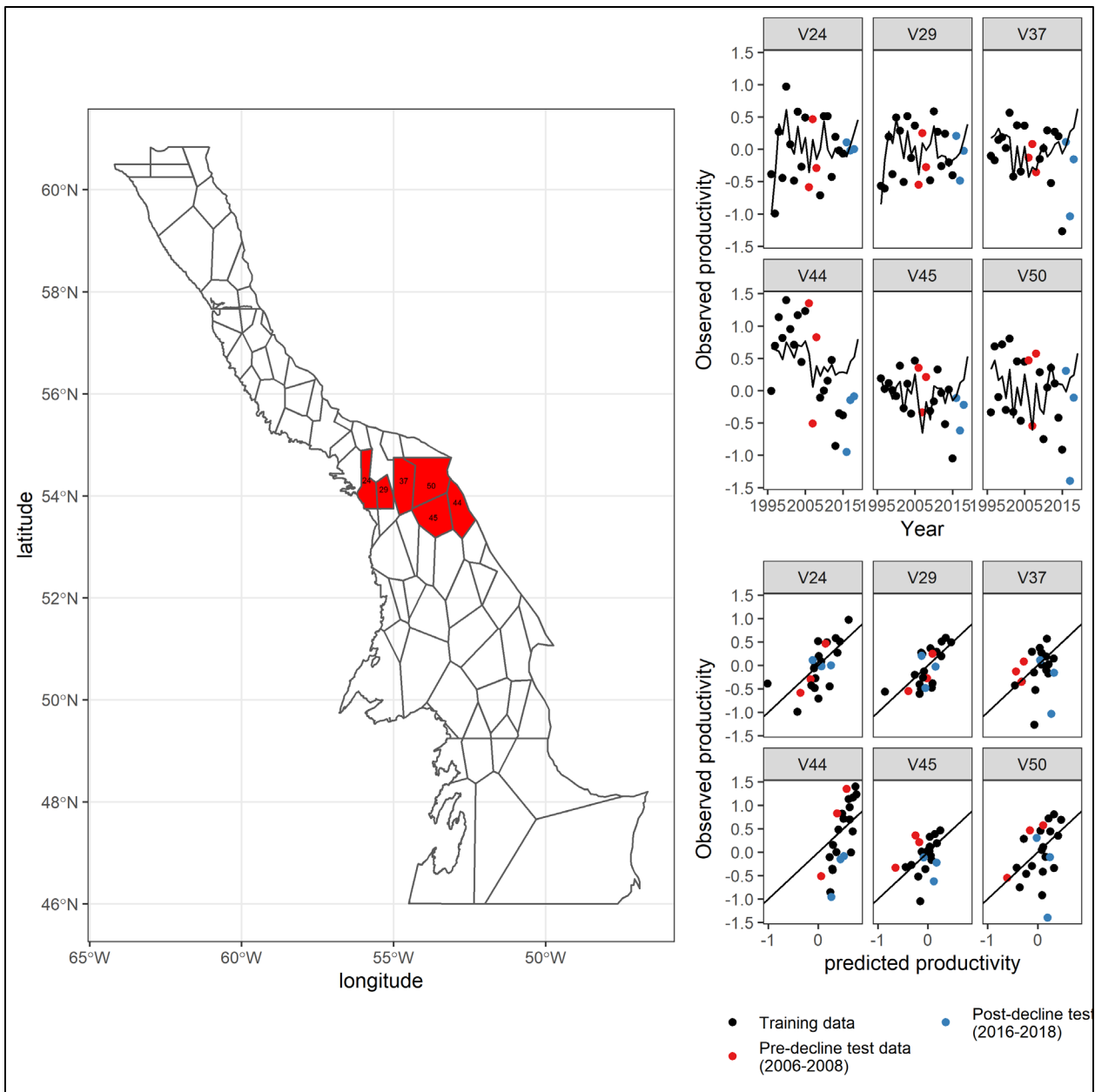


Figure S6: Model fits for patches V24, V29, V37, V44, V45, and V50. Left: map illustrating patch locations. Top right: plot of observed patch-level productivities plotted against time. Black line indicated model-predicted productivity. Bottom right: observed versus expected productivity in each patch in each year. Black line indicates the 1-1 line.

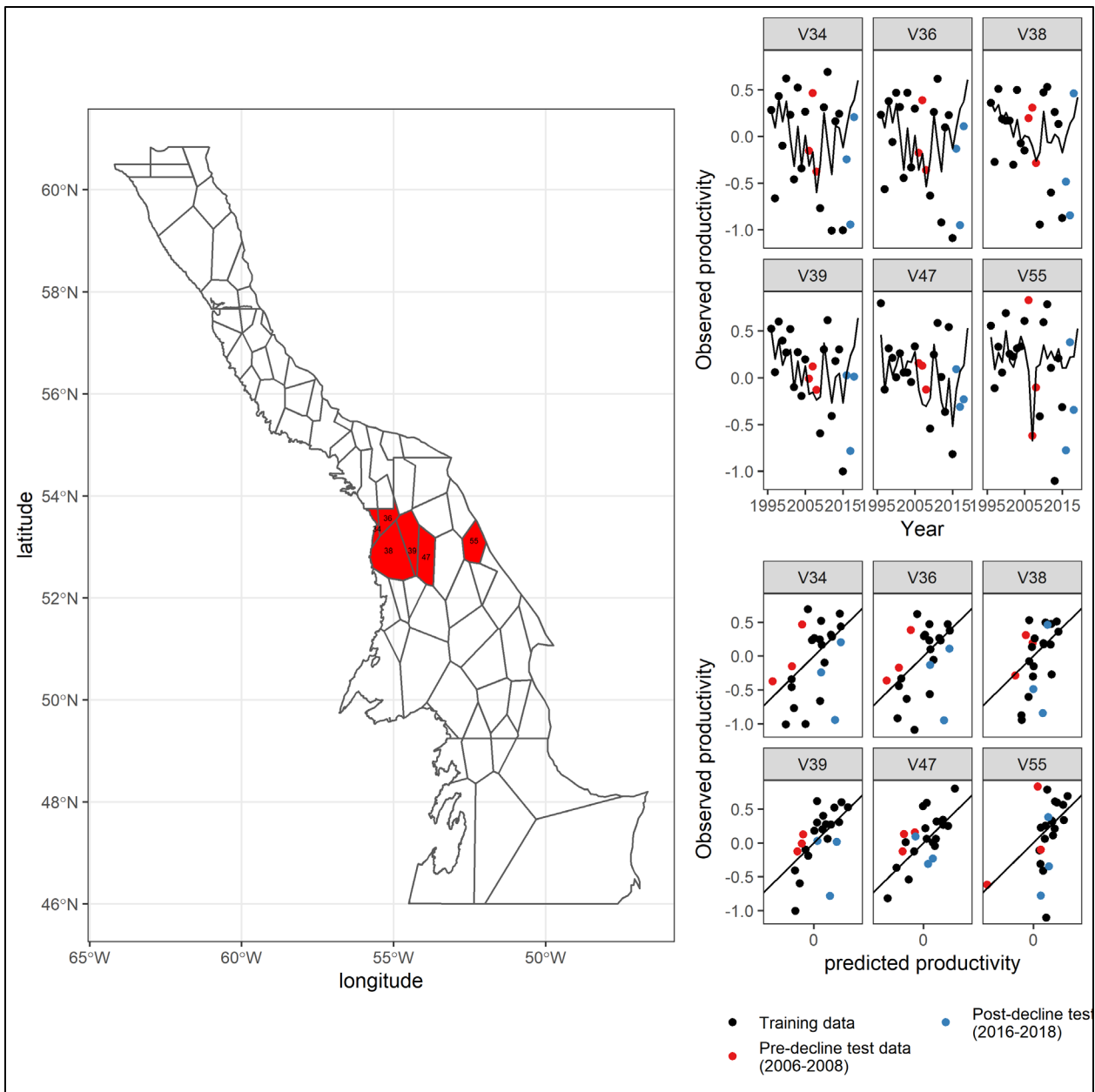


Figure S7: Model fits for patches V34, V36, V38, V39, V47, and V55. Left: map illustrating patch locations. Top right: plot of observed patch-level productivities plotted against time. Black line indicated model-predicted productivity. Bottom right: observed versus expected productivity in each patch in each year. Black line indicates the 1-1 line.

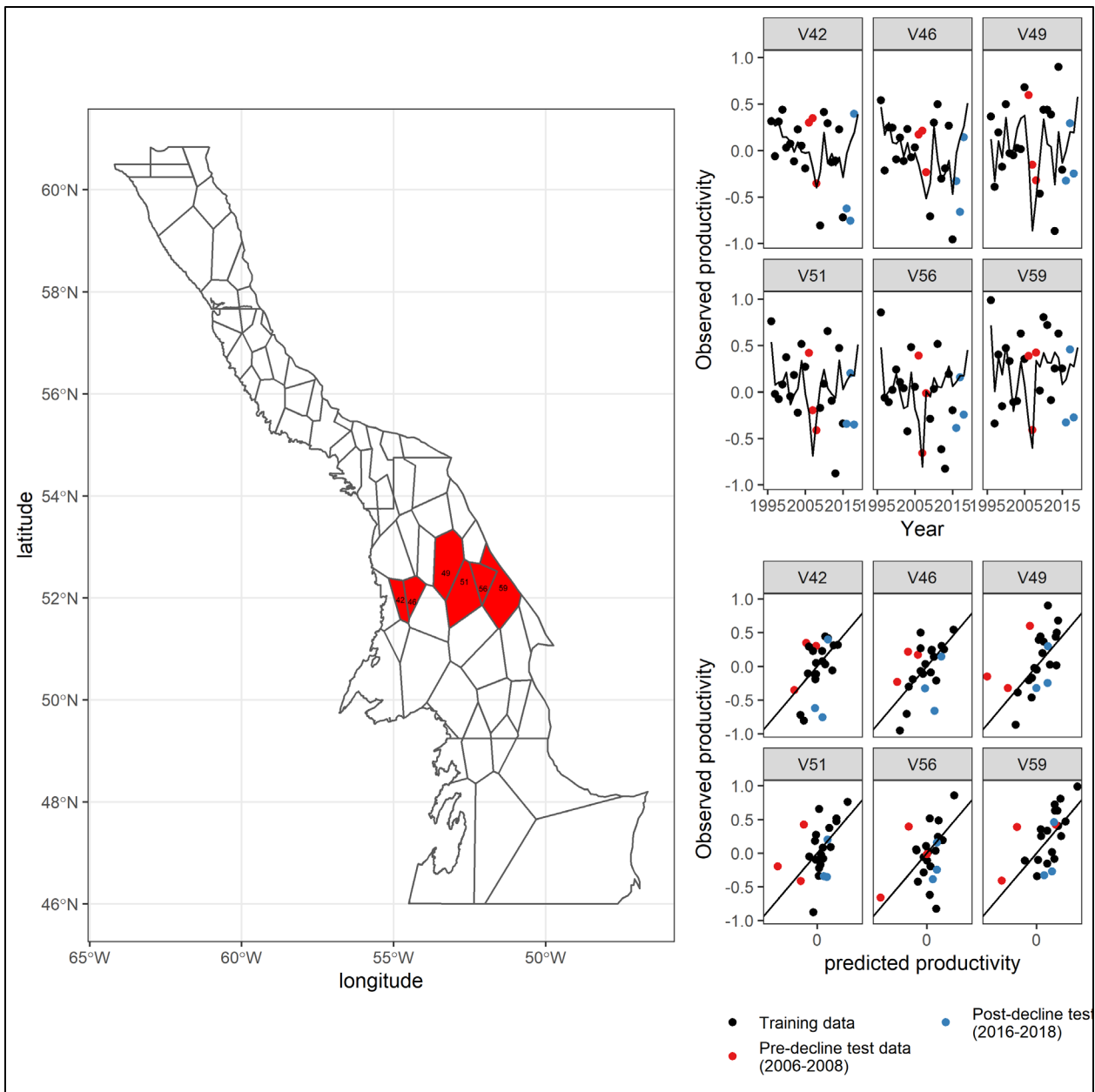


Figure S8: Model fits for patches V42, V46, V49, V51, V56, and V59. Left: map illustrating patch locations. Top right: plot of observed patch-level productivities plotted against time. Black line indicated model-predicted productivity. Bottom right: observed versus expected productivity in each patch in each year. Black line indicates the 1-1 line.

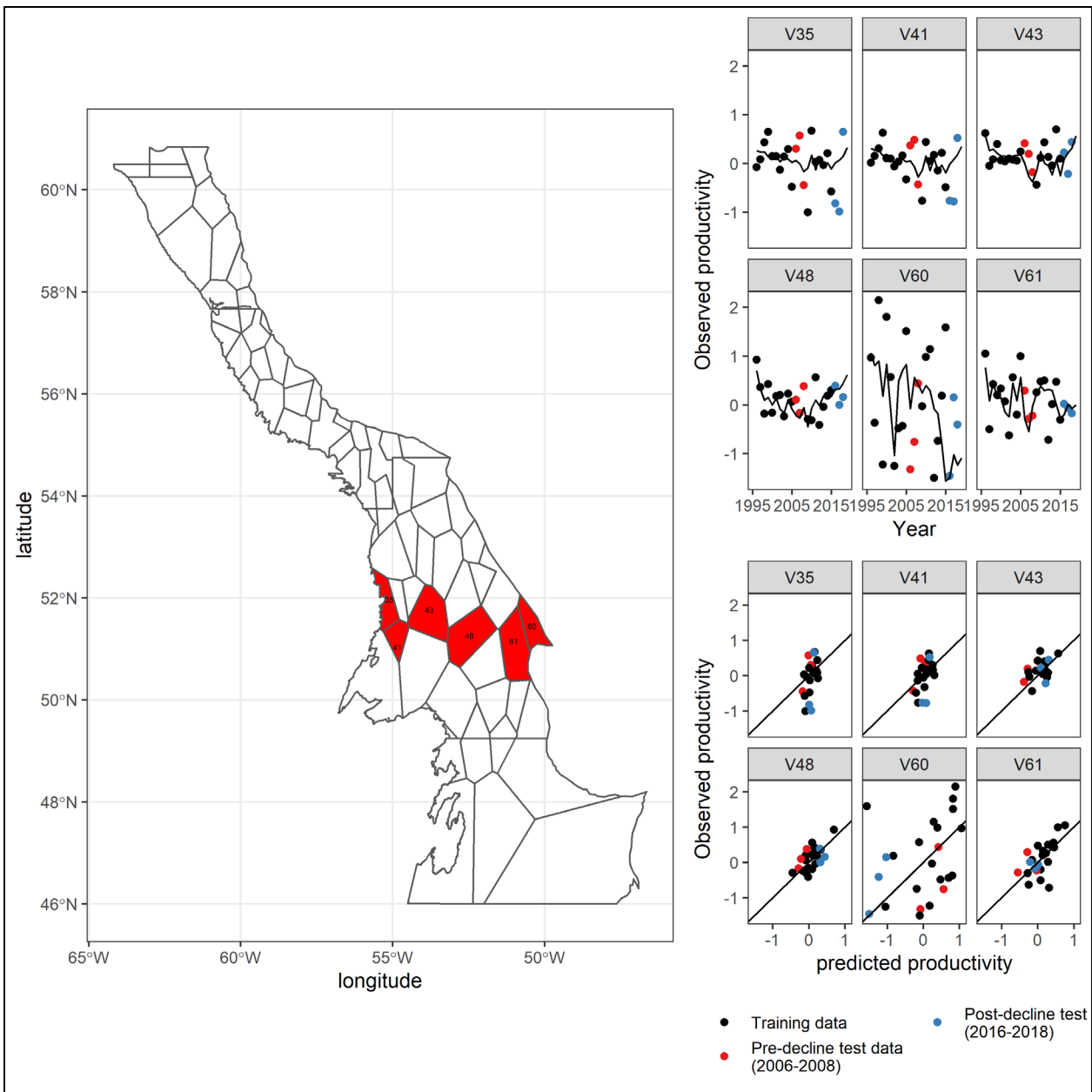


Figure S9: Model fits for patches V35, V41, V43, V48, V60, and V61. Left: map illustrating patch locations. Top right: plot of observed patch-level productivities plotted against time. Black line indicated model-predicted productivity. Bottom right: observed versus expected productivity in each patch in each year. Black line indicates the 1-1 line.

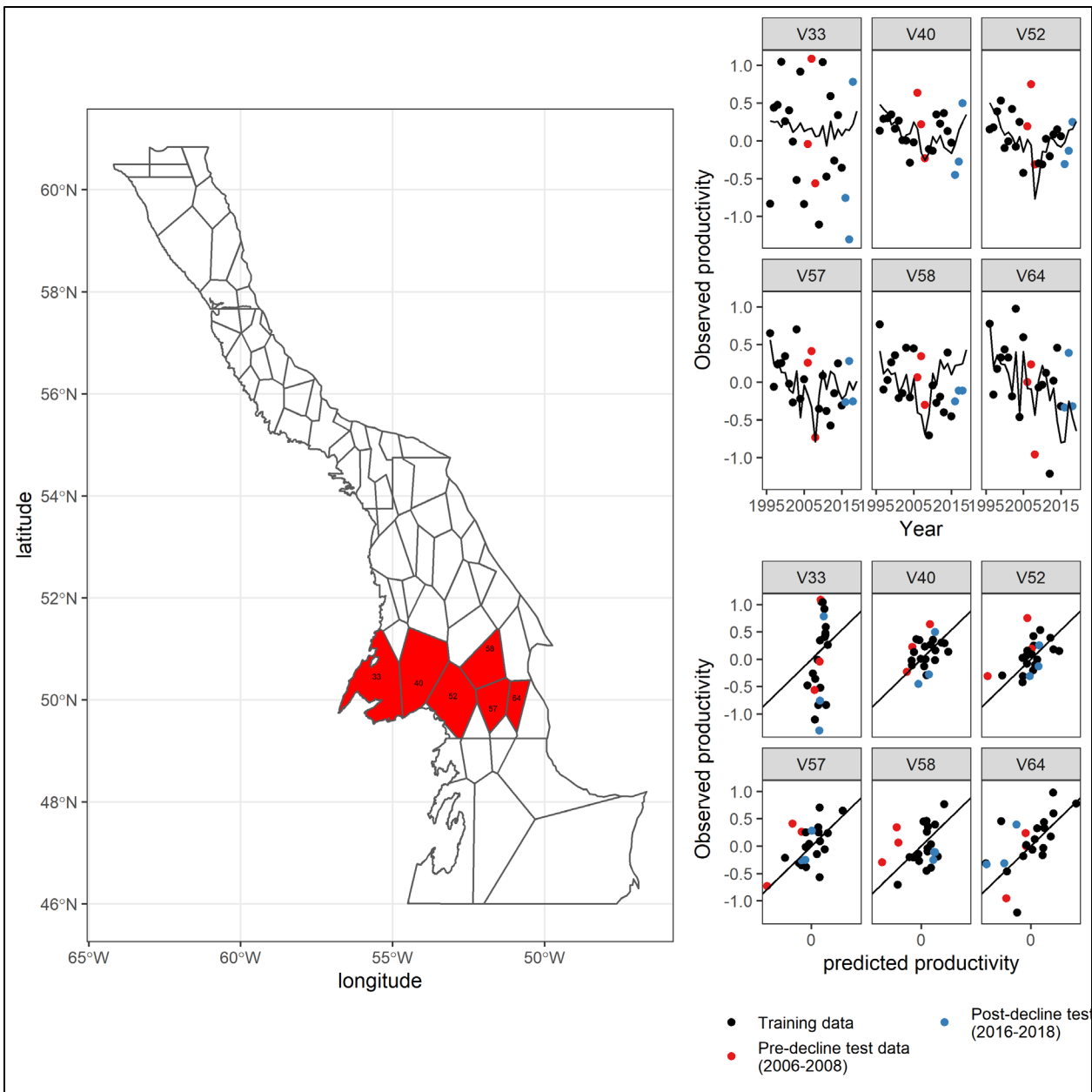


Figure S10: Model fits for patches V33, V40, V52, V57, V58, and V64. Left: map illustrating patch locations. Top right: plot of observed patch-level productivities plotted against time. Black line indicated model-predicted productivity. Bottom right: observed versus expected productivity in each patch in each year. Black line indicates the 1-1 line.

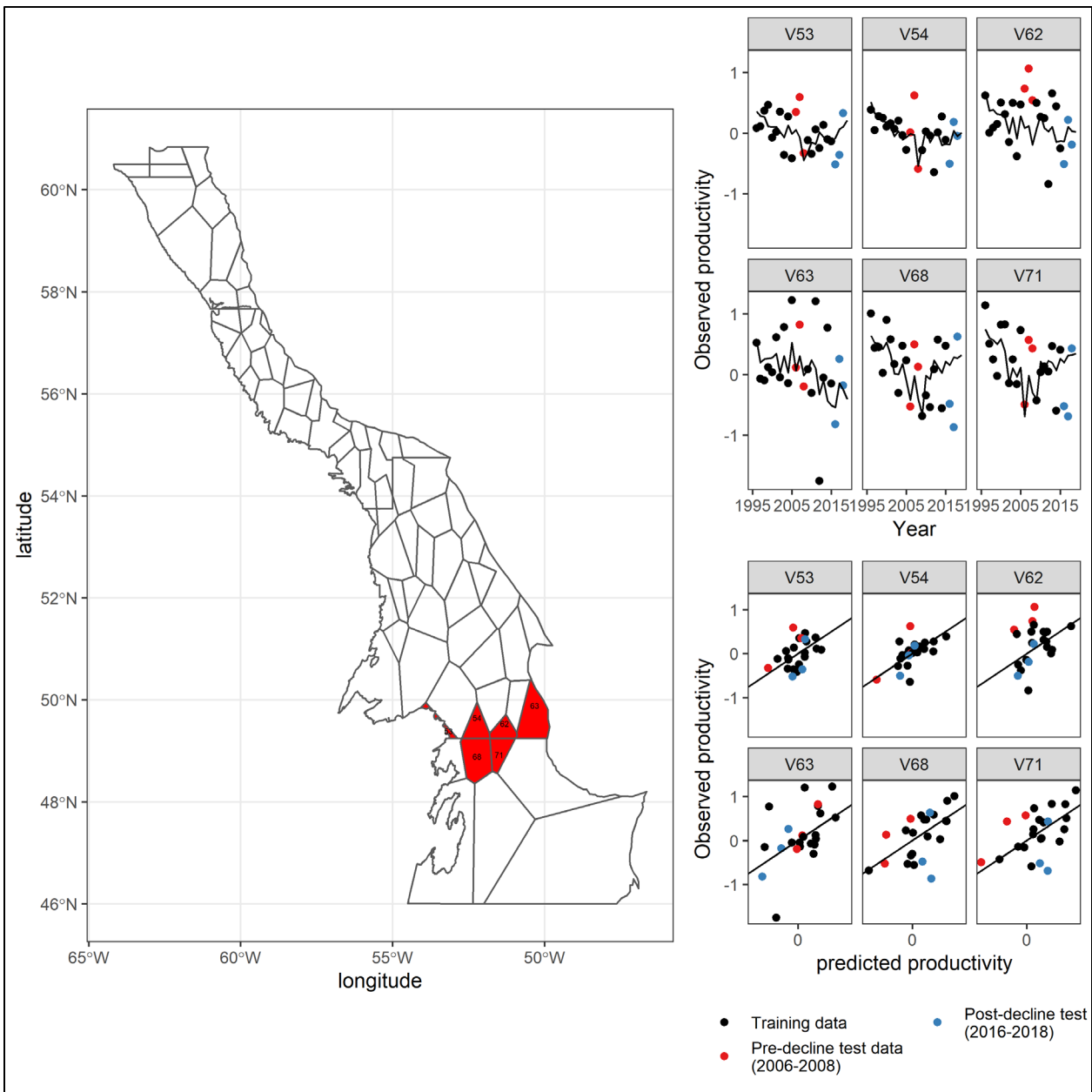


Figure S11: Model fits for patches V53, V54, V62, V63, V68, and V71. Left: map illustrating patch locations. Top right: plot of observed patch-level productivities plotted against time. Black line indicated model-predicted productivity. Bottom right: observed versus expected productivity in each patch in each year. Black line indicates the 1-1 line.

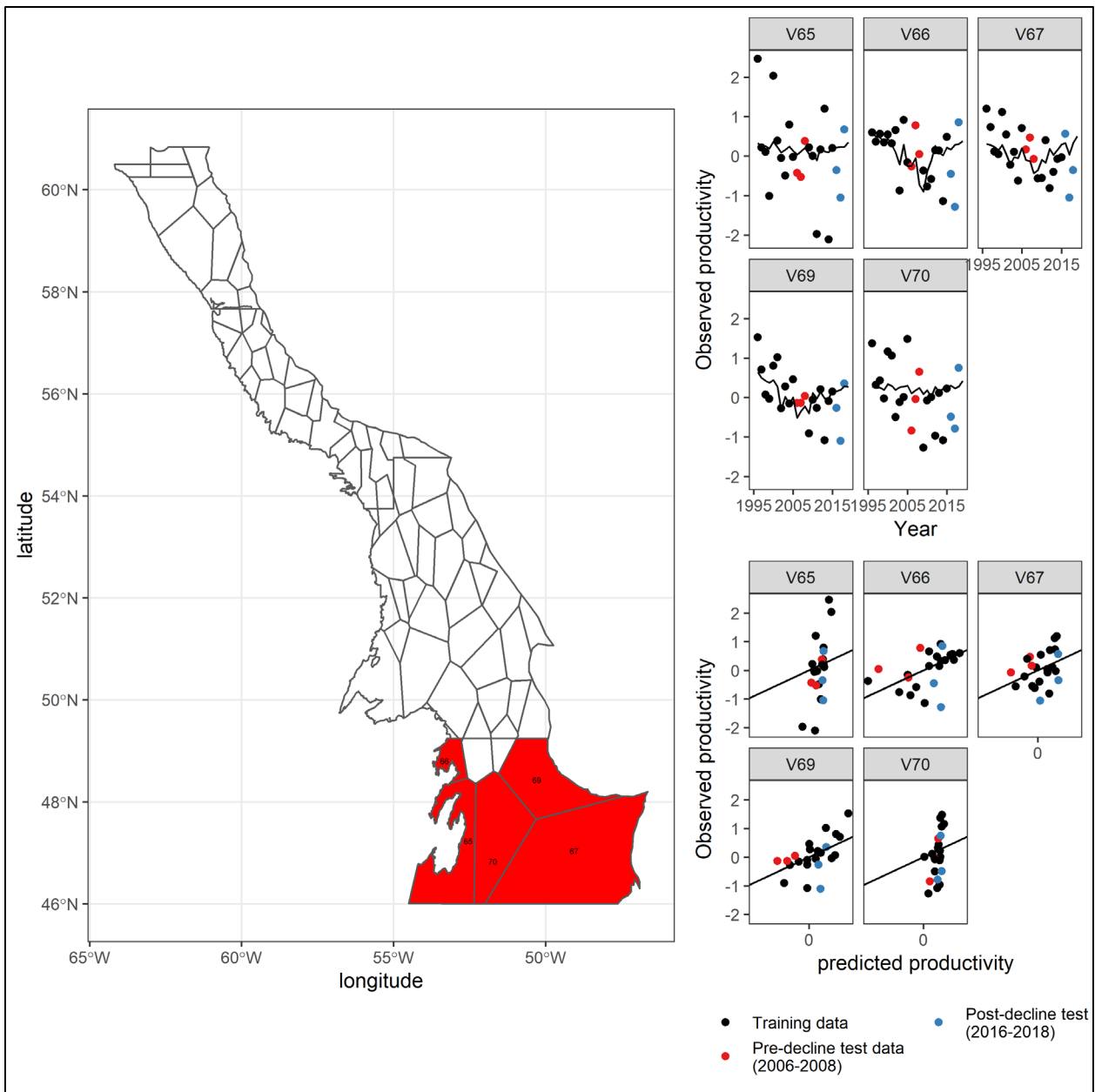


Figure S12: Model fits for patches V65, V66, V67, V69, and V70. Left: map illustrating patch locations. Top right: plot of observed patch-level productivities plotted against time. Black line indicated model-predicted productivity. Bottom right: observed versus expected productivity in each patch in each year. Black line indicates the 1-1 line.

APPENDIX I: AMENDMENT

A mistake in the modelling code for the non-spatial model used in the original version of this document was found. This error added an additional unanticipated interaction into the non-spatial model. The error did not substantially change the overall relative rankings of the models. The corrected values and changes to the text are restricted to values for the root-mean square error (Table 2), visualizations (Figure 25) for the updated non-spatial model, and the Results' paragraphs comparing this model with other modelling results (page 16–17). The corrected paragraphs describing the results, Table 2, and Figure 25 are below.

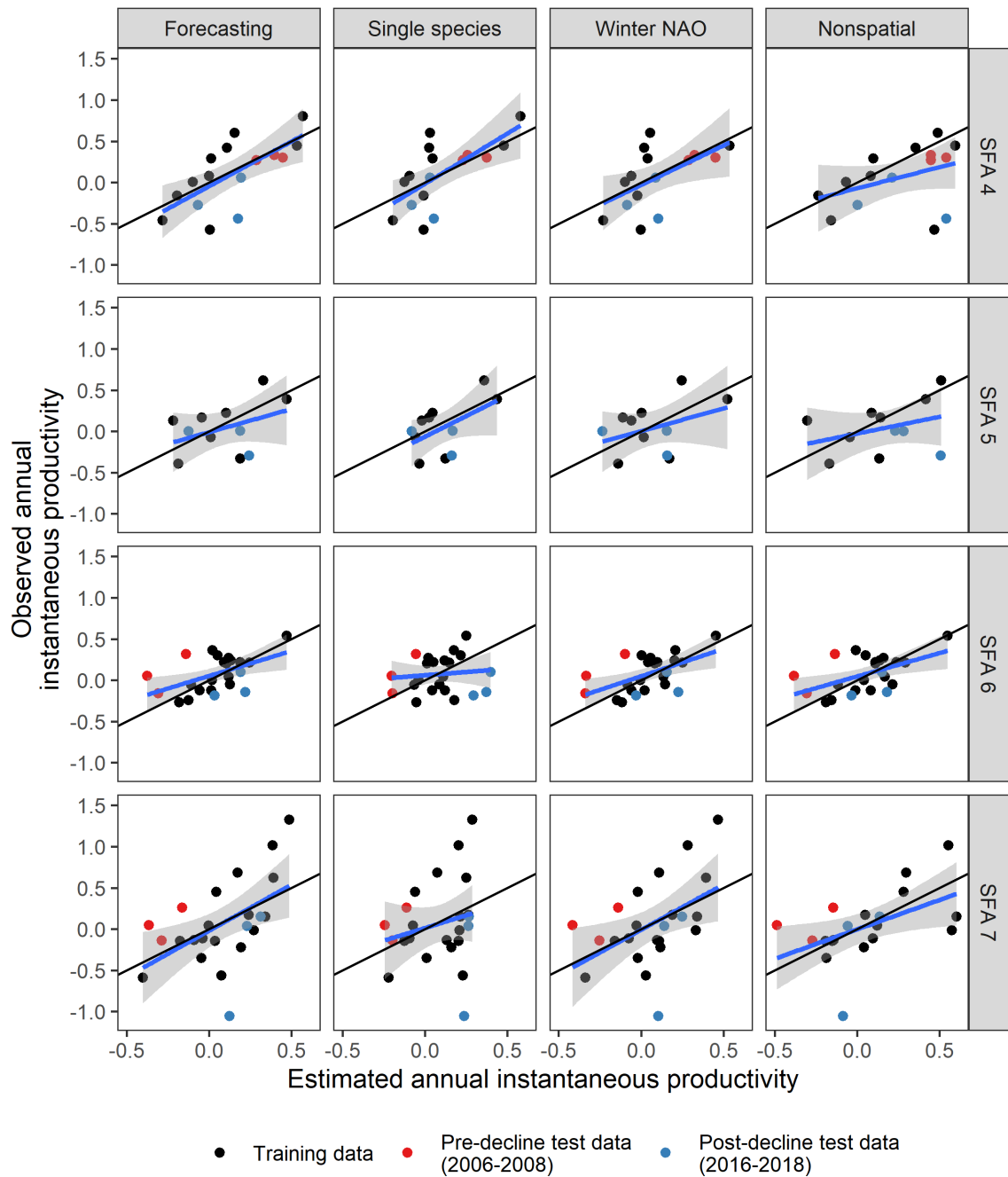
Revised text (page 16–17):

The simplified lag-1 model fit observed yearly productivities better than the single species model in all SFAs except 5 in the training data set, but was outperformed by the single species model in SFA 4 and 5 in the test data set (Table 2). The winter NAO model fit approximately as well as the forecasting model in all SFAs in the training data, and slightly out-performed the forecasting model when predicting trends in the test data set (Table 2). However, the winter NAO term was not actually statistically significant in this model, indicating that the sign of the effect of the winter NAO term was uncertain. The non-spatial model had worse predictive performance than the simplified lag-1 model for SFA 4 and 6 in the training data set, and the same or worse predictive performance in all SFAs except SFA 7 compared to the simplified lag-1 model in the test data set (Table 2).

Overall, the single-species model did a poorer job of predicting periods of rapid increase or decrease in SFA 6 and 7 (Figure 25, column 2), which is consistent with the evidence presented previously that these stocks have undergone at least two large-scale changes productivity in this time series. The winter NAO model fit as well or better than the simplified lag-1 model (Figure 25, column 3). The non-spatial model tended to under-predict periods of both increase and declines in SFA 4 (Figure 25, column 4). Although the simplified lag-1 model was outperformed by alternate models test in some incidences (e.g., multi-year lags, SFA 7 post-decline test data), the simplified lag-1 model was chosen for its relatively simplicity and overall fit and was adopted as the primary model for forecasting changes in this stock. This model was refit using data from all years to ensure that model parameters were estimated using all available data. This refit model was used to generate the remainder of the results in this report, and is hereafter referred to as the forecasting model.

Revised Table 2: SFA-level out-of-sample goodness of fit (RMSE) for model sensitivity comparisons.

	Forecasting	Single species	Winter NAO	Non-spatial
Training data				
SFA 4	0.29	0.32	0.32	0.36
SFA 5	0.27	0.24	0.28	0.24
SFA 6	0.14	0.20	0.14	0.16
SFA 7	0.38	0.47	0.41	0.28
Test data (2006–2008, 2016–2018)				
SFA 4	0.28	0.22	0.24	0.44
SFA 5	0.33	0.28	0.31	0.51
SFA 6	0.30	0.36	0.28	0.30
SFA 7	0.55	0.57	0.54	0.48



Revised Figure 25: Observed SFA-level productivity values for all SFAs for sensitivity tests. Black line indicates the 1-1 equality line, and the blue lines represent a simple linear regressions of observed on predicted values. Red points and lines indicate data from 2006 to 2008, prior to significant Northern Shrimp declines. Blue points and lines indicate data from 2016 to 2018, following the decline in shrimp biomass